國 立 交 通 大 學

電子工程學系 電子研究所碩士班

碩 士 論 文

寬頻無線通道模型及模擬之研究

Study in Broadband Wireless Channel Modeling and Simulation

研 究 生：陳豐進

指導教授：林大衛 博士

中 華 民 國 九 十 九 年 四 月

寬頻無線通道模型及模擬之研究

Study in Broadband Wireless Channel Modeling and Simulation

研究生：陳豐進　　Student: Feng-Chin Chen

指導教授：林大衛 博士　　Advisor: Dr. David W. Lin

國 立 交 通 大 學

電子工程學系　　電子研究所碩士班

碩士論文

A Thesis

Submitted to Department of Electronics Engineering & Institute of Electronics
College of Electrical and Computer Engineering
National Chiao Tung University
in Partial Fulfillment of the Requirements
for the Degree of Master of Science
in
Electronics Engineering
April 2010
Hsinchu, Taiwan, Republic of China

中華民國九十九年四月

寬頻無線通道模型及模擬之研究

研究生：陳豐進　　指導教授：林大衛 博士

國立交通大學

電子工程學系　電子研究所碩士班

摘要

3GPP 長期演進技術 (Long Term Evolution)是近來廣受注目的 4G 行動通訊的規格系統。但是發展通訊規格技術之前，首要目的便是如何能準確地去模擬通道間各種情況，而 3GPP SCM 通道規格和 WINNER 通道模擬計畫便此而產生。

本篇論文主要探討 WINNER 通道模擬技術之研究。首先我們將一一介紹各種常見於通訊技術中的通道模型，其中包括了 Jakes、AR、SCM 以及 WINNER 通道等模型。由於 WINNER 通道的發展初衷便是針對 4G 的環境作設定，所以我們更著重於對 WINNER 通道的研究。但是 WINNER 通道的運算複雜度相當高，這會對未來我們實現於數位訊號處理器（DSP）中時，造成極大的硬體負荷及運算時間；所以我們利用多項式內插法大量減少其複雜度而模擬效果卻不會相差太多，再者我們也利用 AR 模型去討論 WINNER 通道的特性，以便將來能實際應用在 DSP 上。

在系統整合上，我們將先前由學長姐所完成各部份的 C 程式做一個連接；將來，我們便能夠做整個系統的簡單模擬；另外在數位訊號處理器（DSP）上的系統，我們也增加了對上層 (MAC) 的溝通介面。

最後，由於 WINNER 通道模型是能夠做多傳多收的通道模擬，所以我們也特別針對此利用 WINNER 通道去探討該情況下，通道之間相互影響的主要原因及影響程度。

Study in Broadband Wireless Modeling and Simulation

Student: Feng-Chin Chen Advisor: Dr. David W. Lin

Institute of Electronics

Department of Electronics Engineering

National Chiao Tung University

Abstract

3GPP Long Term Evolution is popular standard of 4G mobile communication technique. But before develop any kinds of communication technique, we must be confirm the channel simulation environment and how to actual modeling channel condition. And the 3GPP SCM standard and WINNER channel model were developed by this purpose.

In this thesis, we first present four kinds of popular channel model which were Jakes, SCM, WINNER and Autoregressive (AR) model. We focus on discuss the WINNER channel model, because it was developed by more actual 4G channel environment and could be simulted for twelve secnario. But we realize it would cost a lot of simultion time and complex to generate WINNER channel coefficients. So we discuss the approximation technique to reduce its complex, and we also discuss its statistical properties using the AR model.

In system application part, we combined the different block code in IEEE 802.16e PHY layer, in order to fast simulate and verify their code in total system. Besides, we make the simple connection between PHY layer and MAC layer.

In other application part, we discuss the reason to affect channel spatial correlation by the WINNER channel.

Contents

List of Figures

List of Tables

Chapter 1

Introduction

Long Term Evolution (LTE) is the popular standard technology to develop the 4th generation (4G) mobile communication radio technologies, which is aiming at high capacity, high speed, low latency and packet in cellular mobile communication systems. Although LTE and WiMAX are competitors, there are a lot of similarity, like framing. So we can take our earlier experience and technique in WiMAX study to apply to LTE. But in order to accurately simulate 4G channel system, Jakes' model we used may not satisfied with us. Then we start studying 3GPP SCM and WINNER channel model, and take advantage of these models to implement in our system.

The 3GPP spatial channel model, developed by 3GPP-3GPP2 spatial channel model (SCM) ad-hoc group (AHG) is the standard 3GPP (3rd Generation Partnership Project) channel model. The 3GPP SCM channel model was developed by using radio frequency spectrum around 2 GHz and frequency bandwidth of 5 MHz, but may not be suitable for 4G radio system. So the wireless world initiative new radio (WINNER) group developed the WINNER model based on SCM model, aiming at simulating Beyond-3G (B3G) radio systems using a frequency bandwidth of 100 MHz and a radio frequency spectrum between 2 and 6 GHz. In [2], the chapter 5 (Measurements and Literature Review) were listed a lots of reference documents, and those documents were based on different center frequency, bandwidth and scenarios to discuss the property statistics and correlation of channel parameters. Then, WINNER group developed channel model based on these documents and some actual environment measurement.

According to the public document of Matlab software documentation of WIM2 model [1], the channel models cover WINNER propagation scenarios for indoor, urban macro-cell and micro-cell, stationary feeder, suburban macro-cell, and rural macro-cell. Both geometric-based stochastic channel model and reduced-variability (clustered delay-line) models are presented. This channel system also could be simulate MIMO system and set base station and mobile station antenna array type (UCA/ULA). In chapter 5, we use this model to discuss the spatial channel correlation. By the way, the channel models are mainly based on measurement data.

However, we know the WINNER channel model was developed based on sum-of-sinusoid technique, and the disadvantage of this technique is cost a lot of time to generate channel coefficients using many multiplication and addition. If we want apply WINNER channel model to DSP platform on future, we must consider some of technique to reduce this simulation complex. In the chapter 3, we could take and autoregressive (AR) model to reduce WINNER II channel model simulation complexity.

Our other application study could be divided into two part in chapter 4. In the first part, we integrate the IEEE802.16e PHY system. Because we want to quickly and convenient verify our block function in IEEE802.16e PHY system, combine with before function block code and analyze their power level. In the second part, we establish the mechanism that communicate physical layer and MAC layer.

The thesis is organized as follows. we first introduce the four kinds of popular channel models in chapter 2. Chapter 3, we analyze the WINNER channel model characteristic and use auto-regressive model attempting to reduce WINNER channel simulation complex. In chapter 4, we introduce the process that integrate downlink IEEE 802.16e PHY system with fixed point and connect physical layer and MAC layer. We also discuss the MIMO spatial channel correlation in chapter 5. Finally, the conclusion is given in chapter 6, where we also point out some potential future work.

Chapter 2

Channel Modeling Techniques

In this chapter, we introduce some different methods to simulate realistic channel models.

2.1 Jakes' Model [3]

The Jakes fading model is popularly used model for simulating time-correlation Rayleigh fading waveforms. The model assumes that N equal-strength rays around the moving receiver with uniformly distributed arrival angles $\alpha_n = 2\pi n/N$, such that ray n experiences a Doppler shift $w_n = w_M \cos(\alpha_n)$, where $w_M = 2\pi f v/c$ is the maximum Doppler shift, v is the vehicle speed, f is the carrier frequency, and c is the speed of light.

There is quadrantal symmetry in the magnitude of the Doppler shift, in order to reduce the compute complex, the fading waveform can be modeled with $N_0 + 1$ complex oscillators, where $N_0 = (N/2 - 1)/2$. This gives

$$\begin{aligned} T(t) = K\{&\frac{1}{\sqrt{2}}[\cos(\alpha) + I\sin(\alpha)]\cos(w_M t + \theta_0) \\ &+ \sum_{n=1}^{N_0}[\cos(\beta_n) + I\sin(\beta_n)]\cos(w_n t + \theta_n)\} \end{aligned} \tag{2.1}$$

where I denotes $\sqrt{-1}$, K is a normalization constant, α and β_n are phases, and θ_n are initial phases usually set to zeros.

To generate multiple uncorrelated waveforms, the oscillators must have equal power. This is achieved by reformulating the Jakes model in terms of slightly different arrival angles. Set

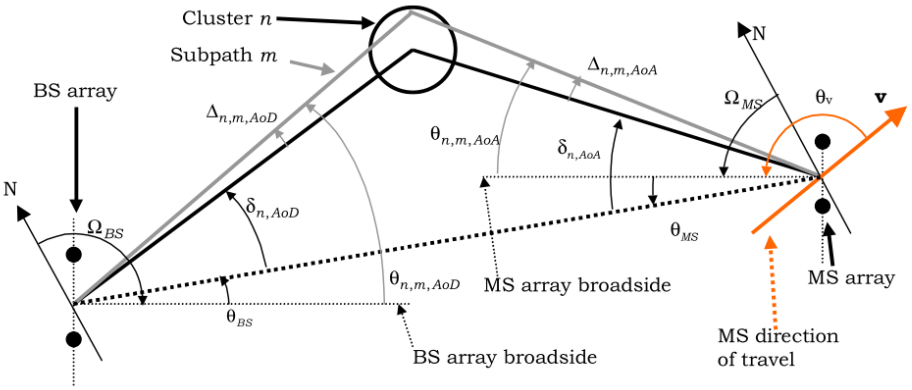

Figure 2.1: SCM channel illustration [4].

the arrival angles $\alpha_n = 2\pi(n - 0.5)/N$, this leads to the model

$$T(t) = \sqrt{\frac{2}{N_0}} \sum_{n=1}^{N_0} [\cos(\beta_n) + I \sin(\beta_n)] \cos(w_n t + \theta_n) \tag{2.2}$$

where $N_0 = N/4$ and the normalization factor $\sqrt{2/N_0}$ give $E\{T(t)T^*(t)\} = 1$. By using $\beta_n = \pi n/N_0$, the real and imaginary parts of $T(t)$ have equal power and are uncorrelated. Randomizing θ_n provides different waveform realizations.

2.2 Spatial Channel Model [4]

According to [4], the Spatial Channel Model (SCM) is developed by 3GPP-3GPP2 spatial channel model ad-hoc group (AHG). This model was based on sum-of-sinusoids method to generate the channel coefficients. The SCM channel is illustrated in Figure 2.1. And these parameters are defined in Table 2.1.

For an S element linear base station (BS) array and a U element linear mobile station (MS) array, the channel coefficients for one of N multi-path components are given by a U-by-S matrix of complex amplitudes. We denote the channel matrix for the nth multi-path component $(n = 1, ..., N)$ as $H_n(t)$. The $(u, s)th$ component $(s = 1, ..., S; u = 1, ..., U)$ of $H_n(t)$ is given by

Table 2.1: SCM Parameters Definition [4]

Parameters	Definition
Ω_{BS}	BS antenna array orientation, defined as the difference between the broadside of the BS array and the absolute North (N) reference direction.
θ_{BS}	LOS AoD direction between the BS and MS, with respect to the broadside of the BS array
$\delta_{n,AoD}$	AoD for the nth ($n = 1...N$) path with respect to the LOS AoD θ_0.
$\Delta_{n,m,AoD}$	Offset for the mth ($m = 1...M$) subpath of the nth path with respect to AoD θ_0.
$\theta_{n,m,AoD}$	Absolute AoD for the mth ($m = 1...M$) subpath of the nth path at the BS with respect to the BS broadside.
Ω_{MS}	MS antenna array orientation, defined as the difference between the broadside of the MS array and the absolute North reference direction.
θ_{MS}	Angle between the BS-MS LOS and the MS broadside.
$\delta_{n,AoA}$	AoA for the nth ($n = 1...N$) path with respect to the LOS AoA $\theta_{0,MS}$.
$\Delta_{n,m,AoA}$	Offset for the mth ($m = 1...M$) subpath of the nth path with respect to to AoA $\delta_{n,AoA}$.
$\theta_{n,m,AoA}$	Absolute AoA for the mth ($m = 1...M$) subpath of the nth path at the MS with respect to the BS broadside.
v	MS velocity vector.
θ_v	Angle of the velocity vector with respect to the MS broadside: $\theta_v = arg(v)$.
P_n	is the power of the nth path.
σ_{SF}	is the lognormal shadow fading), applied as a bulk parameter to the n paths for a given drop
M	is the number of subpaths per-path.
$G_{BS}(\theta_{n,m,AoD})$	is the BS antenna gain of each array element.
$G_{MS}(\theta_{n,m,AoA})$	is the MS antenna gain of each array element.
d_s	is the distance in meters from BS antenna element s from the reference (s = 1) antenna.
d_u	is the distance in meters from MS antenna element u from the reference (u = 1) antenna.

$$h_{u,s,n}(t) = \sqrt{\frac{P_n \sigma_{SF}}{M}} \sum_{m=1}^{M} \begin{pmatrix} \sqrt{G_{BS}(\theta_{n,m,AoD})} \exp(j[kd_s \sin(\theta_{n,m,AoD}) + \Phi_{n,m}]) \times \\ \sqrt{G_{MS}(\theta_{n,m,AoA})} \exp(j[kd_u \sin(\theta_{n,m,AoA})]) \times \\ \exp(jk\|v\| \cos(\theta_{n,m,AoA} - \theta_v)t) \end{pmatrix} \quad (2.3)$$

where these parameters are defined as same as Figure 2.1. The path loss and the log normal shadowing is applied as bulk parameters to each of the sub-path components of the n path components of the channel.

Because the process of generate these parameters is copious and similar to WINNER channel model, we do not present those parameter generation process. People interested in the process can refer to [3].

2.2.1 Propagation Scenarios

In 3GPP spatial channel model, we consider the following three environments.

- Suburban macrocell (approximately 3km distance BS to BS).
- Urban macrocell (approximately 3km distance BS to BS).
- Urban microcell (less than 1km distance BS to BS).

The characteristics of the macro cell environments assume that BS antennas are above rooftop height. For the urban microcell scenario, we assume the BS antenna is at rooftop height. Table 2.2 describes the parameters used in each of the environments.

2.2.2 SCM Path-Loss Model

The SCM path-loss models were considered three environments:

Suburban macrocell and urban macrocell environments

The macrocell pathloss is based on the modified COST 231 Hata urban propagation mode:

$$\begin{aligned} PL[dB] &= (44.9 - 6.55 \log(h_{bs})) \log \frac{d}{1000} + 45.5 + \\ &\quad (35.46 - 1.1 h_{ms}) \log(f_c) - 13.82 \log(h_{bs}) + 0.7 h_{ms} + C \end{aligned} \quad (2.4)$$

Table 2.2: SCM Environment Parameters [4]

Channel Secnario	Suburban Macro	Urban Macro	Urban Micro
Number of paths (N)	6	6	6
Number of sub-paths (M) per-path	20	20	20
Mean AS at BS AS at BS as a lognormal RV $\sigma_{AS} = 10^(\varepsilon_{AS}x + \mu_{AS}), x \sim \eta(0,1)$	$E(\sigma_{AS}) = 5^o$ $\mu_{AS} = 0.69$ $\varepsilon_{AS} = 0.13$	$E(\sigma_{AS}) = 8^o, 15^o$ $8^o : \mu_{AS} = 0.810$ $\varepsilon_{AS} = 0.810$ $15^o : \mu_{AS} = 1.18$ $\varepsilon_{AS} = 0.210$	$NLOS : E(\sigma_{AS}) = 19^o$ N/A
$\gamma_{AS} = \sigma_{AoD}/\sigma_{AS}$	1.2	1.3	N/A
Per-path AS at BS (Fixed)	2deg	2deg	5deg (LOS and NLOS)
BS per-path AoD Distribution standard distribution	$\eta(0, \sigma^2_{AoD})$ where $\sigma_{AoD} = \gamma_{AS}\sigma_{AS}$	$\eta(0, \sigma^2_{AoD})$ where $\sigma_{AoD} = \gamma_{AS}\sigma_{AS}$	U(-40deg,40deg)
Mean AS and MS	$E(\sigma_{AS,MS}) = 68^o$	$E(\sigma_{AS,MS}) = 68^o$	$E(\sigma_{AS,MS}) = 68^o$
Per-path AS at MS (fixed)	35^o	35^o	35^o
MS Per-path AoA Distribution	$\eta(0, \sigma^2_{AoD}(Pr))$	$\eta(0, \sigma^2_{AoD}(Pr))$	$\eta(0, \sigma^2_{AoD}(Pr))$
Delay spread as a lognormal RV $\sigma_{DS} = 10^(\varepsilon_{DS}x + \mu_{DS}), x \sim \eta(0,1)$	$\mu_{DS} = -6.80$ $\varepsilon_{DS} = 0.288$	$\mu_{DS} = -6.18$ $\mu_{DS} = 0.18$	N/A
Mean total RMS Delay Spread	$E(\sigma_{DS}) = 0.17\mu s$	$E(\sigma_{DS}) = 0.65\mu s$	$E(\sigma_{DS}) = 0.251\mu s$
$\gamma_{DS} = \sigma_{delay}/\sigma_{DS}$	1.4	1.7	N/A
Distribution for path delays			N/A
Lognormal shadowing standard deviation,σ_{SF}	8dB	8dB	NLOS: 10dB LOS : 4 dB
Pathloss model (dB), d is meters	$31.5 + 35\log(d)$	$34.5 + 35\log(d)$	NLOS :$34.53 + 38\log(d)$ LOS :$30.18 + 26\log(d)$

where h_{bs} is the BS antenna height in meters, h_{ms} is the MS antenna height in meters, f_c is the carrier frequency in MHz, d is the distance between the BS and MS in meters, and C is a constant factor ($C = 0$ dB for suburban macro and $C = 3$ dB for urban macro) Setting these parameters to $h_{bs} = 32m$, $h_{ms} = 1.5m$, and $f_c = 1900$ MHz, the pathlosses for suburban and urban macro environments become, respectively, $PL = 31.5 + 35\log(d)$ and $PL = 34.5 + 35\log(d)$. The distance d is required to be at least 35 m.

Microcell environments

- Non line-of-sight (NLOS): The microcell NLOS pathloss is based on the COST 231 Walfish-Ikegami NLOS model with the following parameters: BS antenna height 12.5 m, building height 12 m, building to building distance 50 m, street width 25 m, MS antenna height 1.5 m, orientation 30 deg for all paths, and selection of metropolitan center. With these parameters, the equation simplifies to

$$PL[dB] = -55.9 + 38\log(d) + (24.5 + 1.5f_c/925) \cdot \log(f_c). \tag{2.5}$$

  The resulting path-loss at 1900 MHz is: $PL[dB] = 34.53 + 38\log(d)$, where d is in meters. The distance d is at least 20 m. A bulk log normal shadowing applying to all sub-paths has a standard deviation of 10 dB.

- Line-of-sight (LOS): The microcell LOS pathloss is based on the COST 231 Walfish-Ikegami street canyon model with the same parameters as in the NLOS case. The pathloss is

$$PL[dB] = -35.4 + 26\log(d) + 20\log(f_c). \tag{2.6}$$

  The resulting path-loss at 1900 MHz is $PL(dB) = 30.18 + 26\log 10(d)$, where d is in meters. The distance d is at least 20 m. A bulk log normal shadowing applying to all sub-paths has a standard deviation of 4 dB.

2.3 WINNER II Channel Models [5]

The goal of wireless world initiative new radio (WINNER) project is to develop a Beyond-3G (B3G) radio system model using the 100 MHz frequency bandwidth and center frequency somewhere between 2 and 6 GHz in spectrum. In the beginning of project, the most important thing is how to use the accurate and realistic channel model in the simulation to enable reliable simulation results. On the other hand, the 3GPP Spatial Channel Model (SCM) cannot satisfied the WINNER project channel simulation. Then WINNER project group start to rebuild another channel model (WINNER Channel Model).

At first, WINNER Channel Models (Phase I) is explored based on the two standardized models, namely 3GPP/3GPP2 SCM and IEEE 802.11n. The former is used in outdoor simulations and the latter in indoor simulations. Afterward, this initial models is not adequate for the advanced WINNER I simulations. Therefore, new measurements-based models (WINNER I) were developed. The generic model is ray-based double-directional multi-link model that is antenna independent, scalable and capable of modeling channels for MIMO connections. Statistical distributions and channel parameters extracted by measurements at any propagation scenarios can be fitted to the generic model. In the WINNER II channel model, it extended the model features, frequency rang, and the number of scenarios based on WINNER I. From the Table 2.3, we can clearly see the differences between SCM, WIMMER I, and WIMMER II.

2.3.1 Propagation Scenarios

In this section, we list the WINNER II channel model propagation scenarios. Those scenarios can be divided to three parts : Local Area (LA), Metropolitan Area (MA) and Wide Area (WA). Mapping of scenarios to three Groups is shown in the Table 2.4, in column CG.

There are some points that need to be understood about the scenarios and channel models adapted to them. First, those scenarios do not cover all possible environments and

Table 2.3: Channel Numerical Comparison [6]

Parmeter	Unit	SCM	WINNER I	WINNER II
Max.bandwidth	MHz	5	100	100
Frequency range	GHz	2	$2-6$	$2-6$
No.of scenarios		3	7	12
No.of clusters		6	$4-24$	$4-20$
No.mid-paths per cluster		1	1	$1-3$
No.sub-paths per cluster		20	10	20
No.of taps		6	$4-24$	$4-24$
BS angle spread	^{o}	$5-9$	$3.0-38.0$	$2.5-53.7$
MS angle spread	^{o}	68	$9.5-53.0$	$11.7-52.5$
Delay spread	ns	$170-650$	$1.6-313.0$	$16-630$
Shadow fading standard deviation	dB	$4-10$	$1.4-8.0$	$2-8$

conditions: e.g, the mountainous or even hilly rural environments have not been covered. Second, the environments are described in two levels of details called non-grid-based and grid-based models. The non-grid-based models is that only the distance between transmitter and receiver, and not considered their locations. And those grid-based scenarios (A1, A2, B1, B2 and B4), because, defiend in building or streets; there are obstacles in direct path between transmitter and receiver. So the transmitters and receivers must be located and streets or a building layout.

2.3.2 WINNER Generic Channel Model

WINNER channel model is stochastic geometry model. Geometry modelling approach enables separation of propagation parameters and antennas. Antenna geometries and field patterns of channel can be defined by user properly. Channel coefficient are generated by summing of rays with specific small scale parameters like delay, power, angle of arrival (AoA) and angle of departure (AoD) . A number of rays constitute a cluster which be defined diffused in space, either or both in delay and angle domains. The MIMO channel are illustrated in Figure 2.2.

Table 2.4: Propagation Scenarios Specified in WINNER II [5]

Scenario	Definition	LOS/ NLOS	Mob .km/h	Frequency (GHz)	CG
A1 (In building)	Indoor office / residential	LOS/ NLOS	$0-5$	$2-6$	LA
A2	Indoor to outdoor	NLOS	$0-5$	$2-6$	LA
B1 (Hotspot)	Typical urban micro-cell	LOS/ NLOS	$0-70$	$2-6$	LA ,MA
B2	Bad urban micro-cell	NLOS	$0-70$	$2-6$	MA
B3 (Hotspot)	Large indoor hall	LOS/ NLOS	$0-5$	$2-6$	LA
B4	Outdoor to indoor micro-cell	NLOS	$0-5$	$2-6$	MA
B5a (Hotspot Metropol)	LOS stat. feeder, rooftop to rooftop	LOS	0	$2-6$	MA
B5b (Hotspot Metropol)	LOS start.feeder, street-level to street-level	LOS	0	$2-6$	MA
B5c (Hotspot Metropol)	Los start.feeder, below-rooftop to street-level	LOS	0	$2-6$	MA
B5d (Hotspot Metropol)	NLOS start.feeder above rooftop to street-level	NLOS	0	$2-6$	MA
B5f	Feeder link BS -> FRS. Approximately RT to RT level.	LOS/ OLOS/ NLOS	0	$2-6$	WA
C1 (Metropol)	Suburban	LOS/ NLOS	$0-120$	$2-6$	WA
C2 (Metropol)	Typical urban macro-cell	LOS/ NLOS	$0-120$	$2-6$	MA WA
C3	Bad Urban macro-cell	LOS/ NLOS	$0-70$	$2-6$	–
C4	Outdoor to indoor macro-cell	NLOS	$0-5$	$2-6$	MA
D1 (Rural)	Rural macro-cell	LOS /NLOS	$0-200$	$2-6$	WA
D2	a) Moving networks : BS-MRS, rural	LOS	$0-350$	$2-6$	WA
	b) Moving networks : MRS- MS, rural	LOS/ OLOS/ NLOS	$0-5$	$2-6$	LA

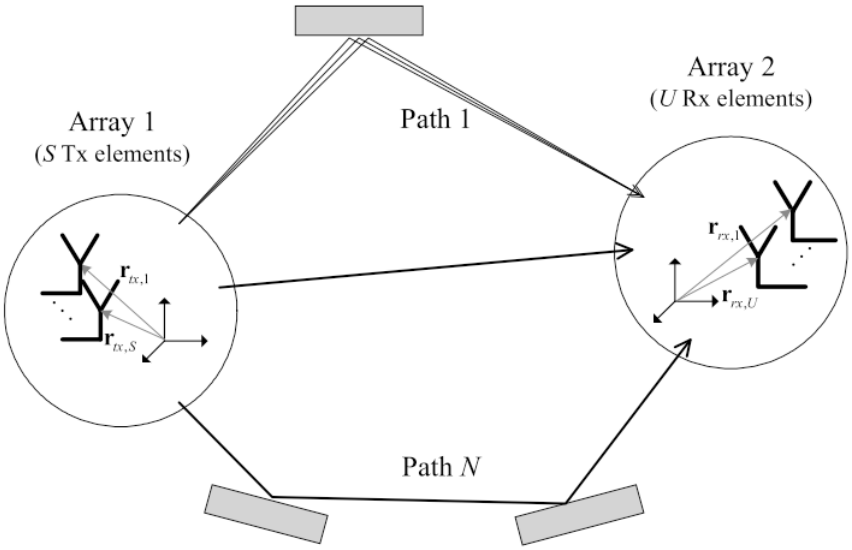

Figure 2.2: The MIMO channel [5].

Transfer matrix of the MIMO channel is

$$H(t;\tau) = \sum_{n=1}^{n} H_n(t;\tau). \tag{2.7}$$

The channel from Tx antenna element s to Rx element u for cluster n is

$$\begin{aligned} H(t;\tau) \;=\; & \sum_{m=1}^{M} \begin{bmatrix} F_{rx,u,V}(\varphi_{n,m}) \\ F_{rx,u,H}(\varphi_{n,m}) \end{bmatrix}^T \begin{bmatrix} \alpha_{n,m,VV} & \alpha_{n,m,VH} \\ \alpha_{n,m,HV} & \alpha_{n,m,HH} \end{bmatrix} \begin{bmatrix} F_{tx,u,V}(\phi_(n,m)) \\ F_{tx,u,H}(\phi_(n,m)) \end{bmatrix} \\ & \times \exp(j2\pi\lambda_0^{-1}(\overline{\varphi}_{(n,m)} \cdot \overline{\gamma}_{(rx,u))}) \exp(j2\pi\lambda_0^{-1}(\overline{\phi}_{(n,m)} \cdot \overline{\gamma}_{(tx,s))}) \\ & \times \exp(j2\pi\nu_{n,m})\delta(\tau - \tau_{n,m}) \end{aligned} \tag{2.8}$$

where $F_{rx,u,V}$ and $F_{rx,u,H}$ are the antenna element u field patterns for vertical and horizontal polarizations respectively, $\alpha_{n,m,VV}$ and $\alpha_{n,m,VH}$ are the complex gains of vertical-to-vertical and horizontal-to-vertical polarizations of ray n,m, respectively, λ_0 is the wave length of carrier frequency, $\overline{\phi}_{n,m}$ is AoD unit vector, $\overline{\varphi}_{n,m}$ is AoA unit vector, $\overline{\gamma}_{tx,s}$ and $\overline{\gamma}_{rx,u}$ are the location vectors of element s and u respectively, and $\nu_{n,m}$ is the Doppler frequency component of ray n,m. If the radio channel is modelled as dynamic, all the above mentioned small scale parameters are time variant, i.e., function of t.

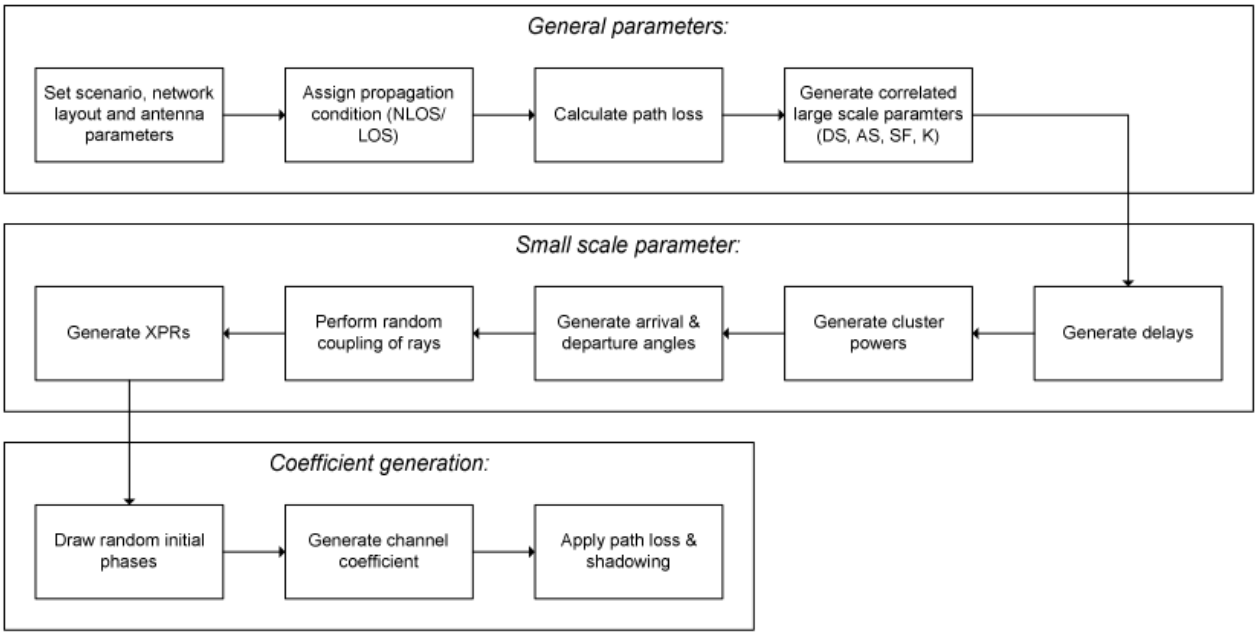

Figure 2.3: Channel coefficient generation procedure [5].

2.3.3 Modelling Process

In this sub-section, we introduce WINNER channel coefficient generation procedure, depicted in Figure 2.3. The following subsection is according to Figure 2.3 modeling process, generate those WINNER channel matrix parameters in (2.8) .

General parameters:

- Step 1: Set the environment, network layout and antenna array parameters
  - Choose one of the scenarios (A1, A2, B1, ...).
  - Give number of BS and MS.
  - Give locations of BS and MS, or equally distances of each BS and MS and relative directions ϕ_{LOS} and φ_{LOS} of each BS and MS.
  - Give BS and MS antenna field patterns F_{rx} and F_{tx}, and array geometries.
  - Give BS and MS array orientations with respect to north (reference) direction.

Table 2.5: Line-of-Sight Probabilities [5]

Scenario	LOS probability as a function of distance d [m]	Note
A1	$P_{LOS} = 1, d \leq 2.5$	
	$P_{LOS} = 1 - 0.9(1 - (1.24 - 0.61 \log d)^3)^{1/3}, d > 2.5$	
B1	$P_{LOS} = min(18/d, 1) \cdot (1 - \exp(-d/36)) + \exp(-d/36)$	
B3	$P_{LOS} = 1, d \leq 10$	For big factory halls,
	$P_{LOS} = 2, d \leq 10$	airport and train stations
C1	$P_{LOS} = \exp(-\frac{d}{200})$	
C2	$P_{LOS} = min(18/d, 1) \cdot (1 - \exp(-d/63)) + \exp(-d/63)$	
D1	$P_{LOS} = \exp(-\frac{d}{1000})$	

- Give speed and direction of motion of MS.
- Give system center frequency.

Large scale parameters:

- Step 2: Assign the propagation condition (LOS/NLOS) according to the probability described in Table 2.5.
- Step 3: Calculate the path loss with formulas of Table 2.12 for each BS-MS link to be modelled.
- Step 4: Generate the correlated large scale parameters.

Small scale parameters:

- Step 5: Generate the delays τ.

  Delays are drawn randomly from the delay distribution defined in Table 2.6. With

exponential delay distribution calculate

$$\tau_n' = -\gamma_\tau \sigma_\tau \ln(X_n). \tag{2.9}$$

where γ_τ is the delay distribution proportionality factor, σ_τ is delay spread, $X_n \sim Uni(0,1)$ and cluster index $n = 1, ..., N$. Normalize the delays by subtracting with minimum delays and sort the normalized delays to descending order as

$$\tau_n = sort(\tau_n' - \min(\tau_n'))). \tag{2.10}$$

In LOS condition, the scaling factor of delays is required to compensate the effect of LOS peak addition to the delay spread. The scaling factor is determined as

$$D = 0.7705 - 0.0433K + 0.0002K^2 + 0.000017K^3, \tag{2.11}$$

where K (in dB) is the Ricean K-factor defined Table 2.6. So the scaled delays are

$$\tau_n^{LOS} = \tau_n / D. \tag{2.12}$$

They are not to be used in cluster power generation.

- Step 6: Generate the cluster powers P.

  The cluster powers are calculated dependent on type of delay distribution defined in Table 2.6. If delay is exponential distribution, then the cluster powers are determined by

$$P_n' = \exp(-\tau_n \frac{\gamma_\tau - 1}{\gamma_\tau \sigma_\tau}) \tag{2.13}$$

  and with uniform delay distribution they are determined by

$$P_n' = \exp(-\tau_n \frac{\gamma_\tau - 1}{\gamma_\tau \sigma_\tau}) \cdot 10^{\frac{-Z_n}{10}} \tag{2.14}$$

  where $Z_n \in (0, \zeta)$ is the per cluster shadowing term in dB. In order to normalize the power, divide the power to sum of power of all cluster

$$P_n = \frac{P_n'}{\sum_{n=1}^{N} P_n'}. \tag{2.15}$$

  Each ray power within a cluster as P_n/M, where M is the number of rays per cluster.

Table 2.6: Parameters for Generic Models [5]

Scenarios		A1		$A2/B4/C4$	B1		B3		C1		C2		D1		D2a
		LOS	NLOS	NLOS	LOS	NLOS	LOS	NLOS	LOS	NLOS	LOS	NLOS	LOS	NLOS	LOS
Delay spread (DS)	μ	-7.42	-7.60	-7.39/-6.62[1)]	-7.44	-7.12	-7.53	-7.41	-7.23	-7.12	-7.39	-6.63	-7.80	-7.60	-7.4
$\log([s])$	σ	0.27	0.19	0.36/0.32[1)]	0.25	0.12	0.12	0.13	0.49	0.33	0.36	0.32	0.57	0.48	0.2
AoD spread (ASD)	μ	1.64	1.73	1.76	0.40	1.19	1.22	1.05	0.78	0.90	1	0.93	0.78	0.96	0.7
$\log([^o])$	σ	0.31	0.23	0.16	0.37	0.21	0.18	0.22	0.12	0.36	0.25	0.22	0.21	0.45	0.31
AoA spread (ASA)	μ	1.65	1.69	1.25	1.40	1.55	1.58	1.7	1.48	1.65	1.7	1.72	1.20	1.52	1.5
$\log([^o])$	σ	0.26	0.14	0.42	0.20	0.20	0.23	0.1	0.20	0.30	0.19	0.14	0.18	0.27	0.2
sadow fading (SF)[dB]	σ	3	4	7	3	4	3	4	4/6[3)]	8	4/6[3)]	8	4/6[3)]	8	4
K-factor(K)[dB]	μ	7	N/A	N/A	9	N/A	2	N/A	9	N/A	7	N/A	7	N/A	7
	σ	6	N/A	N/A	6	N/A	3	N/A	7	N/A	3	N/A	6	N/A	6
$Cross-Correlation$	ASD vs DS	0.7	-0.1	0.4	0.5	0.2	-0.3	-0.1	0.2	0.3	0.4	0.4	-0.1	-0.4	-0.1
	ASA vs DS	0.8	0.3	0.4	0.8	0.4	-0.4	0	0.8	0.7	0.8	0.6	0.2	0.1	0.2
	ASA vs SF	-0.5	-0.4	0.2	-0.5	-0.4	-0.2	0.2	-0.5	-0.3	-0.5	-0.3	-0.2	0.1	-0.2
	ASD vs SF	-0.5	0	0	-0.5	0	0.3	-0.3	-0.5	-0.4	-0.5	-0.6	0.2	0.1	-0.2
	DS vs SF	-0.6	-0.5	-0.5	-0.4	-0.7	-0.1	-0.2	-0.6	-0.4	-0.4	-0.4	-0.5	-0.5	-0.5
	ASD vs ASA	-0.6	-0.3	0	0.4	0.1	0.3	0.3	0.1	0.3	0.3	0.4	-0.3	-0.2	-0.3
	ASD vs K	-0.6	N/A	N/A	-0.3	N/A	0.2	N/A	0.2	N/A	0.1	N/A	0	N/A	0
	ASA vs K	-0.6	N/A	N/A	-0.3	N/A	-0.1	N/A	-0.2	N/A	-0.2	N/A	0.1	N/A	0.1
	DS vs K	-0.6	N/A	N/A	-0.7	N/A	-0.3	N/A	-0.2	N/A	-0.4	N/A	0	N/A	0
	SF vs K	-0.6	N/A	N/A	0.5	N/A	0.6	N/A	0	N/A	0.3	N/A	0	N/A	0
Delay distribution		Exp	Exp	Exp	Exp	Uniform	Exp	Exp	Exp	Exp	Exp	Exp	Exp	Exp	Exp
AoD and AoA distribution		Wrapped Gaussian													
Delay scalig parameter γ_τ		3	2.4	2.2	3.2	–	1.9	1.6	2.4	1.5	2.5	2.3	3.8	1.7	3.8
XPR [dB]	μ	11	10	9	9	8	9	6	8	4	8	7	12	7	3.8
	σ	4	4	11	3	3	4	3	4	3	4	3	8	4	8
Number of clusters		12	16	12	8	16	10	15	15	14	8	20	11	10	8
Number of rays per cluster		20	20	20	20	20	20	20	20	20	20	20	20	20	20
Cluster ASD		5	5	8	3	10	5	6	5	2	6	2	2	2	2
Cluster ASA		5	5	5	18	22	5	13	5	10	12	15	3	3	3
Per cluster shadowing std $\zeta[dB]$		6	3	4	3	3	3	3	3	3	3	3	3	3	3
Correlation distance[m]	DS	7	4	21/10[2)]	9	8	3	1	6	40	40	40	64	36	64
	ASD	6	5	15/11[2)]	13	10	1	0.5	15	30	15	50	25	30	25
	ASA	2	3	35/17[2)]	12	9	2	0.5	20	30	15	50	40	40	40
	SF	6	4	14/7 [2)]	14	12	3	3	40	50	45	50	40	120	40
	K	6	N/A	N/A	10	N/A	1	N/A	10	N/A	12	N/A	40	N/A	40

1) The left value corresponds to A2/B4 microcell and the right value to C4 macrocell.

2) The left value corresponds to A2 Indoor-to-Outdoor and the right value to B4/C4 Outdoor-to-Indoor.

3) Loss models for the C1 LOS and D1 LOS scenarios contain separate shadowing standard deviations.

Table 2.7: Table of Constant C [5]

clusters	4	5	8	10	11	12	14	15	16	20
C	0.779	0.860	1.018	1.090	1.123	1.146	1.190	1.211	1.226	1.289

- Step 7: Generate the azimuth arrival angles φ and azimuth departure angles ϕ

  – NLOS condition :

  According to (2.16), assign the azimuth arrival angles φ by multiplying with the random variable $X_n \sim Uni\{1, -1\}$ and $Y_n \sim N(0, \sigma_{AOA}/5)$ as

$$\varphi_n = X_n \varphi'_n + Y_n + \varphi_{LOS} \tag{2.16}$$

  where φ_{LOS} is the LOS direction defined in Step 1, and φ'_n is determined by

$$\varphi'_n = \frac{2\sigma_{AOA}\sqrt{-\ln(P_n/max(P_n))}}{C}. \tag{2.17}$$

  In (2.17), P_n is the cluster power determined from Step 6, the standard deviation of arrival angles (σ_{AOA}) is equal to $\sigma_\varphi/1.4$ (factor 1.4 is the ratio of Gaussian standard deviation (std)). Constant C is a scaling factor related to total number of clusters and is given in Table 2.7 .

  Finally add the offset angles α_m from Table 2.8 to cluster angles

$$\varphi_{n,m} = \varphi_n + C_{AOA}\alpha_m \tag{2.18}$$

  where C_{AOA} is the cluster-wise rms azimuth spread of arrival angles in Table 2.6.

  – LOS condition:

  In the LOS case, the azimuth arrival equation is changed

$$\varphi_n = (X_n \varphi'_n + Y_n) - (X_n \varphi'_1 + Y_1 - \varphi_{LOS}). \tag{2.19}$$

  And the constant C is substituted by C^{LOS}, which is determined by $C^{LOS} = C \cdot (1.1035 - 0.028K - 0.002K^2 + 0.0001K^3)$, where K (in dB) is the Ricean K-factor defined in Table 2.6. Then the following procedure is same as NLOS.

Table 2.8: Ray Offset Angles Within A Cluster, Given for 1^o rms Angle Spread [5]

Ray number m	Basis vector of offset angles α_m
1,2	± 0.0447
3,4	± 0.1413
5,6	± 0.2492
7,8	± 0.3715
9,10	± 0.5129
11,12	± 0.6797
13,14	± 0.8844
15,16	± 1.1481
17,18	± 1.5195
19,20	± 2.1551

For departure angles φ_n the procedure is analogous.

- Step 7b: If the elevation angles are supported:

  Generate elevation arrival angles ψ and elevation departure angles γ. Draw elevation angles with the same procedure as azimuth angles on Step 7. Azimuth rms angle spread values and cluster-wise azimuth spread values are replaced by corresponding elevation parameters from Table 2.11.

- Step 8: Random coupling of rays within clusters.

  Couple randomly the departure ray angles $\phi_{n,m}$ to the arrival ray angles $\varphi_{n,m}$ within a cluster n, or within a sub-cluster in the case of two strongest clusters (see Step 11 and Table 2.9). If the elevation angles are supported they are coupled with the same procedure.

- Step 9: Generate the cross polarization power ratios (XPR) κ for each ray m of each cluster n. XPR is log-Normal distributed. Draw XPR values as

$$\kappa_{m,n} = 10^{X/10} \tag{2.20}$$

  where ray index ($m = 1, .., M$), $X \sim N(\sigma, \mu)$ is Gaussian distributed with σ and μ from Table 2.6 for XPR.

Coefficient generation:

- Step 10: Draw the random initial phase $\{\Phi_{n,m}^{vv}, \Phi_{n,m}^{vh}, \Phi_{n,m}^{hv}, \Phi_{n,m}^{hh}\}$ for each ray m of each cluster n. Distribution for the initial phases is $Uni(-\pi, \pi)$. In the LOS case draw also random initial phases $\{\Phi_{LOS}^{vv}, \Phi_{LOS}^{hh}\}$ for both VV and HH polarizations.

- Step 11: Generate the channel coefficients for each cluster n

  - NLOS case:

    * For the $N-2$ weakest clusters:

      The channel coefficients are given by

$$\begin{aligned} H_{u,s,n}(t) &= \sqrt{P_n}\sum_{m=1}^{M} \begin{bmatrix} F_{tx,s,V}(\varphi_{n,m}) \\ F_{tx,s,H}(\varphi_{n,m}) \end{bmatrix}^T \begin{bmatrix} \exp(\jmath\Phi_{n,m}^{vv}) & \sqrt{\kappa_{n,m}}\exp(\jmath\Phi_{n,m}^{vh}) \\ \sqrt{\kappa_{n,m}}\exp(\jmath\Phi_{n,m}^{hv}) & \exp(\jmath\Phi_{n,m}^{hh}) \end{bmatrix} \\ &\quad \cdot \begin{bmatrix} F_{rx,u,V}(\phi_{n,m}) \\ F_{rx,u,H}(\phi_{n,m}) \end{bmatrix} \times \exp(jd_s 2\pi\lambda_0^{-1}\sin(\phi_{n,m})) \times \exp(jd_u 2\pi\lambda_0^{-1}\sin(\varphi_{n,m})) \\ &\quad \times \exp(j2\pi\nu_{n,m}t) \end{aligned} \tag{2.21}$$

      where $F_{rx,u,V}$ and $F_{rx,u,H}$ are the antenna element u filed patterns for vertical and horizontal polarizations respectively, d_s and d_u are uniform distances m (in meters) between transmitter and receiver element respectively, and λ_0 is the wave length on carrier frequency. If polarization is not considered, 2×2 polarization matrix can be replaced by scalar $\exp(j\Phi_{n,m})$ and only vertically polarized field patterns applied.

      · B5 scenarios - Fixed feeder link model:

      The Doppler frequency component $\nu_{n,m}$ is tabulated for the first ray of each cluster. For the other rays $\nu_{n,m} = 0$.

      · Other scenarios:

      The Doppler frequency is calculated from

$$\nu_{m,n} = \frac{\|v\|\cos(\varphi_{n,m} - \theta_v)}{\lambda_0}. \tag{2.22}$$

    * For the 2 strongest clusters:

      The clusters ray are spread in delay to three sub-clusters (per cluster), with

Table 2.9: Sub-cluster Information for Intra Cluster Delay Spread Clusters.

Sub-cluster	mapping to rays	power	delay offset
1	1,2,3,4,5,6,7,8,19,20	10/20	0 ns
2	9,10,11,12,17,18	6/20	5 ns
3	13,14,15,16	4/30	10 ns

fixed delay offset $0, 5, 10ns$ (see Table 2.9). Delays of sub-cluster are

$$\tau_{n,1} = \tau_n + 0ns, \;\; \tau_{n,2} = \tau_n + 5ns, \;\; \tau_{n,3} = \tau_n + 10ns. \tag{2.23}$$

– LOS case: Adding single line of sight ray and scaling down the other channel coefficient generated by (2.21). The channel coefficients are given by

$$\begin{aligned} H_{u,s,n}(t) \;\; = \;\; & \sqrt{\frac{1}{K_R+1}} \times H_{u,s,n}(t)' + \delta(n-1)\sqrt{\frac{1}{K_R+1}} \\ & \times \begin{bmatrix} F_{tx,s,V}(\varphi_{LOS}) \\ F_{tx,s,H}(\varphi_{LOS}) \end{bmatrix}^T \begin{bmatrix} \exp(j\Phi_{LOS}^{vv}) & 0 \\ 0 & \exp(j\Phi_{LOS}^{hh}) \end{bmatrix} \begin{bmatrix} F_{rx,u,V}(\phi_{LOS}) \\ F_{rx,u,H}(\phi_{LOS}) \end{bmatrix} \\ & \times \exp(jd_s 2\pi\lambda_0^{-1}\sin(\phi_{LOS})) \times \exp(jd_u 2\pi\lambda_0^{-1}\sin(\varphi_{LOS})) \\ & \times \exp(j2\pi\nu_{LOS}t) \end{aligned} \tag{2.24}$$

where $H_{u,s,n}(t)'$ is the NLOS channel coefficient from the above step, $\delta(\cdot)$ is the Dirac's delta function, and K_R is the Ricean K-factor defined in Table 2.6 converted to linear scale.

- Step 11*b*: If non-ULA arrays: Generate the channel coefficients for each cluster n

  For arbitrary array configurations on horizontal plane, see Figure 2.4. The distance d_u is replaced by

$$d'_{u,n,m} = \frac{\sqrt{x_u^2 + y_u^2}\cos(\arccos(y_u/x_u) - \varphi_{n,m})}{\sin\varphi_{n,m}} \tag{2.25}$$

  where (x_u, y_u) are co-ordinates of uth element A_u and A_0 is reference element.

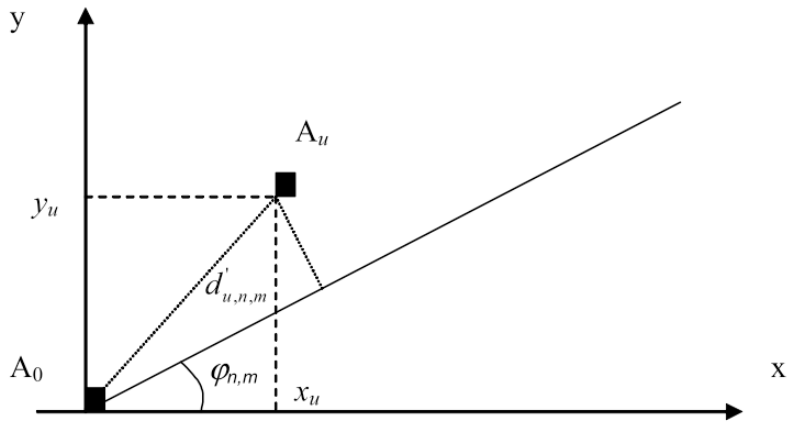

Figure 2.4: Modified distance of antenna element u with non-ULA array. [5]

- Step 11*c*: If the elevation is considered The channel coefficient matrix equation will be written as

$$H_{u,s,n}(t) = \sqrt{P_n}\sum_{m=1}^{M}\begin{bmatrix} F_{tx,s,V}(\varphi_{n,m}) \\ F_{tx,s,H}(\varphi_{n,m}) \end{bmatrix}^T \begin{bmatrix} \exp(j\Phi_{n,m}^{vv}) & \sqrt{\kappa_{n,m}}\exp(j\Phi_{n,m}^{vh}) \\ \sqrt{\kappa_{n,m}}\exp(j\Phi_{n,m}^{hv}) & \exp(j\Phi_{n,m}^{hh}) \end{bmatrix} \cdot \begin{bmatrix} F_{rx,u,V}(\phi_{n,m}) \\ F_{rx,u,H}(\phi_{n,m}) \end{bmatrix} \times \exp(jd_s 2\pi\lambda_0^{-1}\overline{r_s}\overline{\Phi_{n,m}}) \times \exp(jd_u 2\pi\lambda_0^{-1}\overline{r_u}\overline{\Psi_{n,m}}) \times \exp(j2\pi\nu_{n,m}t) \quad (2.26)$$

where scalar product

$$\overline{r}_s \cdot \overline{\Phi}_{n,m} = x_s \cos\gamma_{n,m}\cos\phi_{n,m} + z_s \sin\gamma_{n.m}, \quad (2.27)$$

$\overline{r}_s$ is location vector of Tx array element s, $\overline{\Phi}_{n,m}$ is departure angle unit vector of ray n,m and x_s,y_s and z_s are component of $\overline{r}_s$ to x,y and z-axis respectively. $\phi_{n,m}$ is ray n,m arrival azimuth angle and $\gamma_{n,m}$ is ray n,m arrival elevation angle. $\overline{r}_u \cdot \overline{\Psi}_{n,m}$ is a scalar product of Rx antenna element u and arrival angle n,m. The Doppler component will also be written as

$$\upsilon_{n,m} = \frac{\overline{v}\cdot\overline{\Psi}_{n,m}}{\lambda_0} = \frac{\|v\|\cos\theta_v\cos\gamma n,m\cos\phi n,m + \|v\|\sin\theta_v\cos\gamma n,m\sin\phi n,m}{\lambda_0}. \quad (2.28)$$

- Step 12: Apply the path loss and shadowing for the channel coefficients.

Table 2.10: Far Scatterer Radii and Attenuations for B2 and C3 [5]

Scenario	FS_{min}	FS_{max}	FS_{loss}
B2	150m	500m	4dB/us
C3	300m	1500m	2dB/us

Generation of bad urban channels (B2, C3):

The procedures of bad urban channel realization as modified B1 and C2 NLOS as follows:

- Step 1: Drop five far scatterers within a hexagonal cell, within radius $[FSmin, FSmax]$. For each mobile user determine the closest two far scatters, which are then used for calculating far scatterer cluster parameters. For $FSmin$ and $FSmax$ values see Table 2.10.

- Step 2: For C3 create 20 delays as described for C2 model in section 4.3.2, Step 5. For the shortest 18 delays create a typical urban C2 channel profile (powers and angles) as in section 4.3.2. Similarly, create 16 delays for B1 NLOS, and for the shortest 14 delays create a typical B1 NLOS channel profile as in section 4.3.2. The last two delays in B2 and C3 are assigned for far scatterer clusters.

- Step 3: Create typical urban channel powers P for FS clusters substituting equation of section 4.3.2, Step 6 with $P'_n = 10^{\frac{-Z_n}{10}}$, where $Z_n \sim N(0, \xi)$ is the per cluster shadowing term in dB.

- Step 4: Next create excess delays due to far scatterer clusters as

$$\tau_{excess} = \frac{d_{BS \to FS \to MS} - d_{LOS}}{c}. \tag{2.29}$$

  Attenuate FS clusters as FS_{loss}, given in Table 2.10.

- Step 5: Select directions of departure and arrival for each FS cluster according to far scatterer locations, i.e., corresponding to a single reflection from far scatterer. It is

Table 2.11: Elevation-Related Parameters for Generic Models [5].

Scenarios		A1		A2/B4/C4
		LOS	NLOS	NLOS
Elevation AOD spread(ESD)	μ	0.88	1.06	0.88
	σ	0.31	0.21	0.34
Elevation AoA spread(ESA)	μ	0.94	1.10	1.01
	σ	0.26	0.17	0.43
Cross-Correlations	ESD vs DS	0.5	-0.6	N/A
	ESA vs DS	0.7	-0.1	0.2
	ESA vs SF	-0.1	0.3	0.2
	ESD vs SF	-0.4	0.1	N/A
	ESD vs ESA	0.4	0.5	N/A
Elevation AoD and AoA distrbution		Gaussian		
Cluster ESD		3	3	3
Cluster ESA		3	3	3

worth noticing that depending on the location of the mobile user within the cell the FS clusters may appear also at shorter delays than the maximum C2 or B1 NLOS cluster. In such cases the far scatterers do not necessarily result to increased angular or delay dispersion. Also the actual channel statistics of the bad urban users depend somewhat on the cell size.

2.3.4 Parameter Tables for Generic Models

Table 2.6 provides parameter values corresponding to the WINNER generic channel models. Parameter values related to elevation angles are provided in Table 2.11.

The line-of-sight probability of different scenarios are provided in Table 2.5, except scenarios A2, B2, B4, C2 and C3. Because these scenarios line-of-sight probability is approximated as being zero. The functions are based on relatively limited data sets and/or specific assumptions and approximations regarding the location of obstacles in the direct path, and should therefore not be considered exact.

2.3.5 Path Loss Models

Path loss models have been developed based on results of measurements carried out within WINNER. These models are typically of the form of Equation 2.30, where d is the distance between transmitter and the receiver in meters, f_c is the system frequency in GHz, the parameters A, B, C are decided by different scenarios, and X is an optional, environment-specific term, as follows:

$$PL = A\log(d) + B + C\log(\frac{f_c}{5.0}) + X. \tag{2.30}$$

The models can be applied in the frequency range from 2 to 6 GHz and for different antenna heights, The path-loss models have been summarized in Table 2.12. If the free-space path loss (PL_{free}), that be rewritten as

$$PL_{free} = 20\log(d) + 46.4 + 20\log(\frac{f_c}{5.0}) + X. \tag{2.31}$$

Table 2.12: Summary Table of the Path-Loss Models [5].

Scenarios		Path loss [dB]	Shadow fading std [dB]	Applicability range, antenna height default values
A1	LOS	$A = 18.7, B = 46.8, C = 20$	$\sigma = 3$	$3m < d < 100m$, $h_{BS} = h_{MS} = 1..2.5m$
	NLOS[1)]	$A = 36.8, B = 43.8, C = 20$ and $X = 5(n_w - 1)$ (light walls) or $X = 12(n_w - 1)$ (heavy walls)	$\sigma = 4$	same as A1 LOS, n_w is the number of walls between the BS and the MS ($n_w > 0$ for NLOS)
	NLOS[2)]	$A = 20, B = 46.4, C = 20$, $X = 5n_w$ (light walls) or $X = 12(n_w)$ (heavy walls)	$\sigma = 6$ $\sigma = 8$	same as A1 LOS, n_w is the number of walls between the BS and MS
A2	NLOS	$PL = PL_b + PL_{tw} + PL_{in}$ $PL_b = PL_{Bl}(d_{out} + d_{in})$ $PL_{tw} = 14 + 15(1 - \cos(\theta))^2$ $PL_{in} = 0.5d_{in}$	$\sigma = 7$	n_f is the number of floors $h_{BS} = 3(n_{Fl} - 1) + 2m$ $h_{MS} = 1.5$, see [3]) for explanation
B1	LOS	$A = 22.7, B = 41.0, C = 20$ $PL = 40.0\log(d_l) + 9.45$ $-17.3\log(h'_{BS} \cdot h'_{MS})$ $+2.7\log(f_c/5.0)$	$\sigma = 3$	$10m < d_l < 1000m$, $d'_{BP} < d_l < 5km$, $h_{BS} = 10m, h_{MS} = 1.5m$
	NLOS	$PL = min(PL(d_1, d_2), PL(d_2, d_1))$ where	$\sigma = 4$	$10m < d_1 < 5km$, $w/2 < d_2 < 2km$

Scenarios		Path loss [dB]	Shadow fading std [dB]	Applicability range, antenna height default values
		$PL(d_k, d_l) = PL_{LOS}(d_k) + 20$ $-12.5n_j + 10n_j \log(d_l)$ $+3\log(f_c/5.0)$ and $n_j = max(2.8 - 0.0024d_k, 1.84)$, PL_{LOS} is the path loss LOS scenarios and $k, l \in 1, 2$		$w = 20m$, $h_{BS} = 10m$,$h_{MS} = 1.5m$ When $0 < d_2 < w/2$, the LOS PL is applied.
B2	NLOS	Same as B1.	$\sigma = 4$	
B3	LOS	$A = 13.9, B = 64.4, C = 20$	$\sigma = 3$	$5m < d < 100m$, $h_{BS} = 6m$,$h_{MS} = 1.5m$
	NLOS	$A = 37.8, B = 36.5, C = 23$	$\sigma = 4$	Same as B3 LOS
B4	NLOS	Same as A2, except antenna heights.		$3m < d_{out} + d_{in} < 1000m$, $h_{BS} = 10m$, $h_{MS} = 3(n_{Fl}) + 1.5m$
B5a	LOS	$A = 23.5, B = 42.5, C = 20$	$\sigma = 4$	$30m < d < 8km$, $h_{BS} = 25m$,$h_{MS} = 25m$
B5c	LOS	Same as B1 LOS, except antenna height	$\sigma = 4$	$10m < d < 2000m$, $h_{BS} = 25m$,$h_{MS} = 5m$
B5f	NLOS	$A = 23.5, B = 57.5, C = 23$	$\sigma = 8$	$30m < d < 1.5km$ $h_{BS} = 25m$,$h_{MS} = 1.5m$
C1	LOS	$A = 23.8, B = 41.2, C = 20$	$\sigma = 4$	$30m < d < d_{BP}$
		$PL = 40.0\log(d) + 11.65$ $-16.2\log(h_{BS} \cdot h_{MS}) + 3.8\log(f_c/5)$	$\sigma = 6$	$d_{BP} < d < 5km$ $h_{BS} = 25m$,$h_{MS} = 1.5m$
	NLOS	$PL = (44.9 - 6.55\log(h_{BS}))\log(d)$ $+31.46 + 5.83\log(h_{BS}) + 23\log(f_c/5)$	$\sigma = 8$	$50m < d_{BP} < d < 5km$ $h_{BS} = 25m$,$h_{MS} = 1.5m$
C2	LOS	$A = 26, B = 39, C = 20$	$\sigma = 4$	$10m < d < d^{'}_{BP}$
		$PL = 40\log(d) + 13.47 - 14\log(h^{'}_{BS})$ $-14\log(h^{'}_{MS}) + 6\log(f_c/10)$	$\sigma = 6$	$d^{'}_{BP} < d < 5km$ $h_{BS} = 25m$,$h_{MS} = 1.5m$
	NLOS	$PL = (44.9 - 6.55\log(h_{BS}))\log(d)$ $+34.46 + 5.83\log(h_{BS}) + 23\log(f_c/5)$	$\sigma = 8$	Same as C1 NLOS
C3	NLOS	Same as C2 NLOS		Same as C2 NLOS
C4	NLOS	$PL = PL_{C2}(d_{out} + d_{in}) + 17.4 + 0.5d_{in}$ -0.8_{MS} where PL_{C2} is the path−loss function of C2 LOS/NLOS scenarios	$\sigma = 10$	See[3)] for explanation of Parameter. $h_{BS} = 25m$,$h_{MS} = 1.5m$
D1	LOS	$A = 21.5, B = 44.2, C = 20$	$\sigma = 4$	$30m < d < d_{BP}$
		$PL = 40\log(d) + 10.5 - 18\log(h_{BS})$ $-18.5\log(h_{MS}) + 1.5\log(f_C/10)$	$\sigma = 6$	$d_{BP} < d < 10km$, $h_{BS} = 32m$,$h_{MS} = 1.5m$
	NLOS	$PL = (25.1\log(d)) + 55.4$ $-0.13\log(h_{BS-25})\log(d/100)$	$\sigma = 8$	$h_{BS} = 32m$,$h_{MS} = 1.5m$

Scenarios		Path loss [dB]	Shadow fading std [dB]	Applicability range, antenna height default values
		$-0.9\log(h_{MS}-1.5)+21.3\log(f_c/5)$		
D2a	LOS	Same as D1 LOS		

2.3.6 Clustered Delay Line (CDL) Models

In the CDL model each cluster is composed of 20 rays with fixed offset angles and identical power. In the case of cluster where a ray of dominant power exists, the cluster has 20 + 1 rays. This dominant ray has a zero angle offset. The departure and arrival rays are coupled randomly. The CDL models offer well-defined radio channels with fixed parameters to obtain comparable simulation results with relatively non-complicated channel models. We do not list the CDL tables in this thsis, because there are 20 scenarios tabulated too many tables. However, they are available in [5].

2.4 Autoregressive Model [7]

Autoregressive (AR) models are commonly used to approximate discrete-time random processes. This is due to the simplicity with which their parameters can be computed and due to their correlation matching property. By the way, AR models simulation time is much less than the some sum-of-sinusiods methods (e.g., Jakes models). A complex AR process of order p $[AR(p)]$ can be generated via the time domain recursion

$$X[n] = -\sum_{k=1}^{p} a_k x[n-k] + w[k] \tag{2.32}$$

where $w[n]$ is a complex white Gaussian noise process with uncorrelated real and imaginary components.

Although the Doppler spectrum models proposed for mobile radio are not rational, an arbitrary spectrum can be closely approximated by an AR model of sufficiently large order. The basic relationship between the desired model autocorrelation function (ACF) $R_{xx}[k]$ and

the $AR(p)$ parameters is given by

$$R_{xx}[k] = \begin{cases} -\sum_{m=1}^{p} a_m R_{xx}[k-m], & \text{if } k \geq 1, \\ -\sum_{m=1}^{p} a_m R_{xx}[m] + \sigma_p^2, & \text{if } k = 0. \end{cases}$$

In matrix form this becomes for $k = 1, 2, ..., p$,

$$R_{xx} a = -v \tag{2.33}$$

where

$$\begin{aligned} R_{xx} &= \begin{bmatrix} R_{xx}[0] & R_{xx}[-1] & .... & R_{xx}[-p+1] \\ R_{xx}[1] & R_{xx}[0] & .... & R_{xx}[-p+2] \\ .... & .... & .... & .... \\ R_{xx}[p-1] & R_{xx}[p-2] & .... & R_{xx}[0] \end{bmatrix}, \\ a &= \begin{bmatrix} a_1 & a_2 & .... & a_p \end{bmatrix}^T, \\ v &= \begin{bmatrix} R_{xx}[1] & R_{xx}[2] & .... & R_{xx}[p] \end{bmatrix}^T, \end{aligned} \tag{2.34}$$

and

$$\sigma_p^2 = R_{xx}[0] + \sum_{k=1}^{p} a_k R_{xx}[-k]. \tag{2.35}$$

So if the inverse R_{xx}^{-1} exists and the AR filter coefficients can thus be determined by $a = -R_{xx}^{-1} v$. The generated AR(p) process has the ACF

$$R_{xx}[k] = \begin{cases} R_{xx}[k], & \text{if } k \geq 1, \\ -\sum_{m=1}^{p} a_m \widehat{R}_{xx}[k-m], & \text{if } k \geq p. \end{cases}$$

That is, the simulated process has the attractive property that its sampled ACF perfectly matches the desired sampled ACF up to lag p. The remaining ACF extension is characterized by the property that the generated time series is the most random one (maximum entropy) which has the assigned first $p+1$ ACF lags.

Chapter 3

Channel Simulation Methods

According to the introduction in the last chapter, we realize that to generate WINNER channel coefficients would need to store many parameter tables and use a lot of additions and multiplications. It costs a lot of simulation time, and is hard to implement the WINNER channel model to our DSP board. So we analyze the WINNER channel model characteristics and use some methods in order to reduce the computational complexity and the memory requirement.

In this chapter, we introduce some methods to reduce the channel simulation complex, which taking some known sample to approximate the other unknown sample using different approximation technique. Final, we take autoregressive methods to discuss with WINNER2 channel characteristic, in order to be convenient to implement WINNER channel on DSP board in the future.

3.1 Polynomial Interpolation

In this section, we first introduce how we want to implement interpolation technique on our system, and we list three methods going to reduce the channel simulation complex on DSP board.

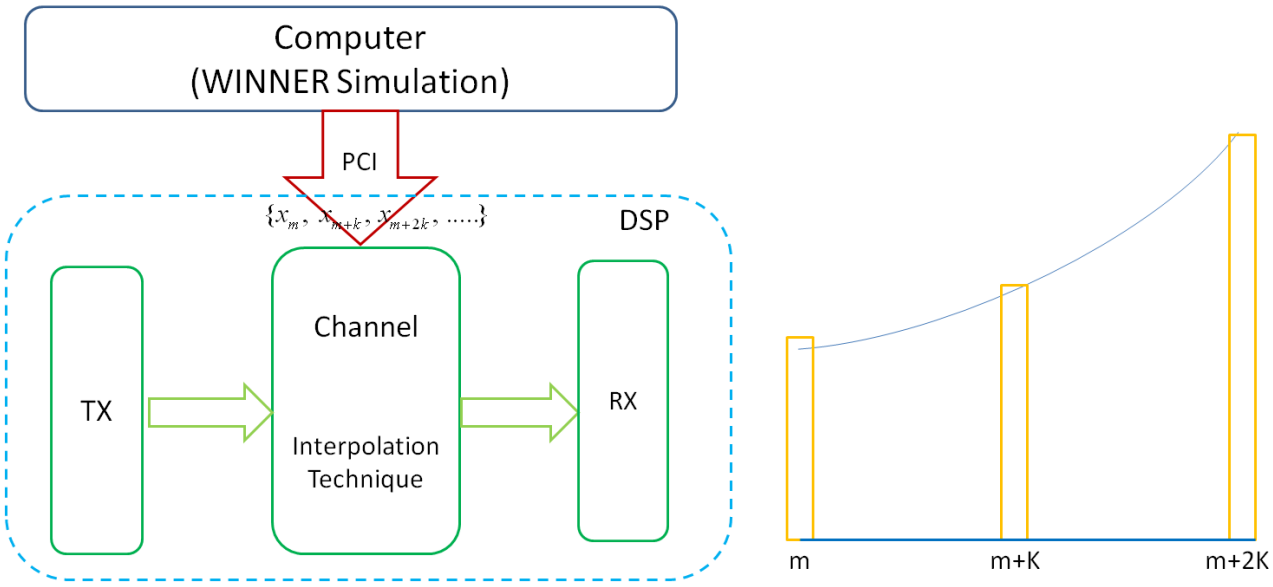

Figure 3.1: Implement interpolation technique on our system and interpolation technique diagram.

3.1.1 Motivation

Because it is very difficult to implement WINNER channel model on our DSP system, the generation process cost a lot of memory requirement and computational complexity. We consider the WINNER channel coefficients generated by computer be transmitted to DSP board through PCI bus. The left figure in Fig. 3.1 is the our system diagram. But we also want to reduce the transmitting number and increase throughput, we transmit $\{m, m+K, m+2K, ...\}$ channel coefficients form computer to DSP, and use interpolation technique to approximate the other channel coefficients, where m is the first transmitting symbol and K is the number interval for next transmitting symbol. The right figure in Fig. 3.1 is the simple interpolation diagram.

According to Fig. 3.2, we realize the DSP internal transmitting data rate and PCI bus between computer and DSP data rate. In general, we usually use the PCI-X edition, so its data rate could be above 500 MBytes/sec. And if we consider the $K = 10$ interpolation case, the the throughput of transmitting channel coefficients through PCI bus could be reach ten time. Then it could be enough to match for the DSP data rate (1 GBytes/sec).

標準	位元	時脈	傳輸速度（雙向）
PCI 2.3	32 Bit	33 MHz	133 MB/sec
PCI 2.3	32 Bit	66 MHz	266 MB/sec
PCI 64	64 Bit	33 MHz	266 MB/sec
PCI 64	64 Bit	66 MHz	533 MB/sec
PCI-X 1.0	64 Bit	66 MHz	533 MB/sec
PCI-X 1.0	64 Bit	100 MHz	800 MB/sec
PCI-X 1.0	64 Bit	133 MHz	1066 MB/sec
PCI-X 2.0 (DDR)	64 Bit	133 MHz	2132 MB/sec
PCI-X 2.0 (QDR)	64 Bit	133 MHz	4264 MB/sec
PCI-Express	1 Lines 8 Bit	2.5 GHz	512 MB/sec
PCI-Express	2 Lines 8 Bit	2.5 GHz	1 GB/sec
PCI-Express	4 Lines 8 Bit	2.5 GHz	2 GB/sec
PCI-Express	8 Lines 8 Bit	2.5 GHz	4 GB/sec
PCI-Express	16 Lines 8 Bit	2.5 GHz	8 GB/sec

Feature	C6416T
DMA / McBSP / Timer	64/3/3
On-chip memory	1056k bytes
Speed	1GHz
Others	UTOPIA Viterbi and Turbo decoders

Figure 3.2: Transmitting data rate for Computer PCI bus [8] and DSP [9].

3.1.2 Linear Interpolation

Linear interpolation is a commonly considered scheme to its low complexity. It does the interpolation between two known data. Linear interpolation is given by

$$H(m+k) = H(m) + [H(m+K) - H(m)]\frac{k}{K} \tag{3.1}$$

where $H(m)$ and $H(m+K)$ are known sample, $H(m+k)(k = 1, 2, \ldots, L-1)$ are approximation sample and K is sampling period.

3.1.3 Second-Order Polynomial Interpolation

Consider more accuracy of channel approximation, we take the three known sample coefficients to generate two order polynomial. The two order polynomial is given by

$$H(m+k) = H(m) + a \cdot k + b \cdot k^2 \tag{3.2}$$

where K is sampling period, $k = 1, 2, \ldots, K-1$, and the parameters of polynomial are given by

$$\begin{aligned} a &= \frac{-H(m+2K) + 4H(m+K) + 3H(m)}{2K}, \\ b &= \frac{H(m+2K) - 2H(m+K) + H(m)}{2K^2}. \end{aligned} \tag{3.3}$$

3.1.4 Third-Order Polynomial Interpolation

If we want to get the more approximation accuracy than two order polynomial, we can use the three order polynomial to approximate. On the other hand, we must use four known data to generate the polynomial, and the more multiplication and addition. The three order polynomial is given by

$$H(m+k) = H(m) + a \cdot k + b \cdot k^2 + c \cdot k^3 \tag{3.4}$$

where K is sampling period, $k = 1, 2, .., K-1$, and the parameters of polynomial are given by

$$\begin{aligned} a &= \frac{2H(m+3K) - 9H(m+2K) + 18h(m+K) - 11H(m)}{6K}, \\ b &= \frac{-H(m+3K) + 4H(m+2K) - 5H(m+K) + 2H(m)}{2K^2}, \\ c &= \frac{H(m+K) - 3H(m+2K) + 3H(m+K) - H(m)}{6K^3}. \end{aligned} \tag{3.5}$$

3.1.5 Simulation

Simulation Environment [1]

In this chapter simulation, we use the public MATLAB code [1], and the Fig. 3.3 is the block diagram of high-level WIM implementation structure. The main channel transmitting

Table 3.1: General Channel Model Parameters, Common for All Links .

Parameters	Definition	Value	Unit
CenterFrequency	The carrier center frequency	3e9	Hz
SampleDensity	Over-sampling factor, number of time samples per half wavelength	-	-
NumTimeSamples	Number of time samples	200000	
FixedPdpUsed	If yes the power and delay parameters taken from the CDL parameter tables otherwise are random variables	no	
FixedAnglesUsed	the definded as same as FixedPdpUsed	no	
PathLossModelUsed	PathLoss Model is used or not	no	
ShadowingModelUsed	Shadowing Model is used or not	no	
RandomSeed	Sets random seed for Matlab random number generators The default value is empty	111	

parameters setting is in wim.m, and the antenna filed patterns parameters is in the ArrayResponse.m. In the generate-bulk-par.m and wim-core.m is the WINNER modeling process to to generate the WINNER channel coefficients according to chapter 2.3.3. If we want to simulate the path loss channel condition, its coefficients were generated from pathloss.m.

This structure is assumed that the user mobility model, which is not specified in [5] is external to the channel matrix generation routine. The path loss model is also implemented as a separate user-supplied function. The default path loss function, complying with [5], is pathloss.m. Interpolation of antenna field patterns is also required since AoD/AoAs can be any values over (−180,180) degrees.

Simulation Parameter [1]

In the MATLAB code, there are a lot of parameter needed to be set by user. Theose parameter defult values and definition were tabling in [1]. Now, we only list usual parameters and our setting value in Tab. 3.1.

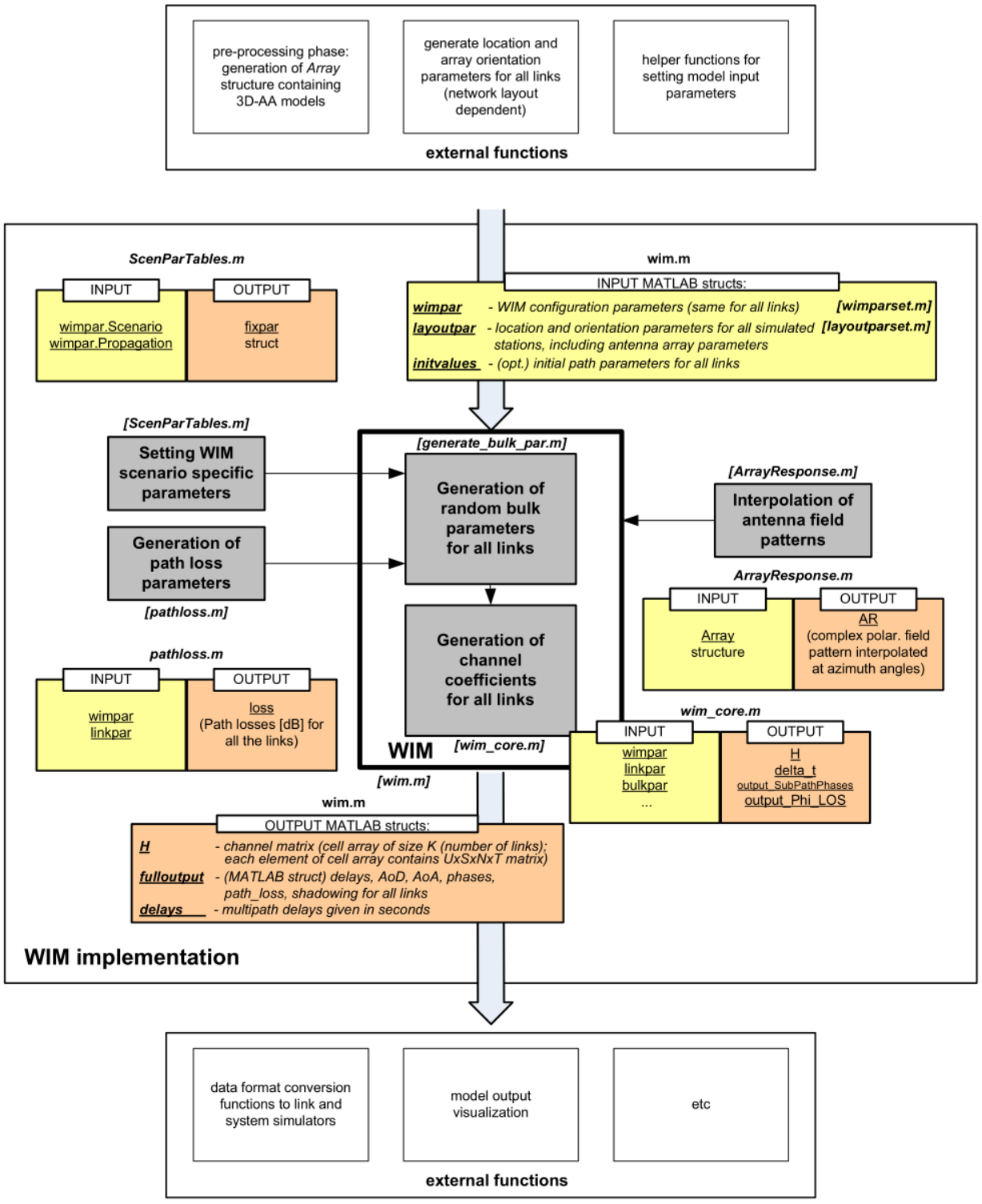

Figure 3.3: High-level description of the WIM computation. The actual WIM model is in the box labeled WIM [1].

Simulation Result

In the cases of comparing different approximation methods, we simulate 20000 samples and take the $\{1, 11, 21, ...\}$ known samples to approximate the other samples. Figures 3.4 to 3.8 shows the approximation performance in usual micro-cell and macro-cell scenarios. Obvious, we can see that the three order polynomial has the best performance on following simulation result, and the two order polynomial performs better than linear interpolation.

The X-label of the Figs. 3.4 to 3.8 is sampling destiny (SampleDensity in Tab. 3.1) which is the oversampling factor that number of time samples per half wavelength, and also equal to $1/\{2f_m \cdot \tau\}$ where f_m is Doppler frequency and τ is sample period. Y-label is mean-square error (MSE) using different technique approximate unknown channel coefficients.

Next, we use the {tic,toc} of MATLAB function to compute the simulation time. By the way, we use MATLAB 7.5.0 (R2007b) edition tool to simulate, if using backward MATLAB edition tool, the simulation time may be different. Form Fig. 3.9, we can see the original simulation time of 200000 samples is 97.175 seconds and we can reduce the simulation time to 90% by using the approximation methods. Fig. 3.10 is the approximation simulation time except the generation WINNER II channel coefficients, and We can see the approximation method of third-order polynomial cost the most time to simulate, and the second-order polynomial method simulation time is closely to linear-interpolation method. So we can make a conclusion that if we do not care about simulation time a lot, third-order polynomial approximation is the best choice for the above approximation methods. But if we care, the second-order polynomial method is the better choice than others, it does not cost much more simulation time than linear-interpolation and its performance of MSE is below linear-interpolation above 10 dB.

3.2 Autoregressive Technique

In this section, we use autoregressive technique to discuss with WINNER channel characteristic, and it could help us to apply WINNER channel and AR technique to DSP

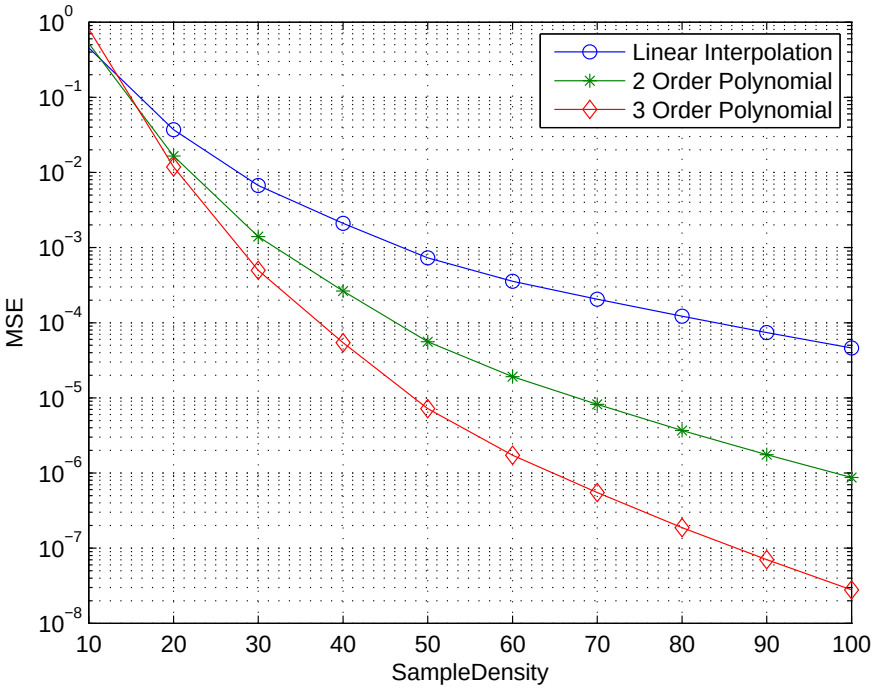

Figure 3.4: MSE for WINNER II Typical Urban micro-cell (B1).

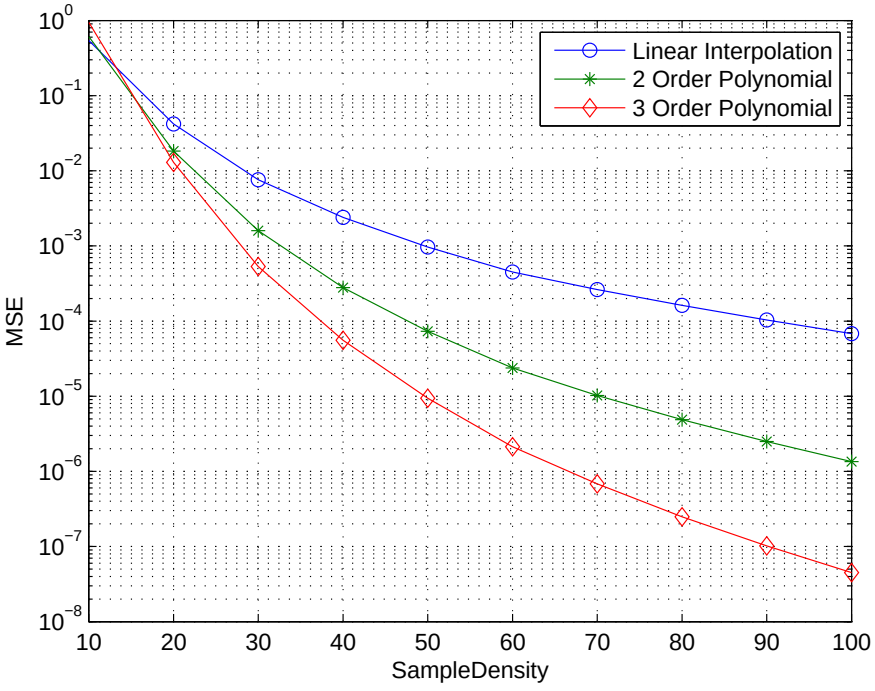

Figure 3.5: MSE for WINNER II Bad Urban micro-cell (B2).

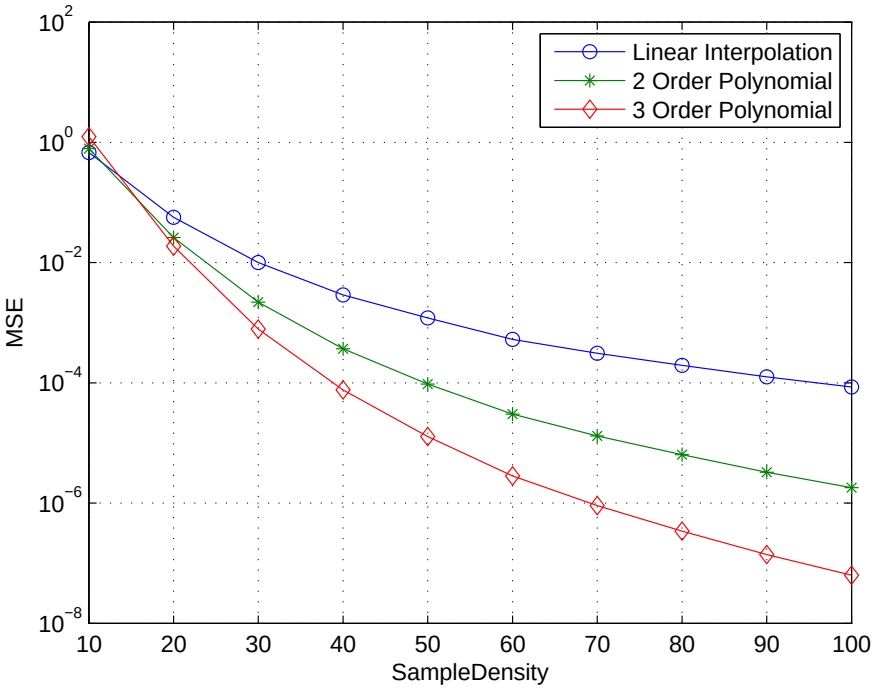

Figure 3.6: MSE for WINNER II Suburban macro-cell (C1).

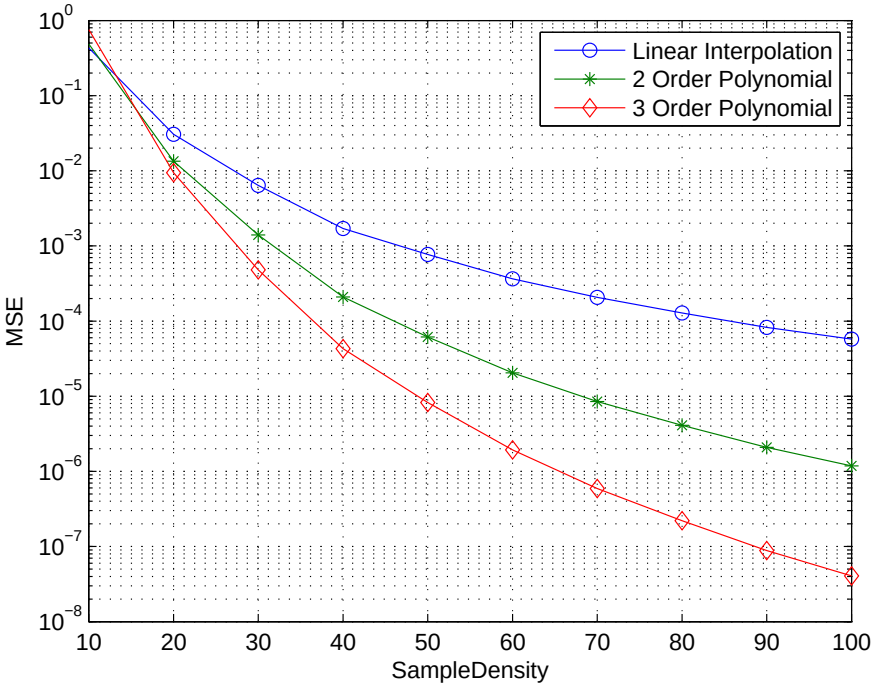

Figure 3.7: MSE for WINNER II Typical Urban macro-cell (C2).

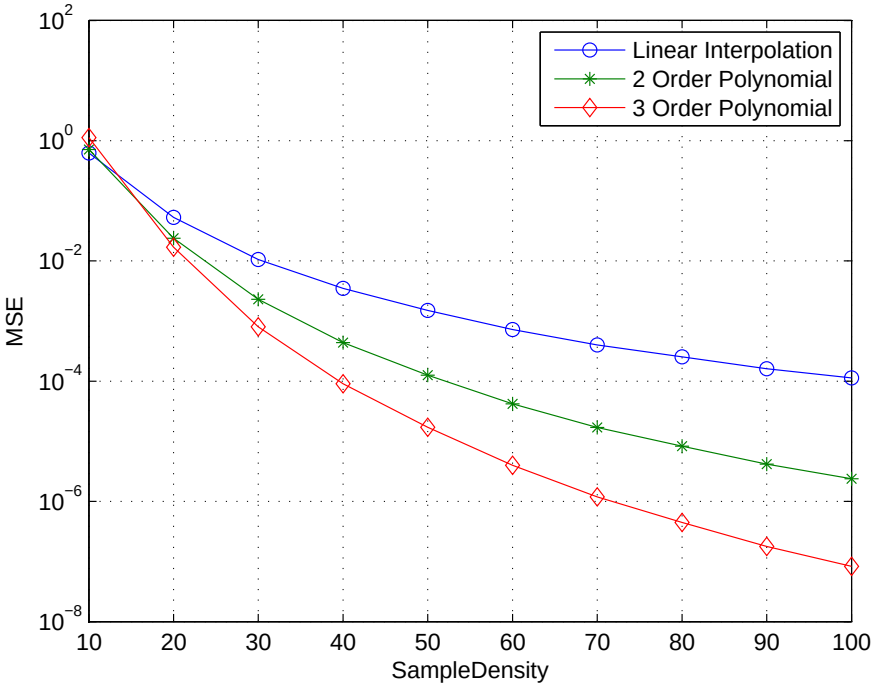

Figure 3.8: MSE for WINNER II Bad Urban macro-cell (C3).

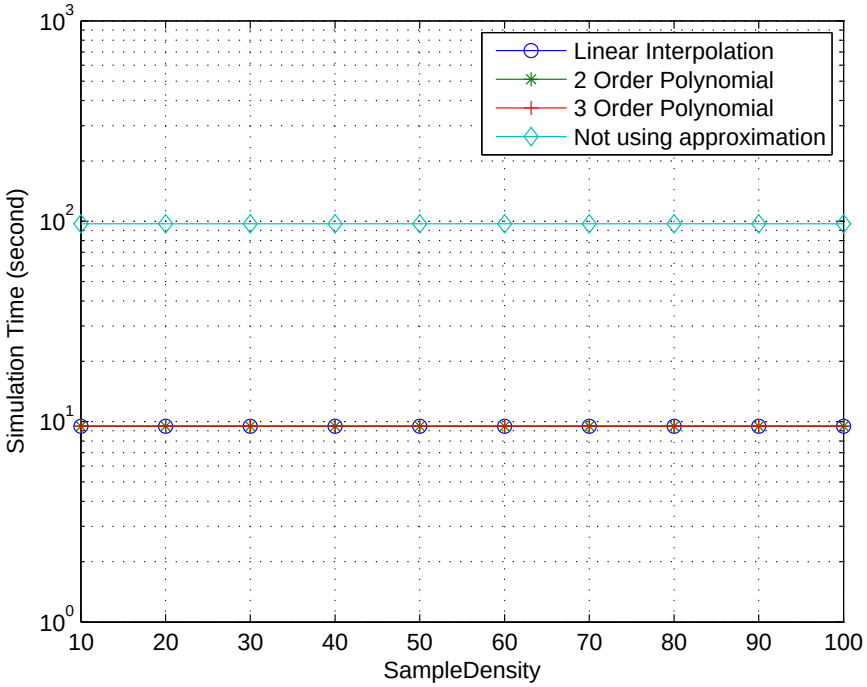

Figure 3.9: Simulation time for different approximation methods and not using approximation method.

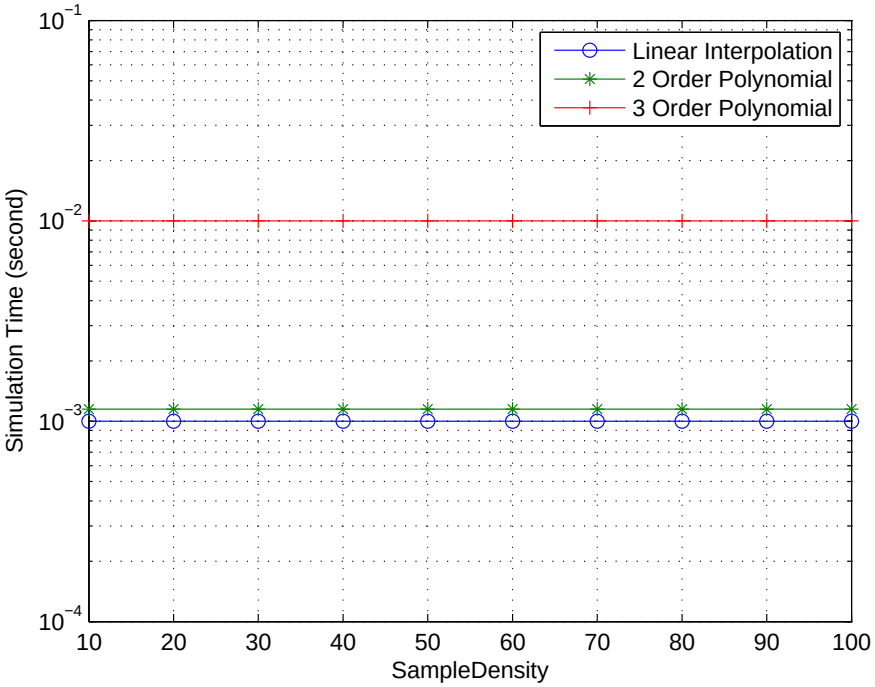

Figure 3.10: Simulation time for different sample destiny.

board.

3.2.1 Motivation

In this part, we introduced how we implement AR technique on our DSP board system on future. As same as polynomial interpolation to reduce the WINNER channel simulation complex, we also try to use AR technique reduced computational complex base on analyzing auto-correlation between WINNER channel coefficients. Fig. 3.11 is our AR implementation system, AR parameters were generated on computer and transmitted from computer to DSP board through PCI bus. On future, We could use some AR parameter, random number generator, and a few additions and multiplications to implement WINNER channel model.

3.2.2 Channel Response Distribution

We use the MATLAB function "normplot" to analyze the WINNER channel coefficients generated by publication MATLAB code from [1]. The normplot MATLAB function displays

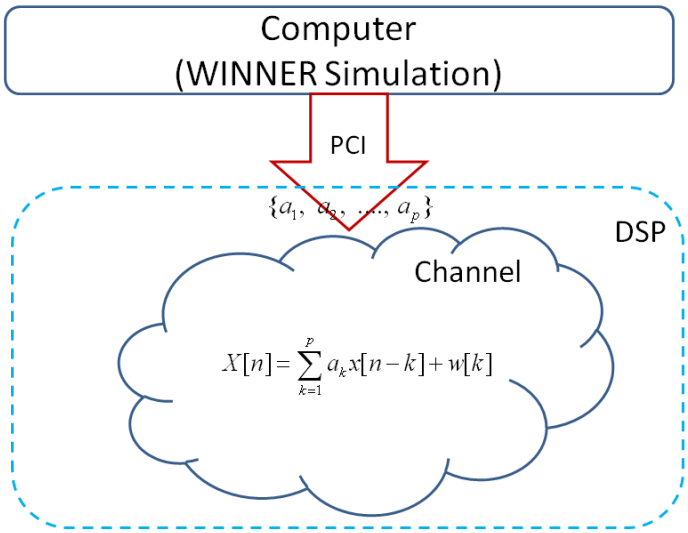

Figure 3.11: Implement AR technique on our system.

a normal probability figure for input data, and if input data closely to Gaussian distribution will be plotted lines.

In the following simulation case as same as before, we use CDL model and take 200000 samples to analyze in usual micro-cell and macro-cell scenarios. Figs. 3.12 to Fig. 3.16 are simulation results for analyze WINNER coefficients of micro-cell and macro-cell scenarios. Obvious, we can see that the WINNER channel coefficients are closely to Gaussian distribution.

3.2.3 Autoregressive Approximation Error Analyze

In this section, we analyze the error of auto-regressive method approximate WINNER channel coefficients.

Approximation Error Distribution

If we could prove the auto-regressive approximation error process $w[n]$ of the following auto-regressive model is a complex white Gaussian noise process with uncorrelated real and imaginary components:

$$X[n] = -\sum_{k=1}^{p} a_k x[n-k] + w[k]. \tag{3.6}$$

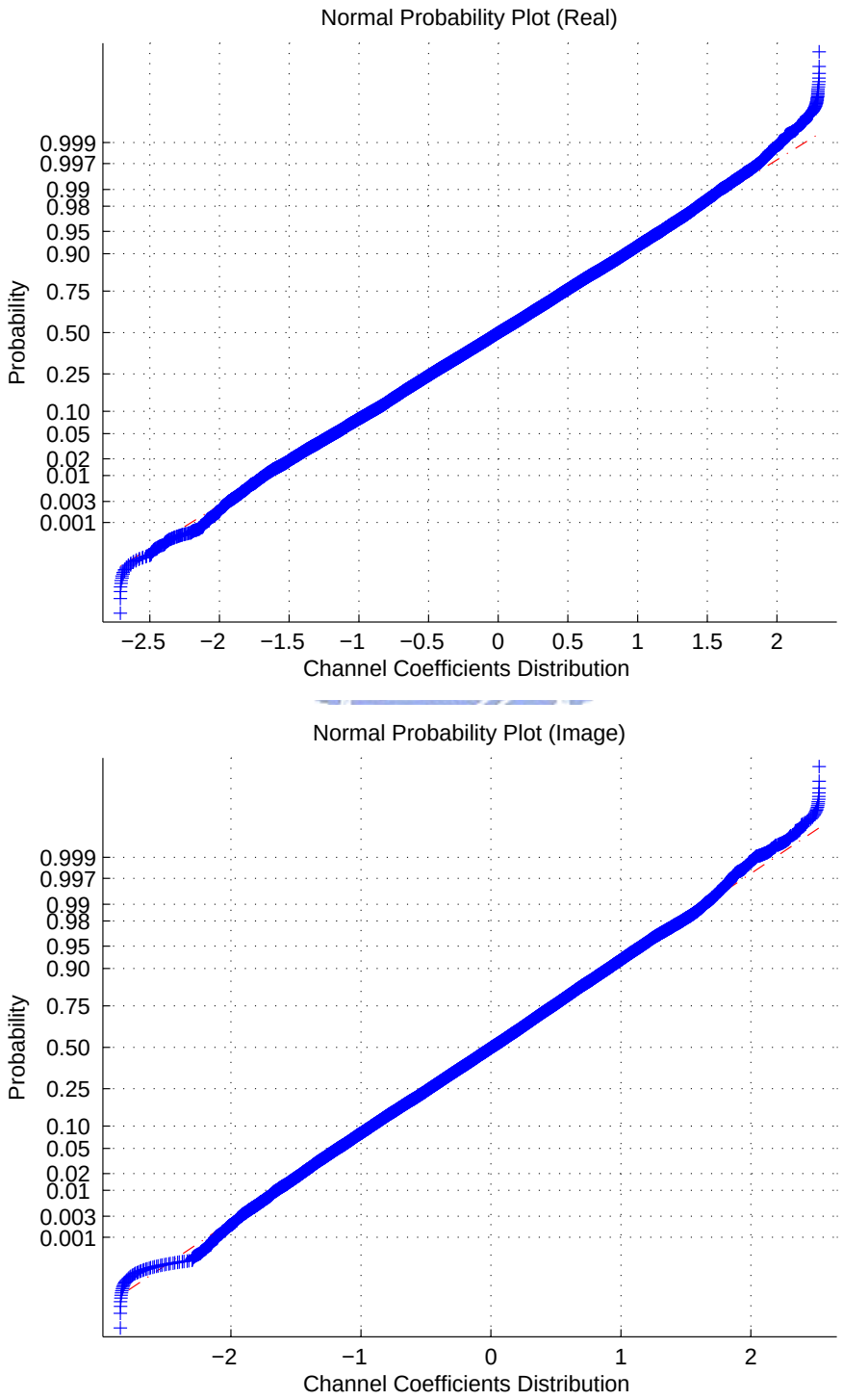

Figure 3.12: NormPlot for WINNER B1 path1 real part channel response and image part channel response.

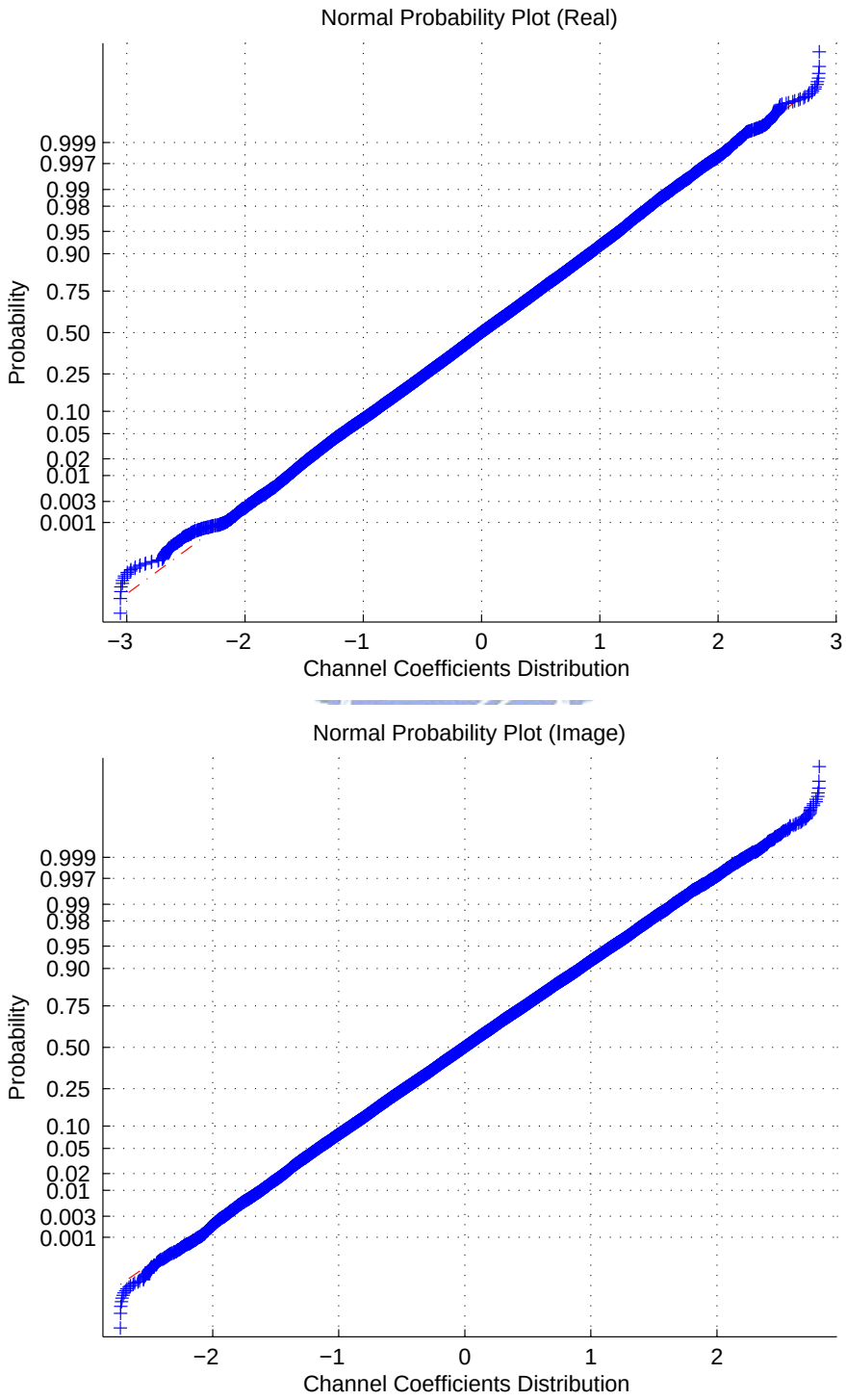

Figure 3.13: NormPlot for WINNER B2 path1 real part channel response and image part channel response.

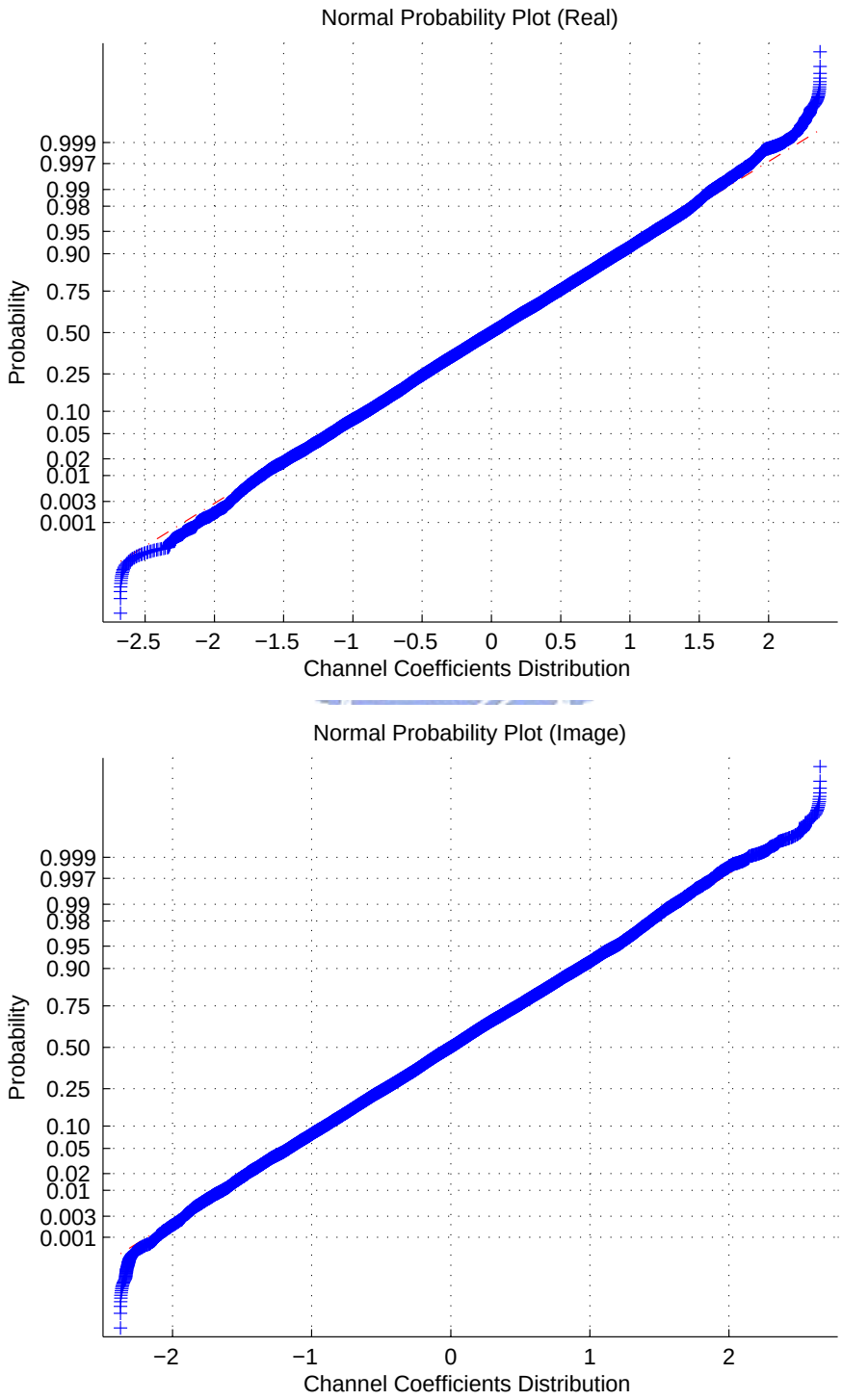

Figure 3.14: NormPlot for WINNER C1 path1 real part channel response and image part channel response.

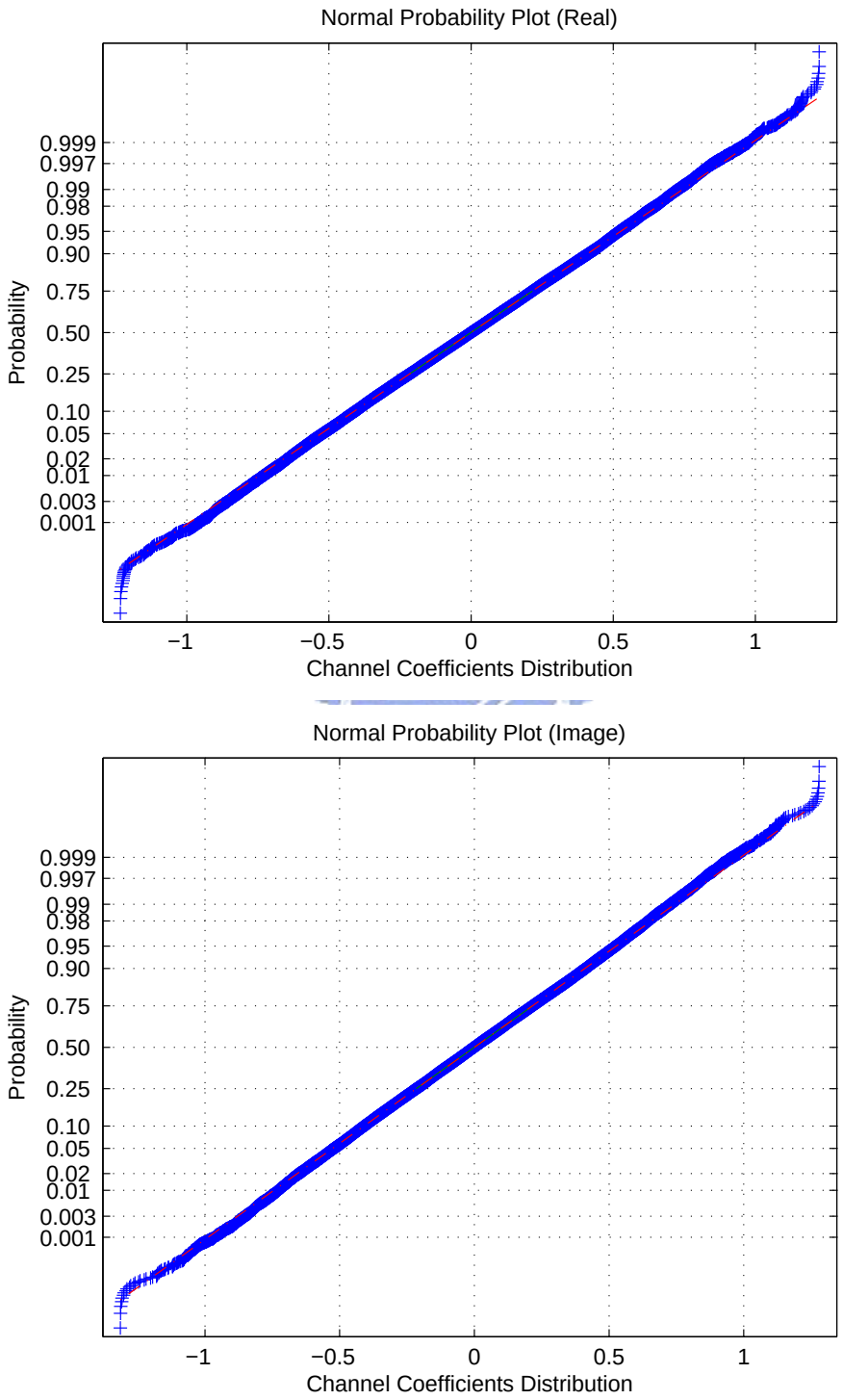

Figure 3.15: NormPlot for WINNER C2 path1 real part channel response and image part channel response.

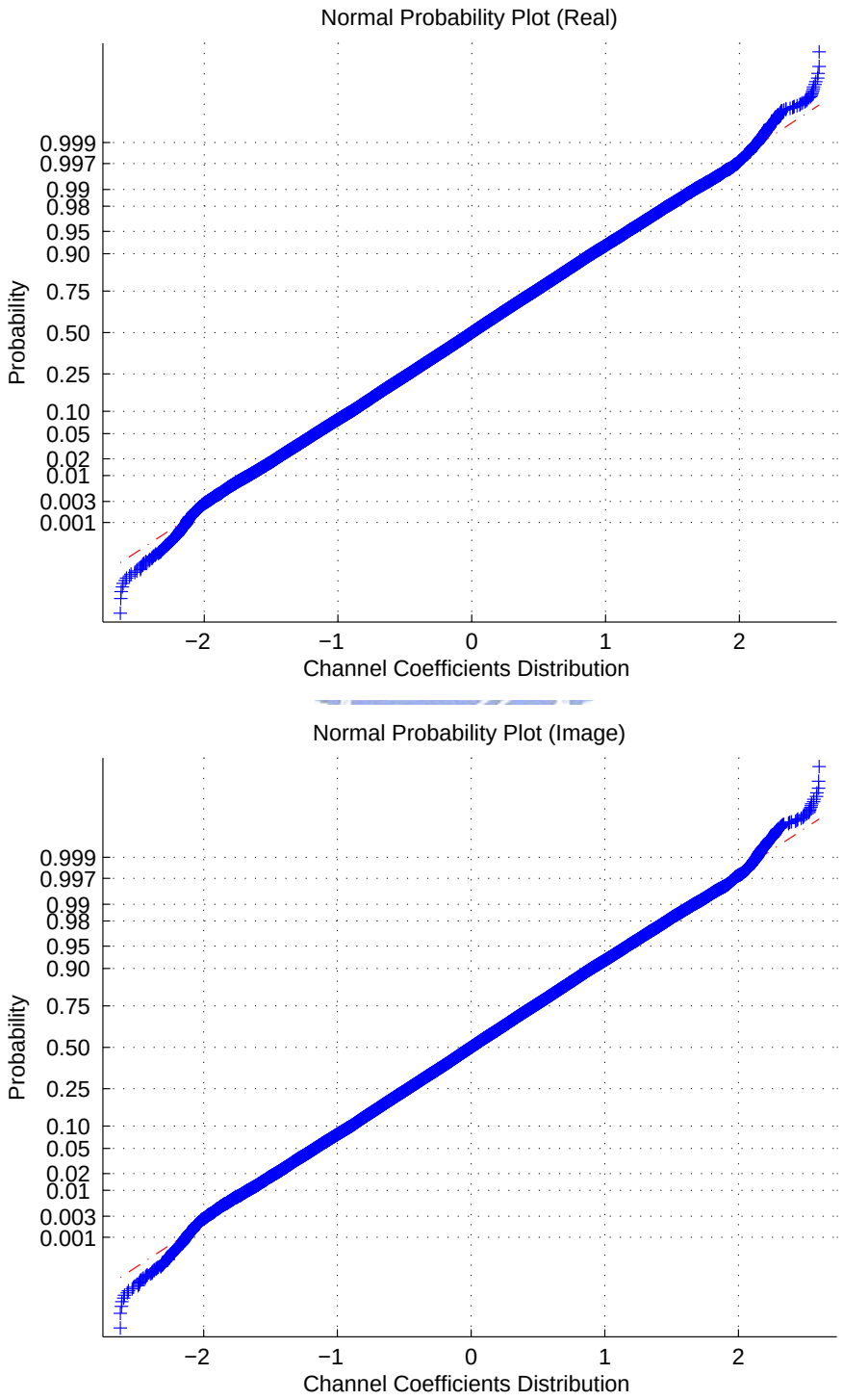

Figure 3.16: NormPlot for WINNER C3 path1 real part channel response and image part channel response.

Then we would not transmit the noise process from PC computer to DSP board, and only need random number generator on DSP board to simulate this noise process reducing computational complex. Figs. 3.17 to 3.21 are simulation results for the five usual scenarios typical urban micro-cell, bad urban micro-cell, suburban, typical urban macro-cell and bad Urban macro-cell defined in [5]. We can see the line of simulate points are closely to the dashed line interval between probability 0.01 and 0.99, even some scenarios case interval between 0.001 and 0.999. So we could make a conclusion that the the error process using auto-regressive method to approximate WINNER channel coefficients is a complex white Gaussian noise process.

Approximation Error Verification

According to the (2.33), the the variance of the driving process is

$$\begin{aligned} \sigma_p^2 &= R_{xx}[0] + \sum_{k=1}^{p} a_k R_{xx}[-k] \\ &= R_{xx}[0] - v^H Rxx^{-1} v \\ &= 1 + v^H a. \end{aligned} \tag{3.7}$$

We use the WINNER channel coefficients generated by publication MATLAB code to calculate the AR process parameter and approximate WINNER coefficients processes. According those approximation error and above equation, to verify our approximate is accuracy.

The Figs.3.22 to 3.26 are simulation results that we test five different scenarios approximation accuracy. In the case between 10 and 100 AR model order, we can see that the variance of error process line calculated by AR approximate WINNER channel coefficients as same as the other generated from above equation. In the other case for 100 to 1000 AR model order, 0.5 percentage error could be tolerated in 1000 AR model order between MSE and theory value. So the AR technique can approximate the WINNER channel coefficients well.

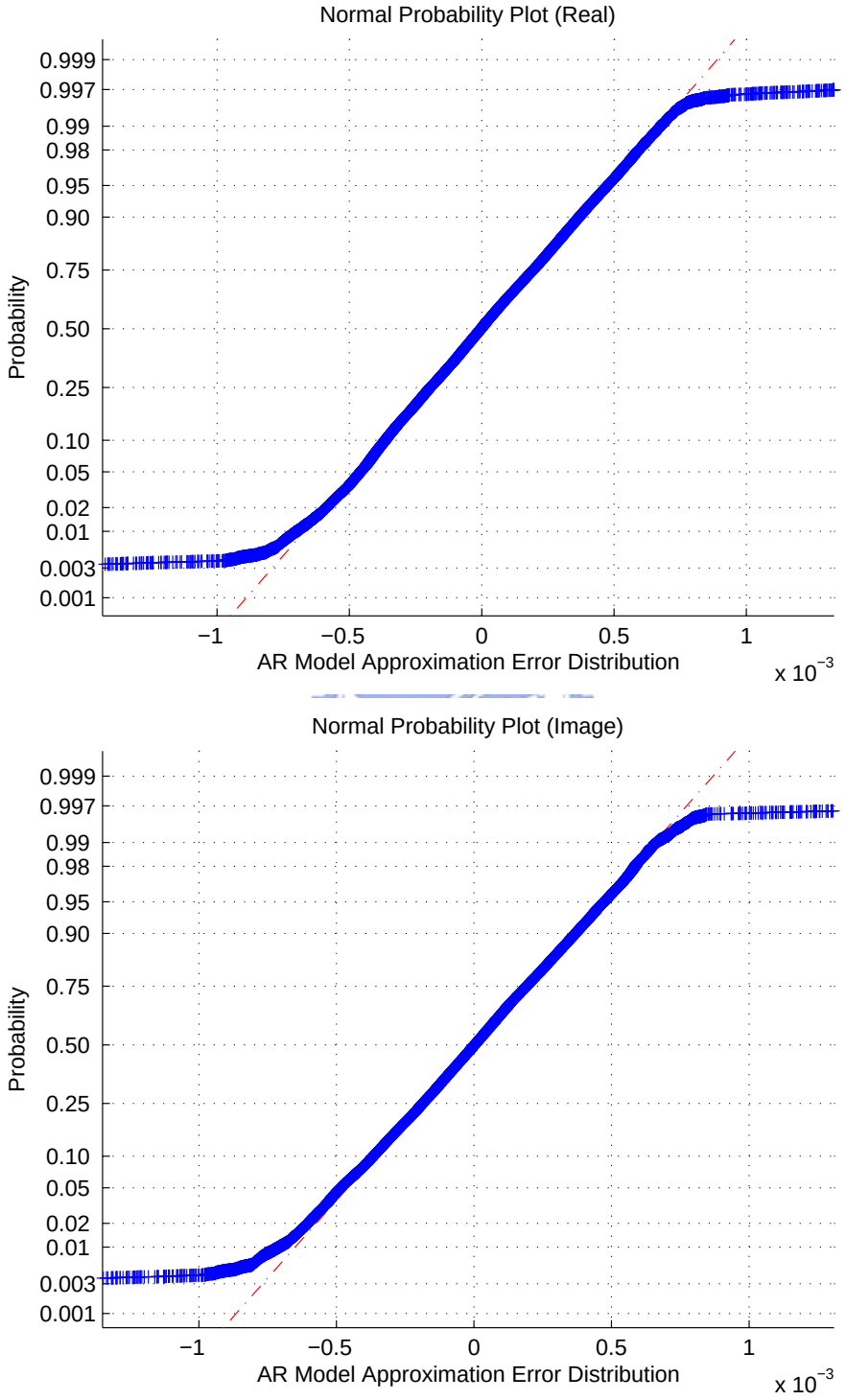

Figure 3.17: NormPlot B1 path1 for AR approximation error of real part and image part.

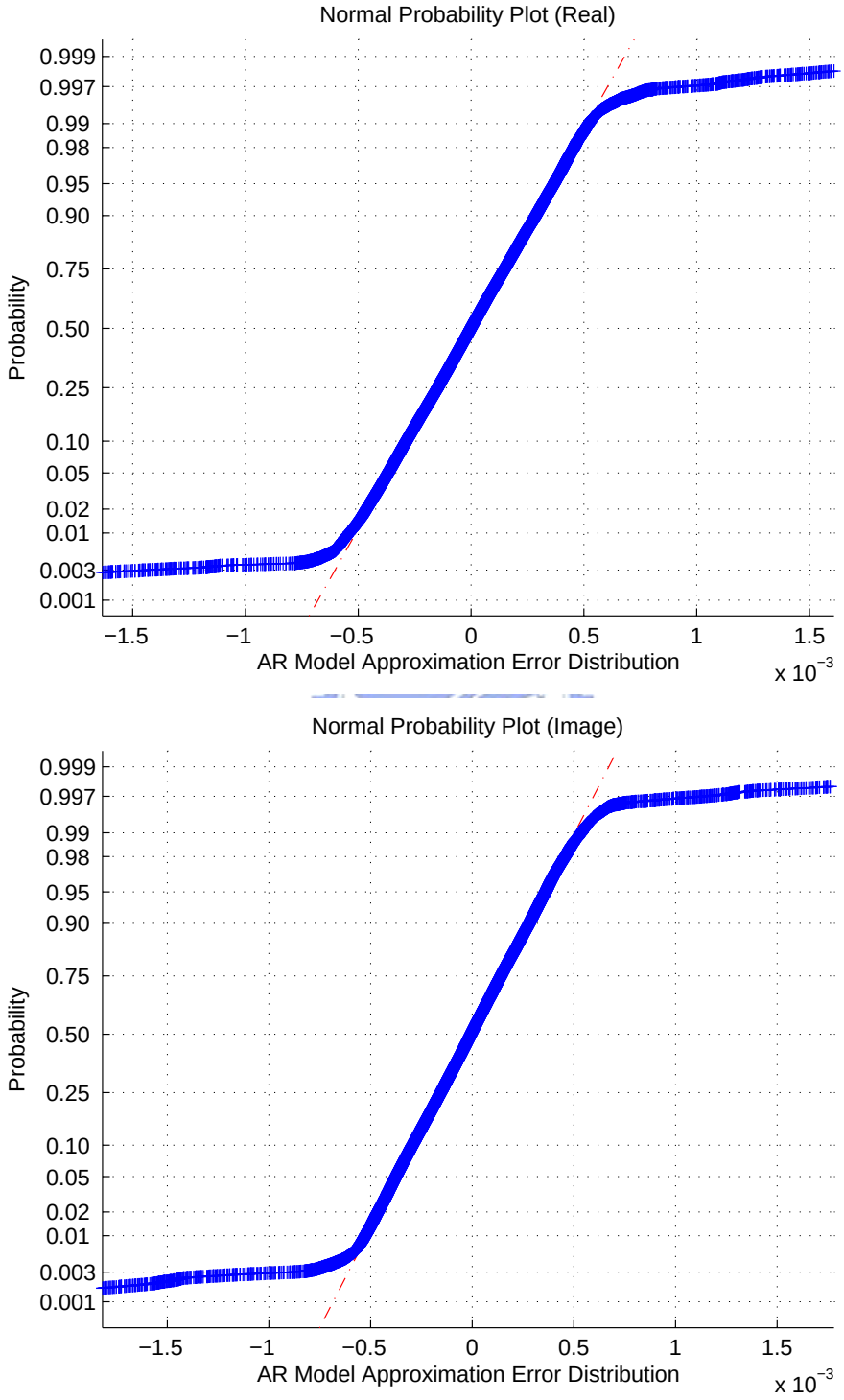

Figure 3.18: NormPlot B2 path1 for AR approximation error of real part and image part.

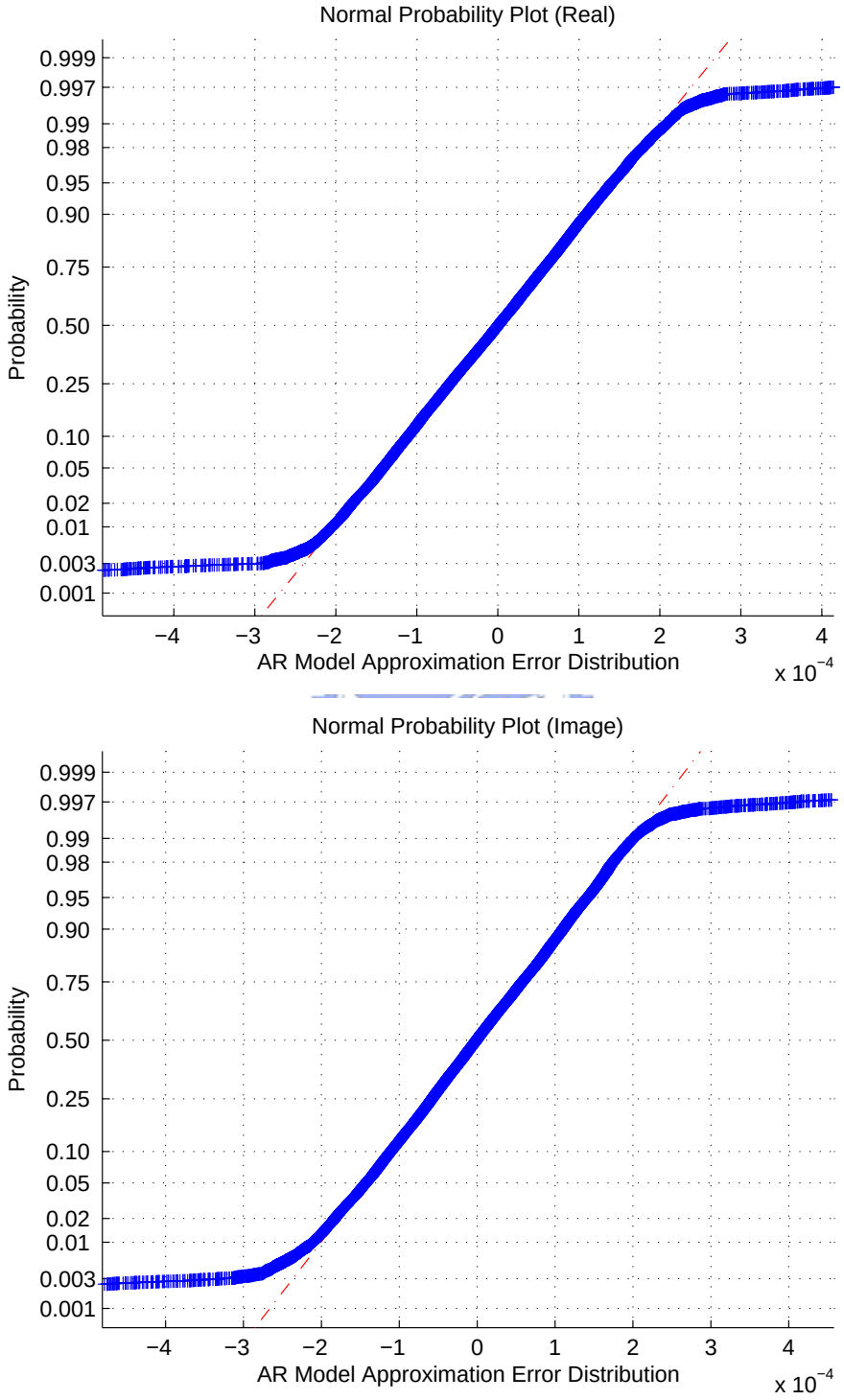

Figure 3.19: NormPlot C1 path1 for AR approximation error of real part and image part.

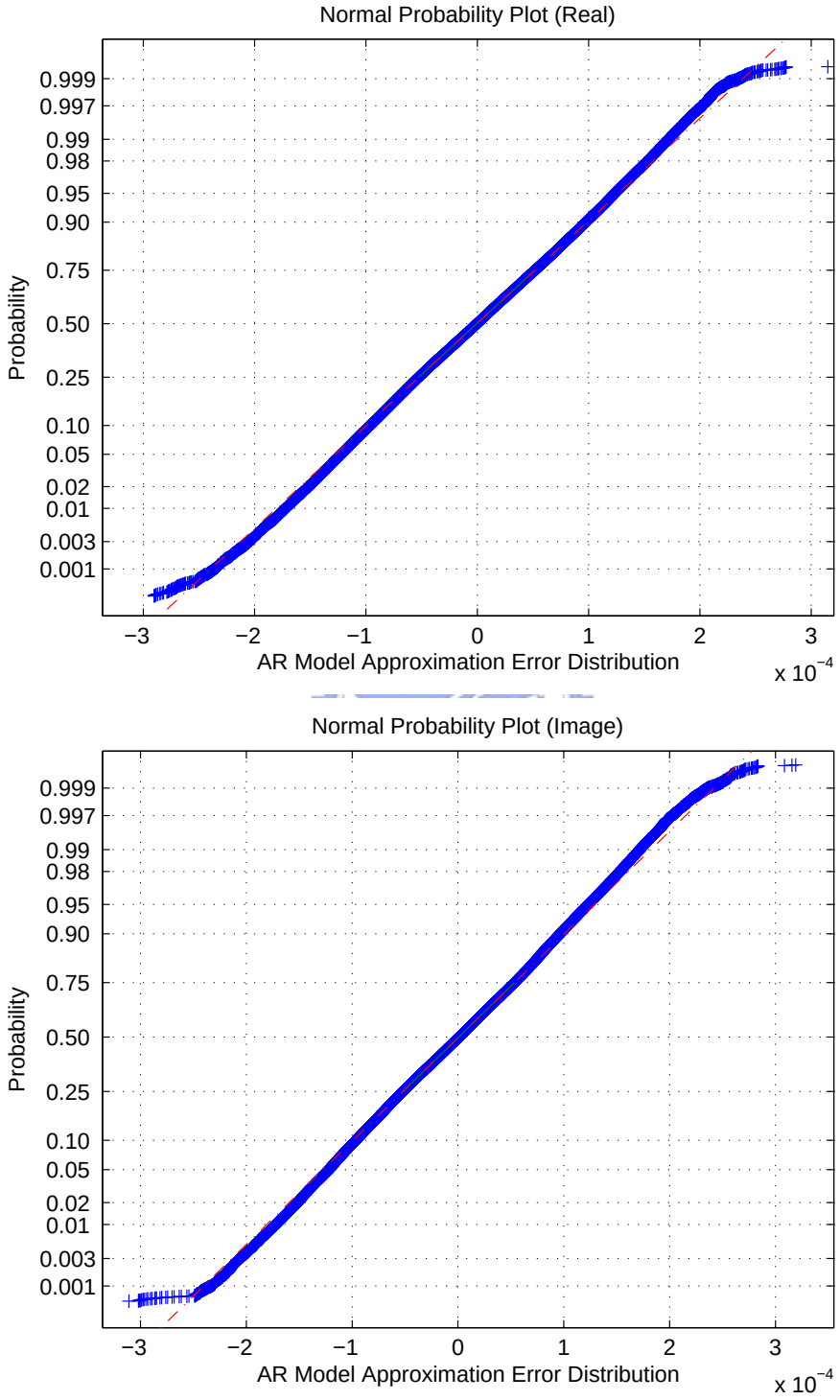

Figure 3.20: NormPlot C2 path1 for AR approximation error of real part and image part.

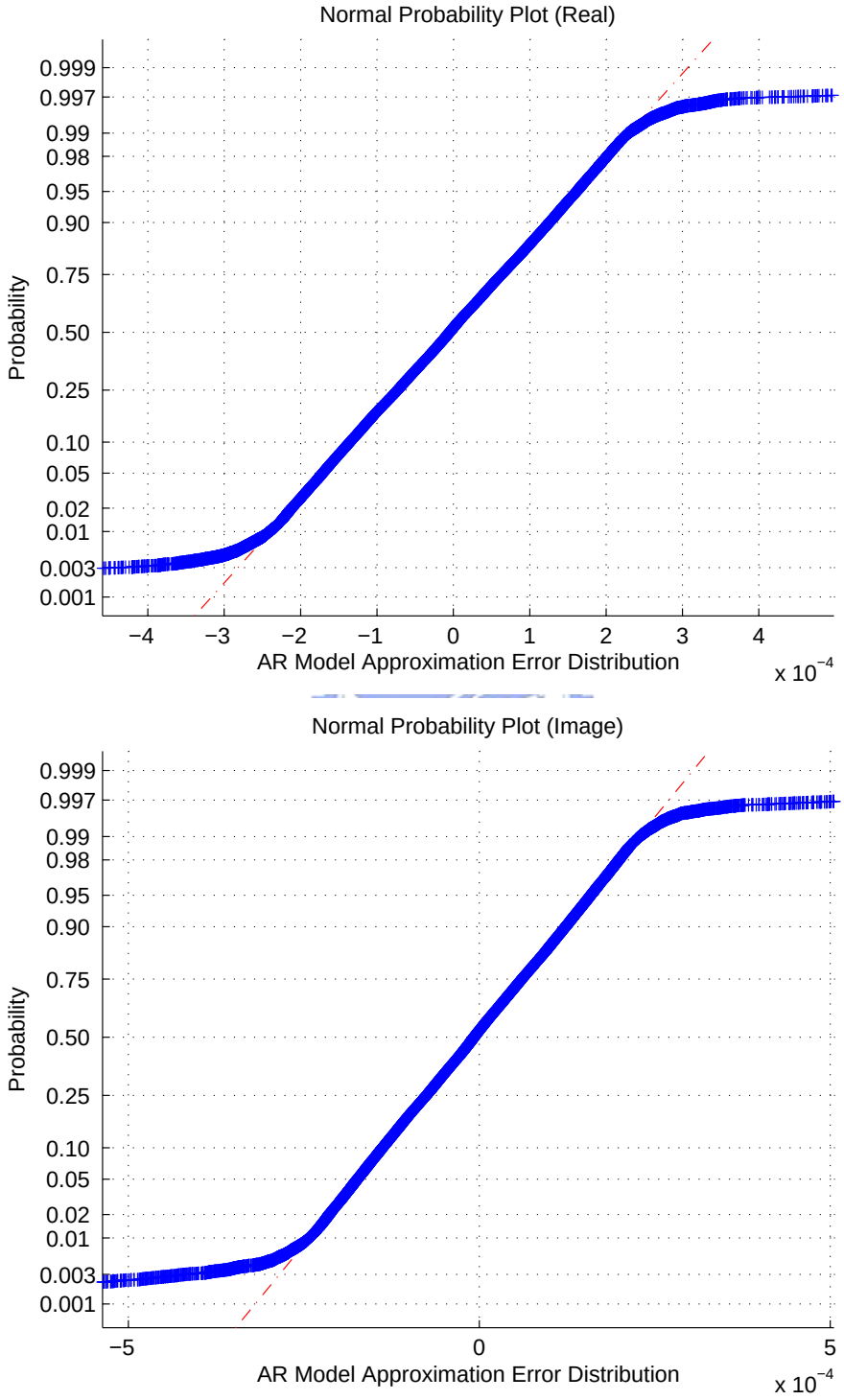

Figure 3.21: NormPlot C3 path1 for AR approximation error of real part and image part.

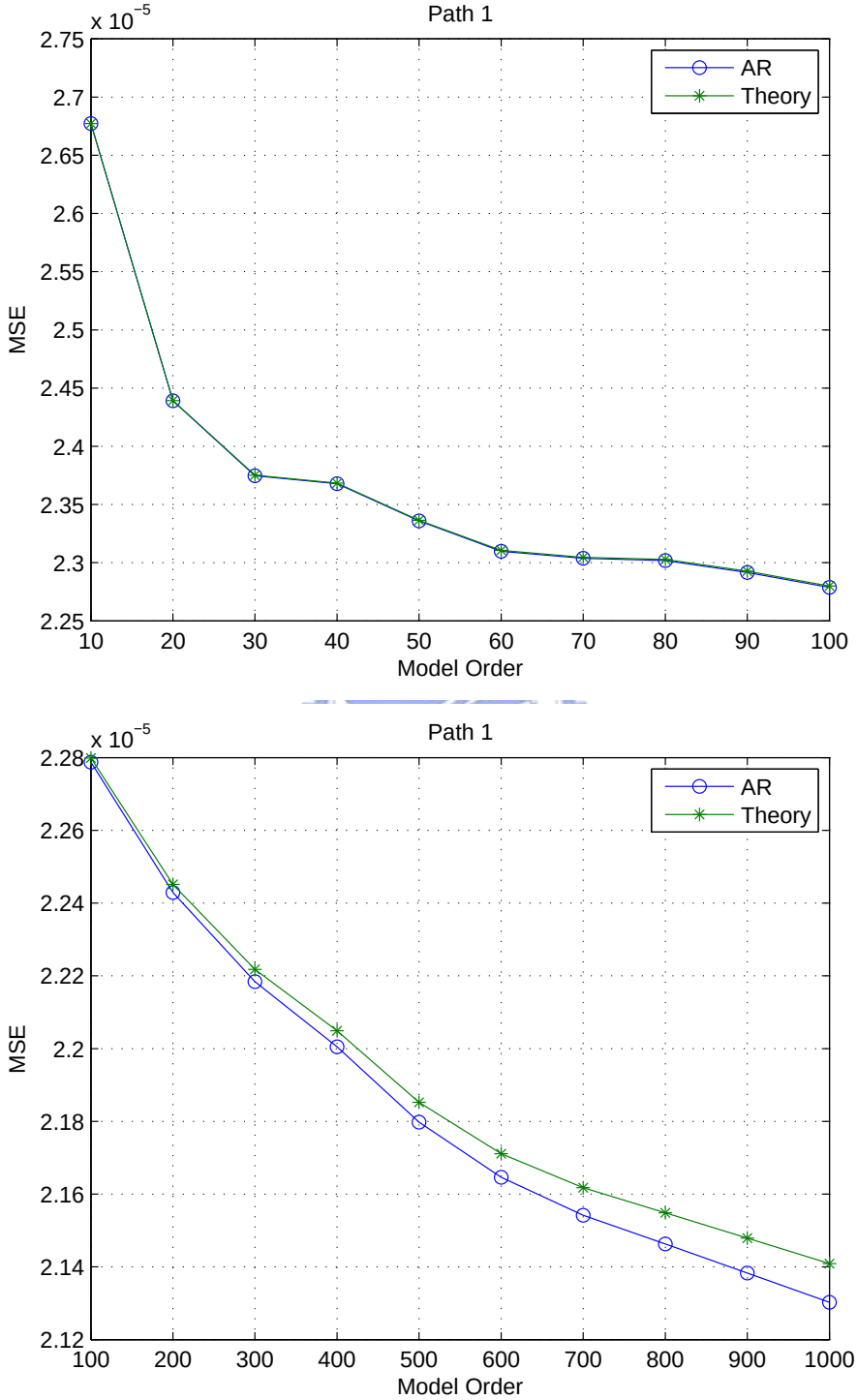

Figure 3.22: Verify the approximation error for WINNER II Typical Urban micro-cell (B1).

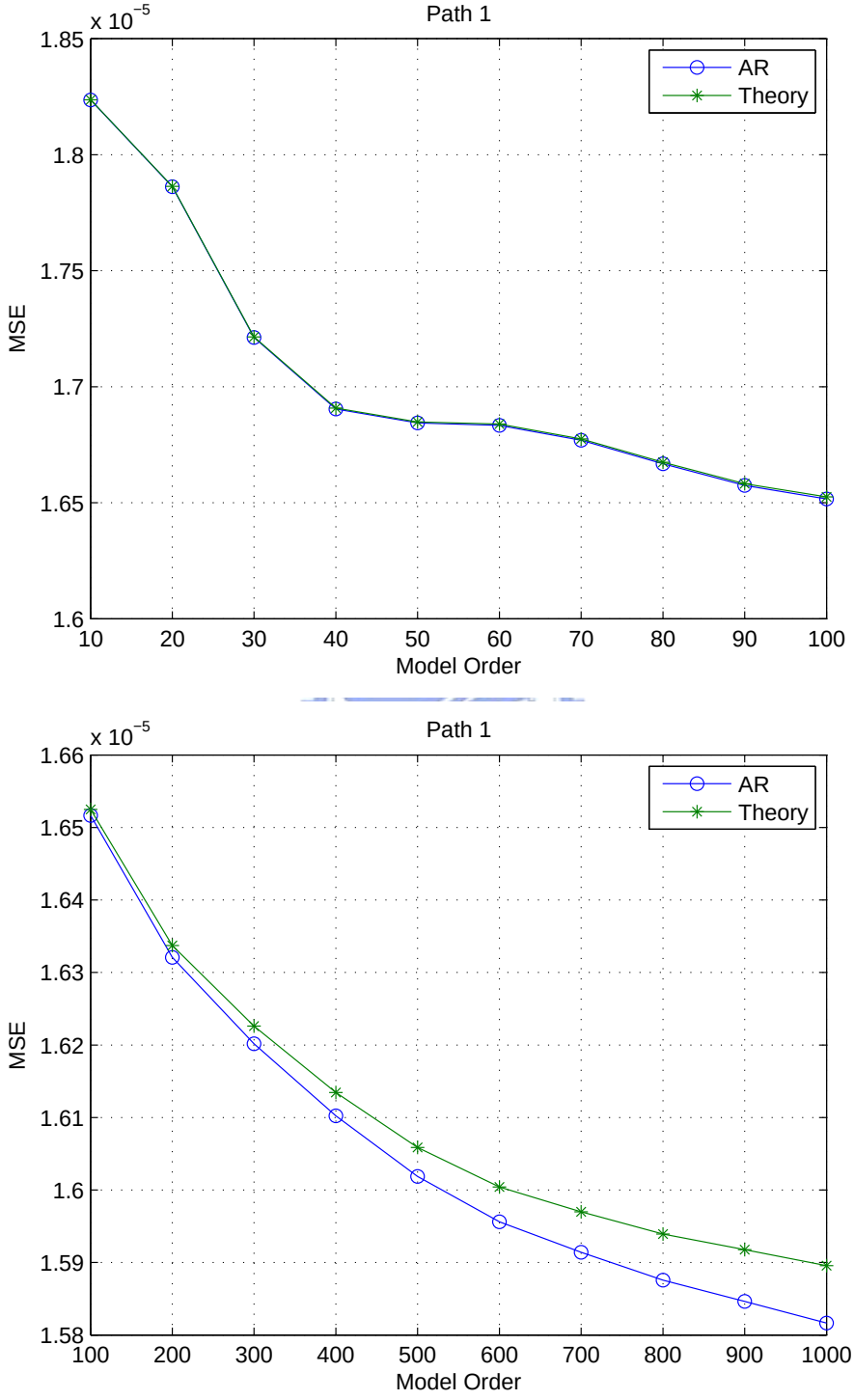

Figure 3.23: Verify the approximation error for WINNER II Bad Urban micro-cell (B2).

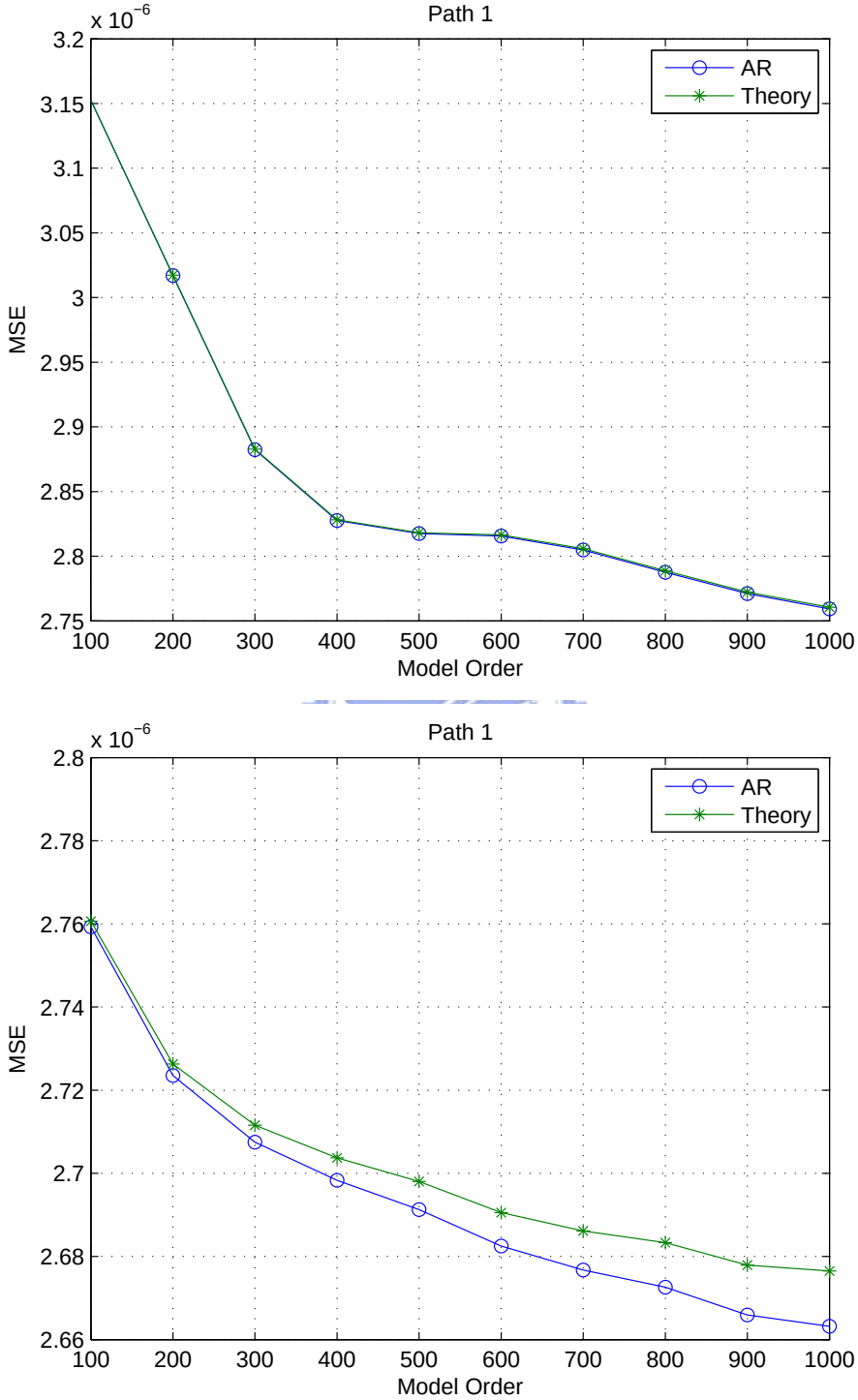

Figure 3.24: Verify the approximation error for WINNER II Suburban macro-cell (C1).

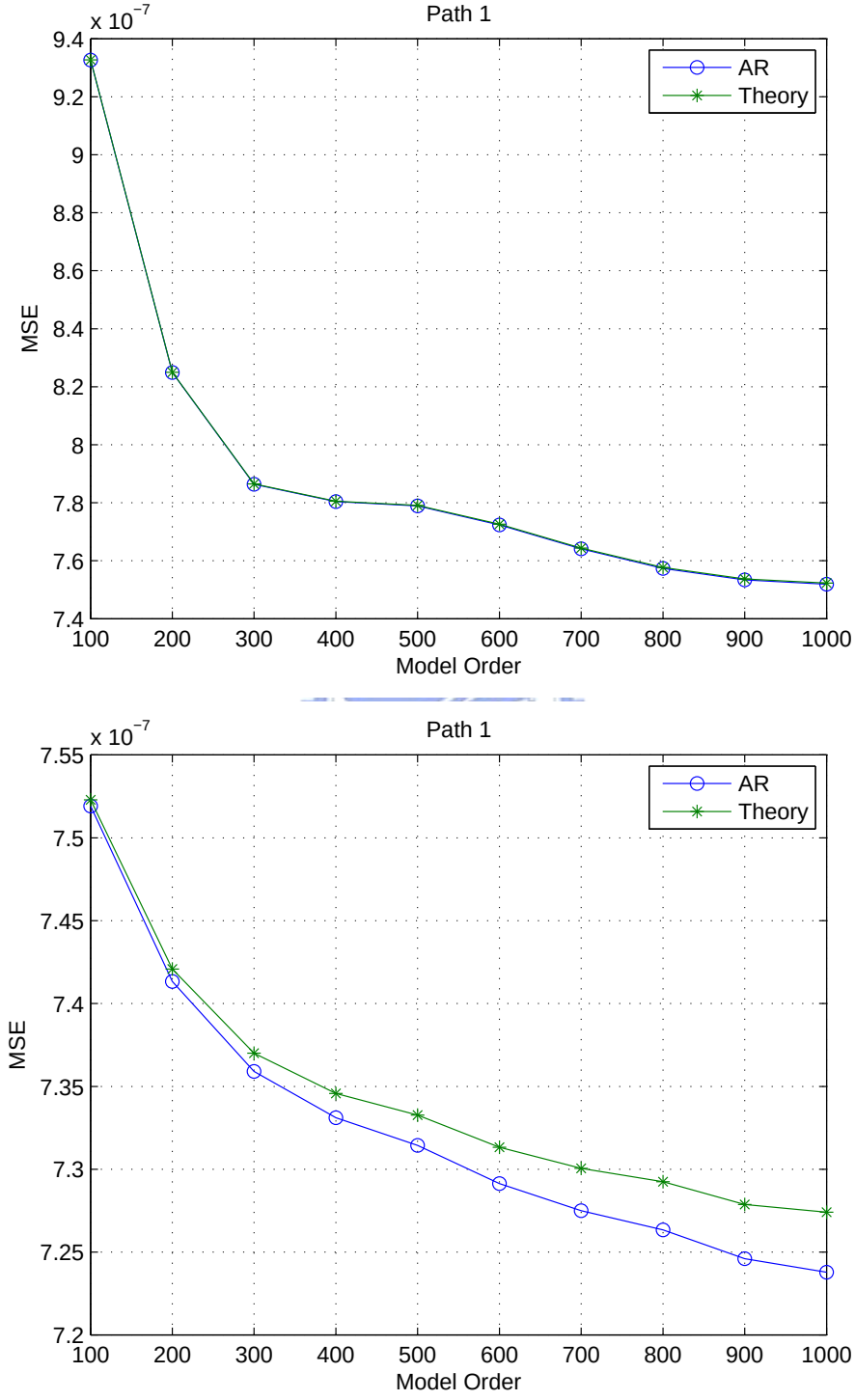

Figure 3.25: Verify the approximation error for WINNER II Typical Urban macro-cell(C2).

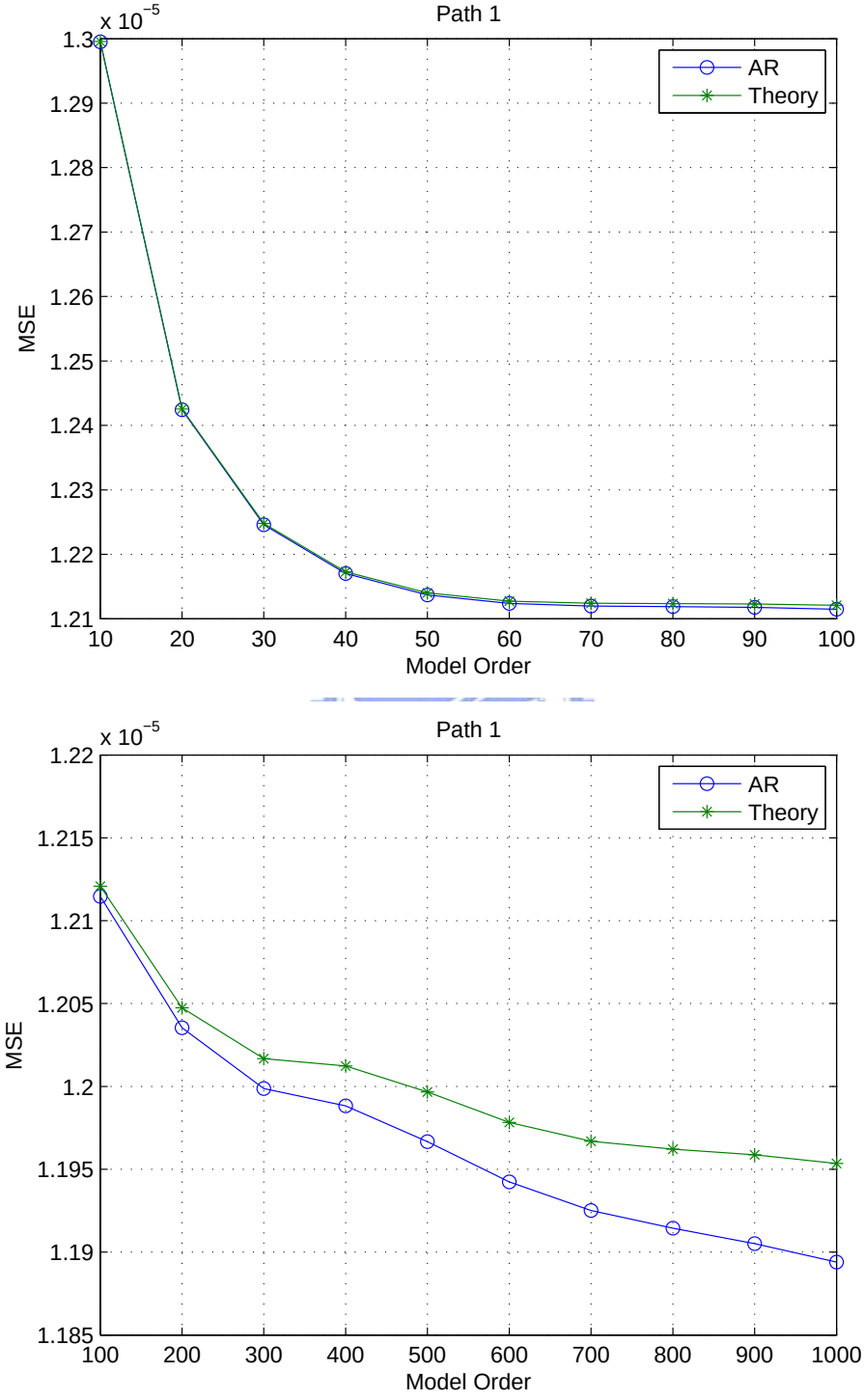

Figure 3.26: Verify the approximation error for WINNER II Bad Urban macro-cell (C3).

Chapter 4

IEEE 802.16e Physical Layer System Integration

In this chapter, we first introduce some function block of IEEE 802.16e physical layer system integration work and analyze each function block power level. Second, we introduced the connection between PHY layer with MAC layer.

4.1 Integration of IEEE 802.16e OFDMA TDD Downlink Transceiver System

In the beginning of system integration for IEEE 802.16e PHY layer downlink transmission, we take the original simply IEEE 802.16e system found by order students to test channel estimation. Figure 4.1 illustrate the block diagrams of our simulated system. The order system be assumed perfect synchronization and omit it in our simulation. Because the preamble is all pilots, there is no need to do DeFraming and DeFEC. For data transmission simulation, we do not do FEC and DeFEC. The integration work is that add those before neglected function to system included synchronization and channel coding.

4.1.1 Power Level Analyze

Because each function block was found by different older students; their fixed point code were defined not the same. We must unify fixed-point data formats at different points in the system integration. The Fig. 4.2 is our system integration final edition.

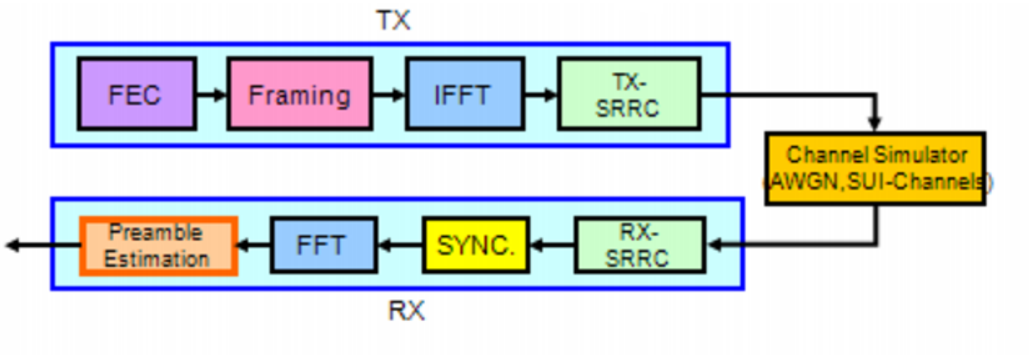

(a)

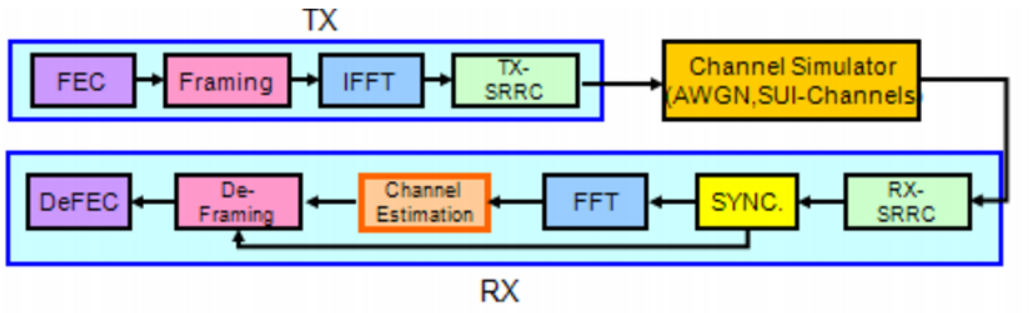

(b)

Figure 4.1: Downlink transmission simulation flow [10]. (a) Preamble (b) Data symbols

In order to add noise to our system, we must consider power level with data signal and noise. So we analyze function block power level before channel in the Fig. 4.2. Table. 4.1 is our set up to analyze power level in the transmitter.

Figs. 4.3 and 4.4 are our analyzing result, the right side value was calculated by C program, and the left side value was our inferred from the system parameter. After QPSK modulation, the widest range occurs in QPSK, which is $[\sqrt{2}, -\sqrt{2}]$. The pilot power is more than data power level about 1/3, and there are 12 data and 2 pilot in one cluster. So one cluster power is 15.554, and we only use the 12 cluster in 1024-FFT OFDMA subcarrier. The average power is 0.18229 before IFFT and 0.00017801 after IFFT. But, if we consider implement to DSP board, so some function block must be considered fixed point. Since the signals after the IFFT are in the range $[-1, 1]$, we choose Q.15 as the data format after IFFT and before FFT. Also, the data format of the input to and the output from the SRRC

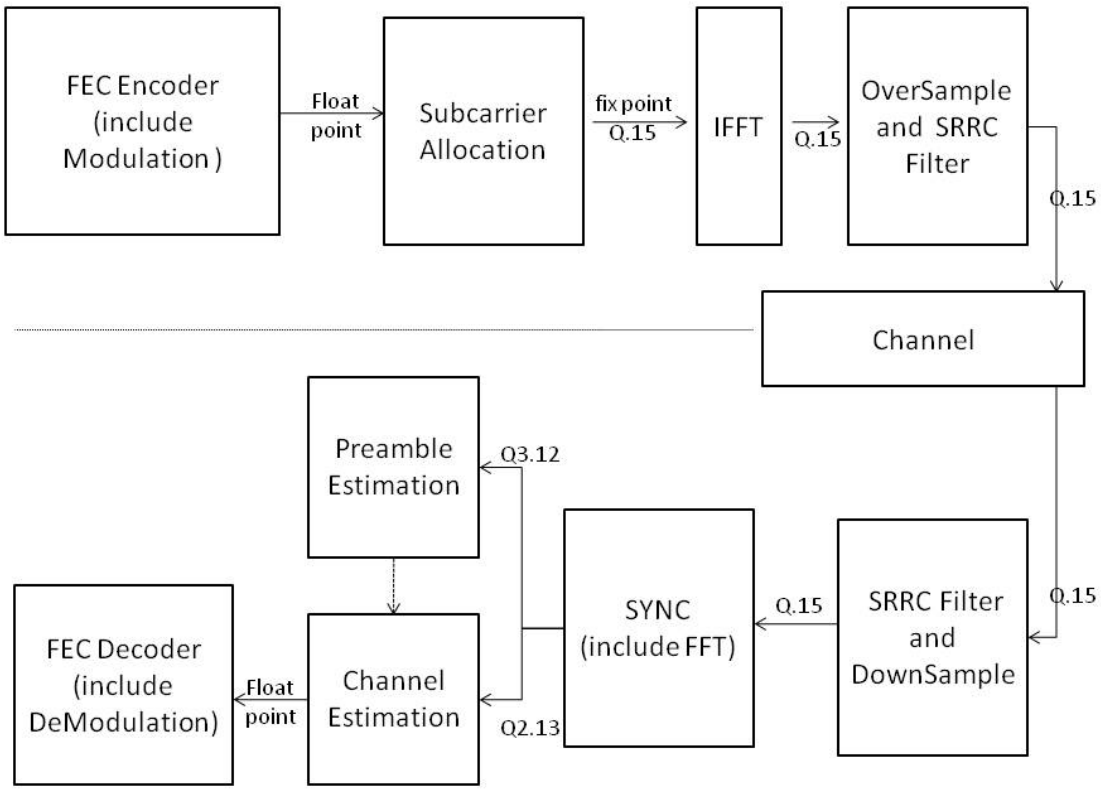

Figure 4.2: Fixed-point data formats used at different points.

filter are the same. So the fixed point power of before SRRC and after SRRC are 0.0001639 and 0.00004116. Between after IFFT with before SRRC power are not the same, and we consider it is float point and fix point switch error. In order to make sure our noise power is normalization or not, and we defined the $SNR = 0$ dB that the white noise total power must be same as the signal power. In the Fig. 4.4 red frame, 4 is cause of after SRRC filter, 1.086 is switch error, and 5.485 is because we only use $168(= 12 \times 14)$ cluster (major group) in 1024-FFT OFDMA subcarrier. According to calculated, we can make sure noise power level is correct.

Table 4.1: System Parameters Used in Our Study

Parameters	Values
Channel	AWGN
SNR	0(dB)
Modulation Type	QPSK
System Channel Bandwidth (MHz)	10
Sampling Frequency (MHz)	11.2
FFT Size	1024
Cluster Number	12
Guard Time (μsec)	11.4
OFDMA Symbol Time (μsec)	102.9

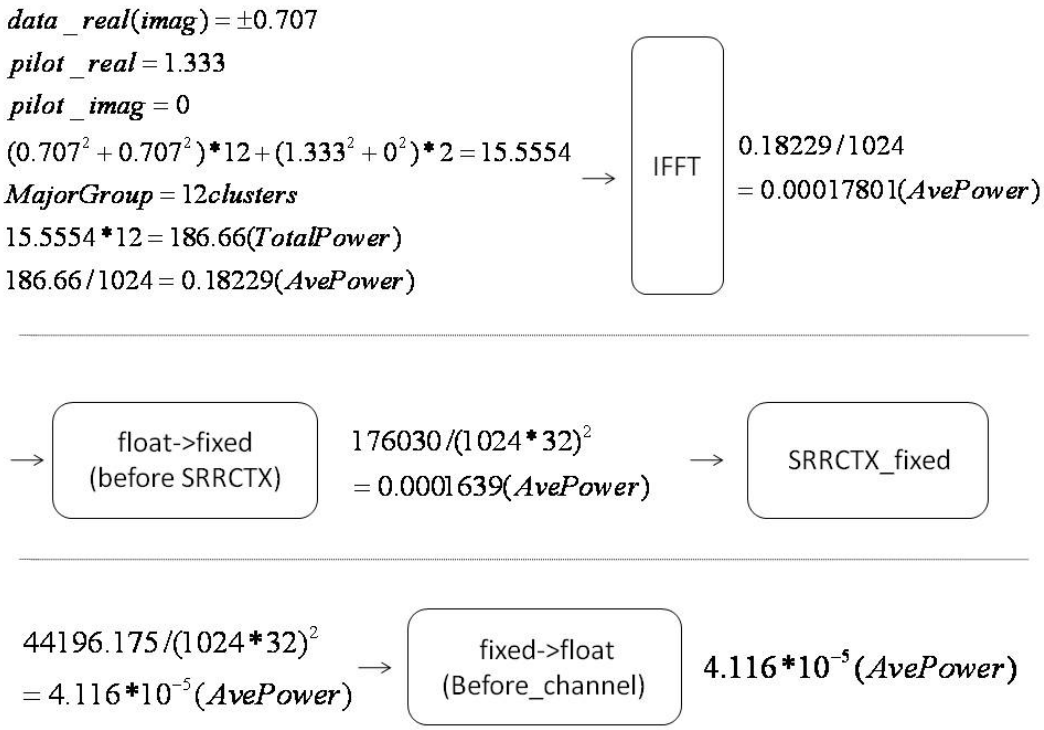

Figure 4.3: Fixed-point data formats used at different points in the transmitter.

4.2 Connect with MAC [11]

In this section, we introduced the other system implementation, establish the connection between IEEE802.16e physical layer (PHY) and MAC layer. Fig. 4.5 is the diagram of before our design the upper-PHY block, and the message of Modulation type, FEC Code Type, Last codeword length, Preamble Presence were defined by ourself. But, now we rewrite the

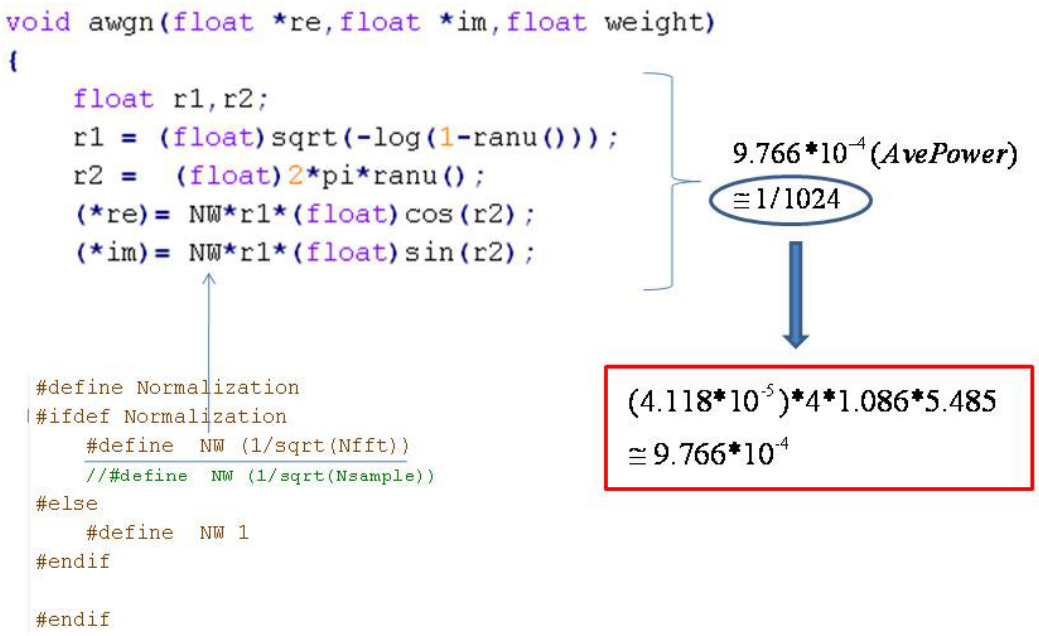

Figure 4.4: Analyze white noise power level.

upper-PHY block code, the above parameter are defined ,according to MAC layer message. Fig. 4.6 is our rewritten upper-PHY block code diagram.

The downlink burst profile message is included in DCD message, and uplink message is in UCD. Figs. 4.7 to 4.8 are the format of DCD and UCD messages. According to different Messagement Message Type would be corresponded to different TLV encoding. If we want to find out the modulation and FEC code type, and only see the Messagement Message Type = 150 TLV encoding variable. Fig. 4.9 is the table of DCD to define the wirelessMAN-OFDMA downlink burst profile, and from the figure we could know DCD message correspond to the message of modulation and FEC code type in PHY layer. But our system was based on the 2007 project of Institute for Information Industry, there were only support convolutional coding (CC) in FEC code type. So we must limit the TLV Variable parameter in DCD message to between 0 and 6, and the modulation type message also in TLV Variable. In the

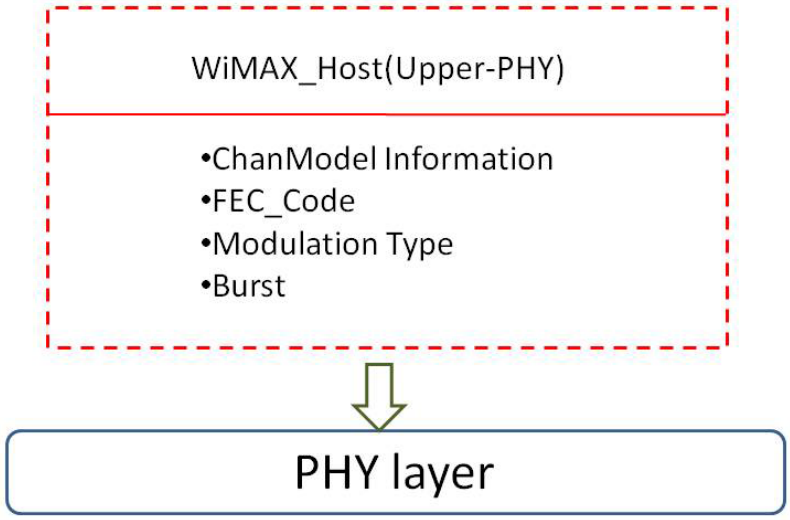

Figure 4.5: Before upper-PHY diagram.

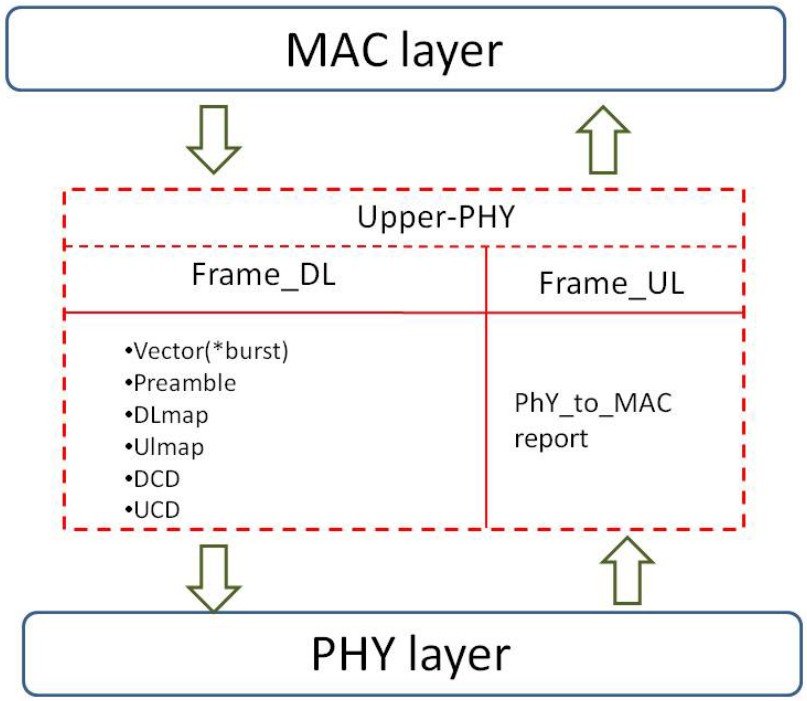

Figure 4.6: After upper-PHY diagram.

Syntax	Size (bit)	Notes
DCD_Message_Format() {	—	—
Management Message Type = 1	8	—
Reserved	8	Shall be set to zero
Configuration Change Count	8	—
TLV Encoded information for the overall channel	*variable*	TLV-specific
Begin PHY-specific section {	—	See applicable PHY subclause
for (i = 1; i <= n; i++) {	—	For each DL burst profile 1 to n
Downlink_Burst_Profile	—	PHY-specific
}	—	—
}	—	—
}	—	—

Figure 4.7: DCD message format [11].

other way, if we want to know uplink burst profile information, we could refer to Table 4.10. Besides, we also must report the channel model information from PHY layer to MAC layer in upper-PHY block (PHY-to-MAC report in Fig. 4.6) included Channel Model Type and Channel Offset.

Syntax	Size (bit)	Notes
UCD_Message_Format() {	—	—
Management Message Type = 0	8	—
Configuration Change Count	8	—
Ranging Backoff Start	8	—
Ranging Backoff End	8	—
Request Backoff Start	8	—
Request Backoff End	8	—
TLV Encoded information for the overall channel	*variable*	TLV-specific.
Begin PHY-specific section {	—	See applicable PHY subclause.
for (i = 1; i <= n; i++) {	—	For each UL burst profile 1 to n.
Uplink_Burst_Profile	*variable*	PHY-specific.
}	—	—
}	—	—
}	—	—

Figure 4.8: UCD message format [11].

Name	Type (1 byte)	Length	Value (variable length)
FEC Code type and modulation type	150	1	0 = QPSK (CC) 1/2 1 = QPSK (CC) 3/4 2 = 16-QAM (CC) 1/2 3 = 16-QAM (CC) 3/4 4 = 64-QAM (CC) 1/2 5 = 64-QAM (CC) 2/3 6 = 64-QAM (CC) 3/4 7 = QPSK (BTC) 1/2 8 = QPSK (BTC) 3/4 or 2/3 9 = 16-QAM (BTC) 3/5 10 = 16-QAM (BTC) 4/5 11 = 64-QAM (BTC) 2/3 or 5/8 12 = 64-QAM (BTC) 5/6 or 4/5 13 = QPSK (CTC) 1/2 14 = *Reserved* 15 = QPSK (CTC) 3/4 16 = 16-QAM (CTC) 1/2 17 = 16-QAM (CTC) 3/4 18 = 64-QAM (CTC) 1/2 19 = 64-QAM (CTC) 2/3 20 = 64-QAM (CTC) 3/4 21 = 64-QAM (CTC) 5/6 22 = QPSK (ZT CC) 1/2 23 = QPSK (ZT CC) 3/4 24= 16-QAM (ZT CC) 1/2 25= 16-QAM (ZT CC) 3/4 26= 64-QAM (ZT CC) 1/2 27= 64-QAM (ZT CC) 2/3 28= 64-QAM (ZT CC) 3/4 29 = QPSK (LDPC) 1/2 30 = QPSK (LDPC) 2/3 A code 31 = QPSK (LDPC) 3/4 A code 32 = 16-QAM (LDPC) 1/2 33 = 16-QAM (LDPC) 2/3 A code 34 = 16-QAM (LDPC) 3/4 A code 35 = 64-QAM (LDPC) 1/2 36 = 64-QAM (LDPC) 2/3 A code 37 = 64-QAM (LDPC) 3/4 A code 38 = QPSK (LDPC) 2/3 B code 39 = QPSK (LDPC) 3/4 B code 40 = 16-QAM (LDPC) 2/3 B code 41 = 16-QAM (LDPC) 3/4 B code 42 = 64-QAM (LDPC) 2/3 B code 43 = 64-QAM (LDPC) 3/4 B code 44 = QPSK (CC with optional interleaver) 1/2 45 = QPSK (CC with optional interleaver) 3/4 46 = 16-QAM (CC with optional interleaver) 1/2 47 = 16-QAM (CC with optional interleaver) 3/4 48 = 64-QAM (CC with optional interleaver) 2/3 49 = 64-QAM (CC with optional interleaver) 3/4 50 = QPSK (LDPC) 5/6 51 = 16-QAM(LDPC) 5/6 52 = 64-QAM(LDPC) 5/6 53...255 = *Reserved*

Figure 4.9: DCD burst profile encodings-wirelessMAN-OFDMA [11].

Name	Type (1 byte)	Length	Value (variable length)
FEC Code type and modulation type	150	1	0 = QPSK (CC) 1/2 1 = QPSK (CC) 3/4 2 = 16-QAM (CC) 1/2 3 = 16-QAM (CC) 3/4 4 = 64-QAM (CC) 1/2 5 = 64-QAM (CC) 2/3 6 = 64-QAM (CC) 3/4 7 = QPSK (BTC) 1/2 8 = QPSK (BTC) 3/4 9 = 16-QAM (BTC) 3/5 10 = 16-QAM (BTC) 4/5 11 = 64-QAM (BTC) 5/8 12 = 64-QAM (BTC) 4/5 13 = QPSK (CTC) 1/2 14 = *Reserved* 15 = QPSK (CTC) 3/4 16 = 16-QAM (CTC) 1/2 17 = 16-QAM (CTC) 3/4 18 = 64-QAM (CTC) 1/2 19 = 64-QAM (CTC) 2/3 20 = 64-QAM (CTC) 3/4 21 = 64-QAM (CTC) 5/6 22 = QPSK (ZT CC) 1/2 23 = QPSK (ZT CC) 3/4 24= 16-QAM (ZT CC) 1/2 25= 16-QAM (ZT CC) 3/4 26= 64-QAM (ZT CC) 1/2 27= 64-QAM (ZT CC) 2/3 28= 64-QAM (ZT CC) 3/4 29 = QPSK (LDPC) 1/2 30= QPSK (LDPC) 2/3 A code 31= QPSK (LDPC) 3/4 A code 32 = 16-QAM (LDPC) 1/2 33 = 16-QAM (LDPC) 2/3 A code 34 = 16-QAM (LDPC) 3/4 A code 35 = 64-QAM (LDPC) 1/2 36 = 64-QAM (LDPC) 2/3 A code 37 = 64-QAM (LDPC) 3/4 A code 38 = QPSK (LDPC) 2/3 B code 39 = QPSK (LDPC) 3/4 B code 40= 16-QAM (LDPC) 2/3 B code 41 = 16-QAM (LDPC) 3/4 B code 42 = 64-QAM (LDPC) 2/3 B code 43 = 64-QAM (LDPC) 3/4 B code 44 = QPSK (CC with optional interleaver) 1/2 45 = QPSK (CC with optional interleaver) 3/4 46 = 16-QAM (CC with optional interleaver) 1/2 47 = 16-QAM (CC with optional interleaver) 3/4 48 = 64-QAM (CC with optional interleaver) 2/3 49= 64-QAM (CC with optional interleaver) 3/4 50 = QPSK (LDPC) 5/6 51 = 16-QAM(LDPC) 5/6 52 = 64-QAM(LDPC) 5/6 53..255 = *Reserved*
Ranging data ratio	151	1	Reducing factor in units of 1 dB, between the power used for this burst and power should be used for CDMA ranging. It shall be encoded as signed integer.

Figure 4.10: UCD burst profile encodings-wirelessMAN-OFDMA [11].

Chapter 5

Analysis of Spatial Correlation for MIMO System

In this chapter, we first introduce how to generate the WINNER channel antenna array pattern, then discuss the correlation between different links on MIMO channel, according different antenna array. We also fit the correlation function by simulated data to discuss the relationship between channel cross-correlation and those auto-correlation.

5.1 Construction of Antenna Array Model [1]

In order to discuss spatial channel correlation, we must consider the antenna array geometry. WINNER channel model uses structure array for representation 3D Antenna array model. For construction of array structure MATLAB function AntennaArray.m is provided. If one would like to verify created 3D-AA model, this can be performed by AntennaResponse.m function. In order to make array it is necessary to define its geometry (positions and rotation of elements), and to provide element field patterns. The arguments provided to AntennaArray.m are always processed in predefined way: first array geometry is created and after that field patterns are assigned. we can set up antenna position and what kind of antenna elements distribute in first part, and coordinate system was defined in second part. Fig. 5.1 is the antenna array construction. We will illustrate this antenna array construction in following sub-section.

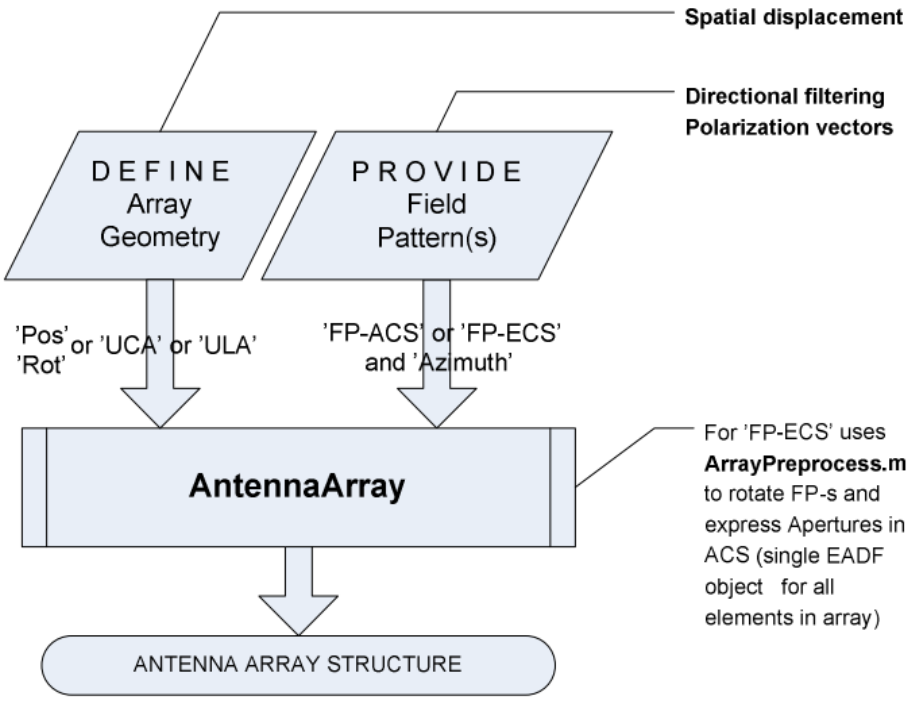

Figure 5.1: Construction of antenna array [1].

5.1.1 Antenna Geometry Representation

Table 5.1 is the input parameter based on our need for antenna geometry. Geometry can be defined explicitly using *Pos* and *Rot* arguments followed by $ELNUM * 3$ matrix, where $ELNUM$ is the number of elements. Alternatively, common array types Uniform-Circular-Array (UCA) and Uniform-Linear-Array (ULA) could be defined with few parameters only. For UCA elements are placed starting from x-axis ($\varphi = 0$) every $\Delta\varphi = \frac{2\pi}{N}$, and n^{th} element is rotated for $(n-1)\Delta\varphi$ in positive mathematical direction. ULA elements are placed along x-axis is such a way that the center of the array is at $[0; 0; 0]$ (for even N there is no antenna element at [0;0;0]). If there are no parameters defining geometry default is single antenna positioned at center of ACS, without rotation.

5.1.2 Field Pattern(FP) Representation

Before introducing the antenna field pattern, we list the different types of coordinate in WINNER channel model.

Table 5.1: Input Parameters for Antenna Geometry [1].

Parameter	Definition	Default value	Unit
Position	ELNUM*3 matrix, where n-th row contains [x,y,z] position of n-th antenna element in ACS.	-	m
Rotation	ELNUMx3 matrix, where n-th row contains $[Rot_x; Rot_y; Rot_z]$ rotation of n-th antenna element a found axes of ACS.	0_{N*3}	rad
ELNUM	Number of physical antenna elements in array.	-	-
r	Radius of UCA.	1	m
d	Distance between antenna elements in ULA.	1/ELNUM	m

- Global coordinate system (GCS): used to define radio-network system layout, and as a reference system for polarization
- Array coordinate system (ACS): describes array geometry and rotated radiation patterns of antenna elements
- Element coordinate system(ECS): represent radiation pattern of each antenna element.

Fig. 5.2 is three kind of coordinate diagram. Additionally, the EADF (effective-aperture-density-functions) in the following introduction is represented the simplify process that will reduce memory storage requirements and provide effective way of interpolating the field pattern for arbitrary angle.

The field patterns of individual array elements are described using the EADF defined in ACS. This was done because EADF has proven to be superior in terms of memory requirements and interpolation errors. EADF representation is created from a sampled field pattern(FP) that is provided as an input to AntennaArray.m. The number of provided field patterns (FP_{NUM}) for FP-ACS and FP-ECS should be equal to number of elements in array ($ELNUM$), however:

- if FP_{NUM} is equal to 1, same Field-Pattern will be apply to all antennas;
- if $1 < FP_{NUM} < ELNUM$ the error will be issued;
- if $FP_{NUM} > ELNUM$ take only first N.

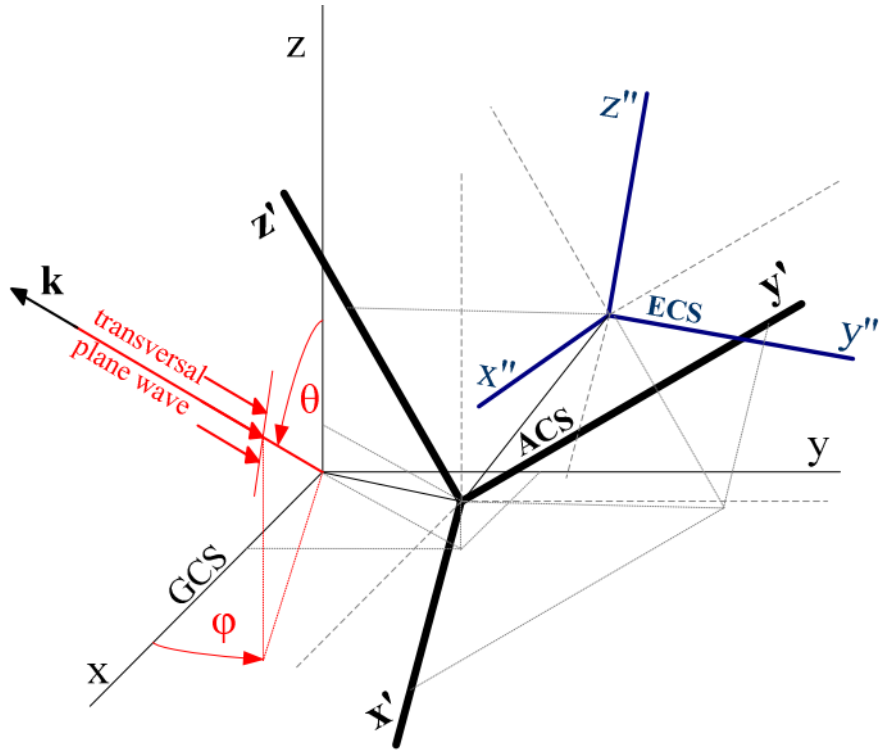

Figure 5.2: Coordinate system definitions [1].

Reference Coordinating System

In order to distinguish between FPs that are expressed in ECS and ACS it was necessary to define different argument types: FP-ECS and FP-ACS. However, in both cases input argument FP has the same structure.

Sampling Grid

In order to calculate 2D Fourier transformation of FP equidistant sampling points are required. If non-uniform samples are provided, additional interpolation (e.g., spline) of FP, before calculating its EADF, is necessary. This may introduce significant errors in the FP representation and therefore we would assume that uniform sampling is always used. This would mean that the azimuth angles must be equidistant from -180 to (but not including) 180 degrees.

Polarization

Since 3D-Antenna-Array-Model generally allows arbitrary rotation of antenna elements, it is necessary to calculate projections to referent polarization vectors in GCS. Using of $wimpar.PolarizedArrays = no$ option in wimparset.m with 3D-Antenna Array is not directly applicable since the representation of the polarization for single-polarized but rotated antenna still requires two orthogonal reference polarization vectors-what is equivalent to previous polarized option ($wimpar.PolarizedArrays = yes$). Otherwise, only single (vertical or horizontal) projection of polarization vector will be handled, what is obviously wrong. Therefore control parameter wimpar.PolarizedArrays can not be used (in general) to reduce complexity channel coefficients will be always based on polarized FP (after rotation).

5.1.3 Simulation Environment

According to [1], helper function arrayparset.m is provided to illustrate construction of arrays. It shows construction of ULA 2/4/8 and UCA 4/8 with synthetic field pattern defined in ECS. Slanted dipole and isotropic radiation patterns are used for that purpose. To simulate 2×2 MIMO system condition, we set the base station and mobile station antenna array were that ULA with 2 elements and use the example antenna pattern in example-syntetic-arrays.m. According to these example pattern, we discuss that the antenna arrays affect spatial channel correlation in next section.

Fig. 5.3 is the position figure of base station and mobile station. The circle is the clusters position of 20 paths for each links. In Fig. 5.3, antenna positions were generated by random number generator (BS: [147;132;32], MS: [96;15;1.5]) ([x;y;z] position in GCS) and velocity of mobile station is 10 m/s. Antenna element rotation were default value ($0_N * 3$), and element distance and mobile station moving distance (sample density) were adjusted respective in following section. Table 5.2 is table of our simulation global parameter.

Table 5.2: Global System Parameters in Chapter 5

Parameters	Values
Center Frequency	3e9
System Channel Bandwidth (MHz)	10
Scenario	Typical urban macro-cell(C2)
Sample Number	1000
Number of clusters	20
Number of paths in each cluster	20
Antenna construction	ULA
BS antenna position	[147;132;32]
MS antenna position	[96;15;1.5]
Number of BS antenna element	2
Number of MS antenna element	2
Antenna rotation	$(0_N * 3)$
Path Loss mode	no
Shadowing Model	no
CDL model	no
Polarized Arrays	no
Random Seed	111

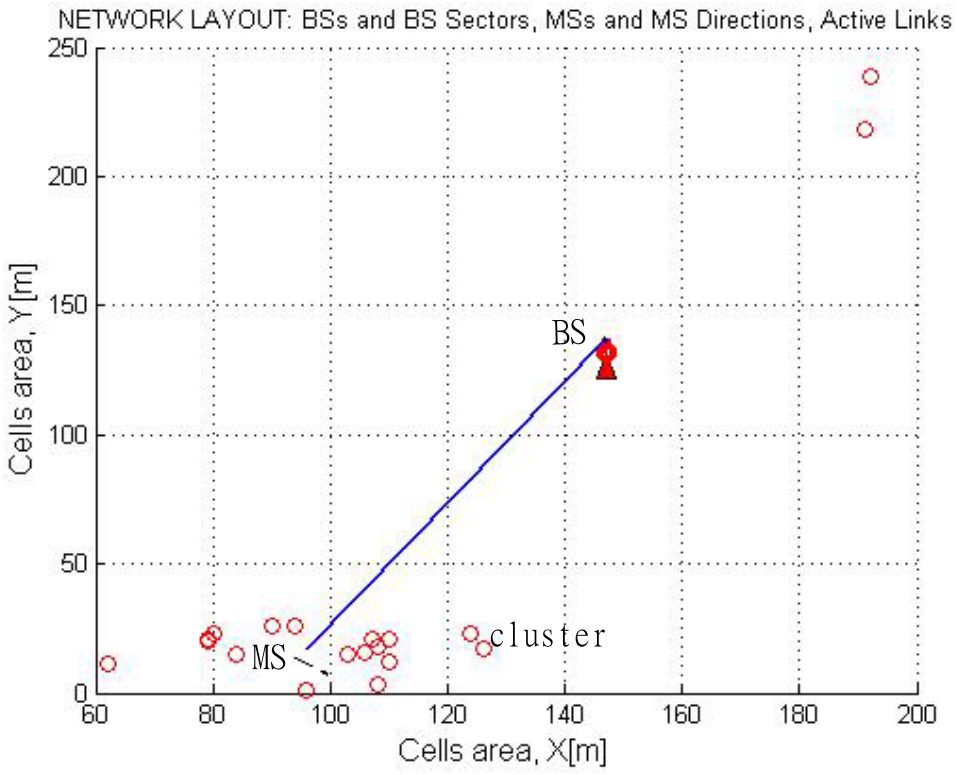

Figure 5.3: Location of base station, mobile station, and cluster.

Table 5.3: Channel Environment Parameter to Test Fit Function

Parameters	Values
Sample Density	5
BS elements distance	5(m)
MS elements distance	0.01(m)

5.2 Fit Correlation Function

In this section, we introduce how did we fit the auto-correlation and cross-correlation function, in order to discuss their relationship in next section. Eq. (5.1) is the 2×2 MIMO channel correlation matrix, and diagonal term are two different links channel auto-correlation function. The others term are cross-correlation, and we maybe base on auto-correlation function to fit cross-correlation function, when those auto-correlation were similar. Eq. (5.2) is simply equation separate only amplitude and phase terms.

$$CorrelationMatrix = \begin{bmatrix} \frac{b_1 \times \exp^{jc_1 f}}{1+ja_1 f} & * \\ * & \frac{b_2 \times \exp^{jc_2 f}}{1+ja_2 f} \end{bmatrix} \tag{5.1}$$

$$= \begin{bmatrix} \frac{b_1}{\sqrt{1+a_1 f^2}} \times \exp^{\{c_1 f - \arctan a_1 f\}} & * \\ * & \frac{b_2}{\sqrt{1+a_2 f^2}} \times \exp^{\{c_2 f - \arctan a_2 f\}} \end{bmatrix} \tag{5.2}$$

According the MATLAB fit function and channel coefficients generated by WINNER II model, we can fit the parameter $\{a_1, b_1, c_1, a_2, b_2, c_2\}$ in diagonal term of (5.1). But MATLAB fit function do not be used to fit the complex number, and we must respective fit amplitude and phase terms, according to (5.2). In the following case, we first fit the phase term, then using already fit phase parameters to fit amplitude term. Besides Table 5.2, the Table 5.3 is also simulation parameter in this section to test fit function.

Fig. 5.5 were the simulation result of fitting auto-correlation from single BS antenna element to double MS antenna elements. And the respective fit result were $\frac{1.438 \times \exp^{\{j(-0.9283)f\}}}{1+j(-0.5314)f}$ and $\frac{1.417 \times \exp^{\{j(-0.9254)f\}}}{1+j(-0.5232)f}$, and those mean square error (mse) between fit function and simulation data were $mse_{amplitude} = 4.122 \times 10^{-2}$ and $mse_{phase} = 2.765 \times 10^{-3}$ for link 1, and $mse_{amplitude} = 4.389 \times 10^{-2}$ and $mse_{phase} = 2.626e \times 10^{-3}$ for link 2.

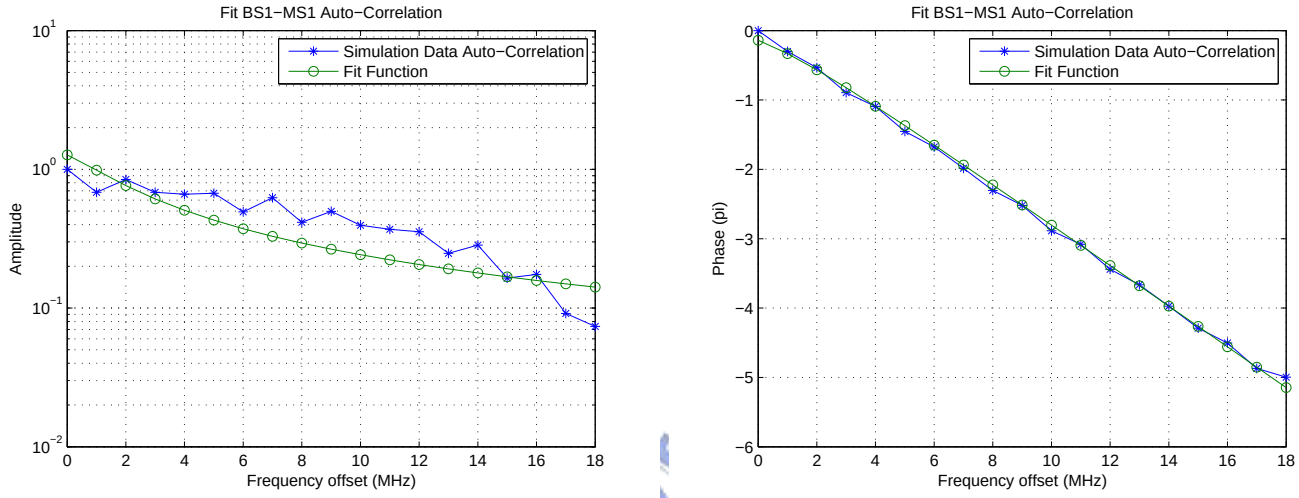

Figure 5.4: Fit auto-correlation link1 (BS1-MS1).

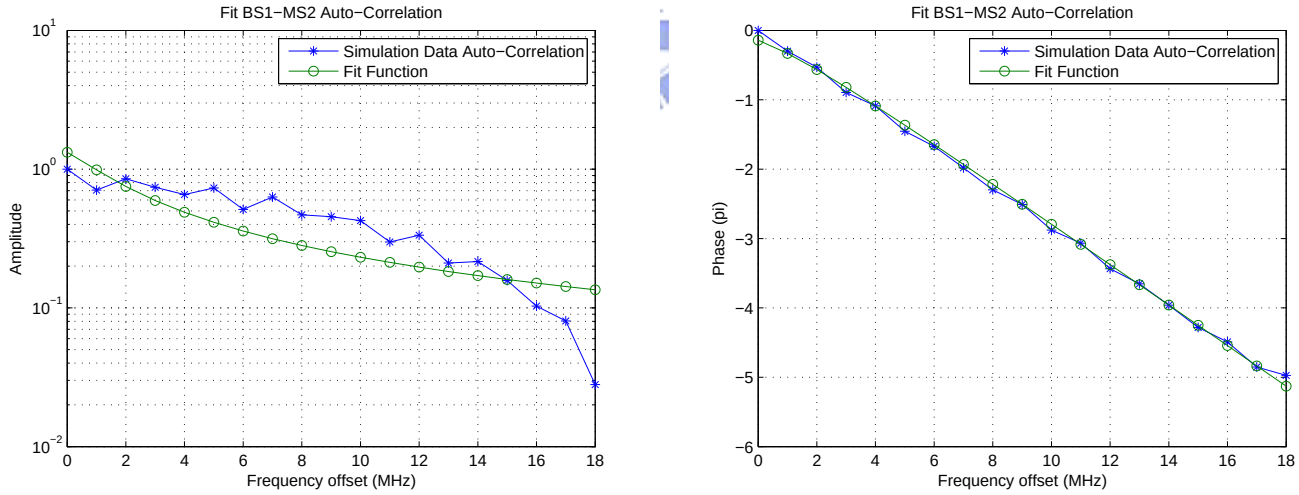

Figure 5.5: Fit auto-correlation link2 (BS1-MS2).

From Fig. 5.5 and those fitting result, we can see those parameter were similar for different links. So their cross-correlation function maybe also the similar, we suppose the cross-correlation function term is the product collection of their fitted auto-correlation functions and some constant number. Eq. (5.3) is our suppose equation; $\{a_1, b_1, c_1\}$ and $\{a_2, b_2, c_2\}$ were the fitted auto-correlation parameter, and $\{p, q\}$ was we want to fit according simulated cross-correlation data:

$$* = \sqrt{\frac{b_1 b_2}{\sqrt{1 + a_1 f^2} \times 1 + a_2 f^2}} \times \exp^{j\{\frac{c_1 + c_2 - \arctan(a_1 f) - \arctan(a_2 f)}{2}\}} \times p \cdot \exp^{j\{q\}} . \tag{5.3}$$

Fig. 5.6 was the fitting result, and the parameter in (5.3) were $p = 0.9994$ and $q = 0.4715$. The mean square error (mse) of fit function were $mse_{amplitude} = 2.577 \times 10^{-2}$ and $mse_{phase} = 4.514 \times 10^{-3}$. And we could see if those auto-correlation function were the same, their cross-correlation could be fitted well used by auto-correlation equation parameter. So the following simulation case were the same process to fit their cross-correlation, and we also use (5.3) in following case to verify our supposition based on the mse values.

5.3 Reason of Affect Channel Cross-Correlation

In this section, we discuss two popular reason to affect the channel spatial correlation.

5.3.1 Antenna Element Distance

In this part, we discuss the relationship between antenna elements distance and channel correlation. We will adjust BS and MS antenna elements distance respective in following section.

Base Station Antenna Element Distance Effect

Now, we adjust base station two antenna element distance to discuss the effect of MIMO channel correlation. And the globe simulation parameter were as same as Table 5.2. Fig. 5.7 is the amplitude figure with simulation result of channel coefficients correlation from two BS antenna elements to one MS antenna element. Because there were low correlation between

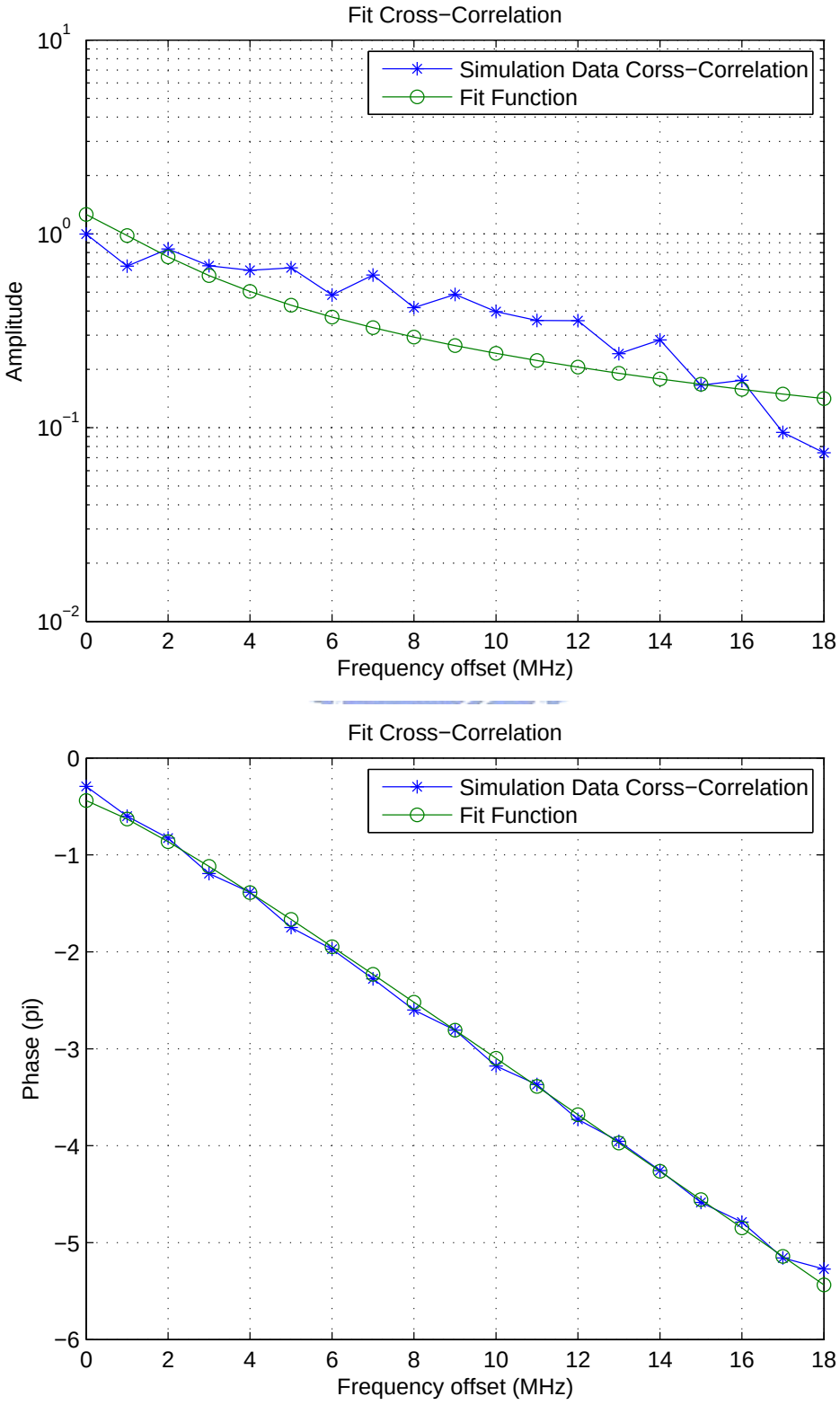

Figure 5.6: Fit cross-correlation for different links.

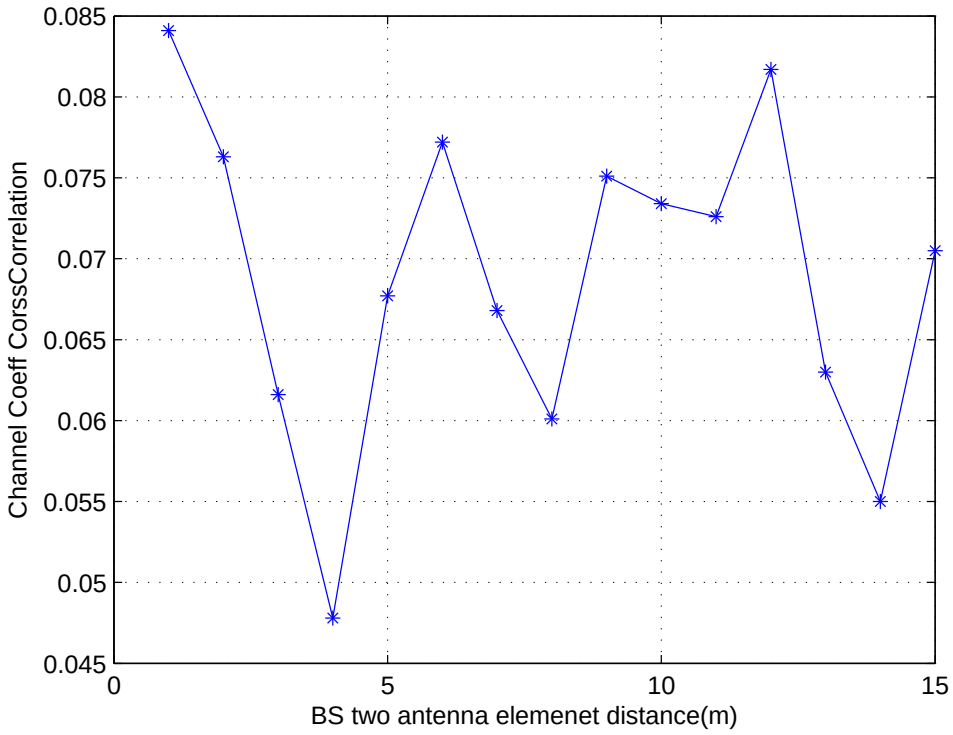

Figure 5.7: Base station antenna element distance (C2).

0.085 and 0.045, and those correlation are not direct relationship to base station antenna element distance.

Because the degree of cross-correlation is lower and may not the BS antenna elements function, we did not discuss the fitting cross-correlation in this part.

Mobile Station Antenna Element Distance Effect

In this part, we consider the relationship between MS antenna element distance and those channel correlation. Figs. 5.8 and 5.9 are simulation results, and we can see that the correlation and element distance are almost inverse proportion. But when elements distance is 50 cm, its correlation was the lowest between 10 cm and 100 cm element distance. Fortuitously, the 50 cm distance is just same as the half wavelength, and the other simulation (Figs. 5.10 and 5.11) with 6 GHz center frequency, were also the same result that half wavelength is 25 cm almost same as the element distance with the lower correlation. We

may infer the reason that half wavelength distance is same as wave crest to the wave trough, and this two point are the highest amplitude distance and phase changed which correlation is relative lower. So the mobile antenna elements distance could direct affect the channel cross-correlation from single BS antenna element to double MS antenna elements.

Fit Cross-Correlation Function

Now, we use fit function before introduced and simulation data to the above correlation matrix. First fitting auto-correlation in diagonal terms use (5.2), then fitting cross-correlation data use (5.3). Fig. 5.12 was the simulation result of sum square error between fit function and data. There are two simulation case: first, only fitting auto-correlation function parameter in cross-correlation equation. Second, fitting not only auto-correlation but also cross-correlation parameters in equation.

Form the Fig. 5.12, we can see the amplitude part of cross-correlation could only used those parameter fitted from auto-correlation (not to fit p parameter of (5.3). But the phase term, it must to fit q parameter of (refeq:cross-correlation function term), otherwise cross-correlation phase error must be a lot. Final, we can make a conclusion in this section, if channel cross-correlation are higher, and its correlation function may be the similar to their auto-correlation function. And cross-correlation could be fitted by auto-correlation function parameter and some constant number.

5.3.2 Mobile Station Moving Distance

In this part, we discuss the mobile station moving distance to affect the channel correlation. According to the above section, we realize the case of cross-correlation in double BS antenna element to single MS antenna element was closely to un-correlation. So we only discuss the spatial channel correlation with single BS antenna element to double MS antenna element in this section.

In the following simulation case, we adjust the *wimpar.SampleDensity* parameter to discuss the channel correlation. According to [1], we realize the *wimpar.SampleDensity* was

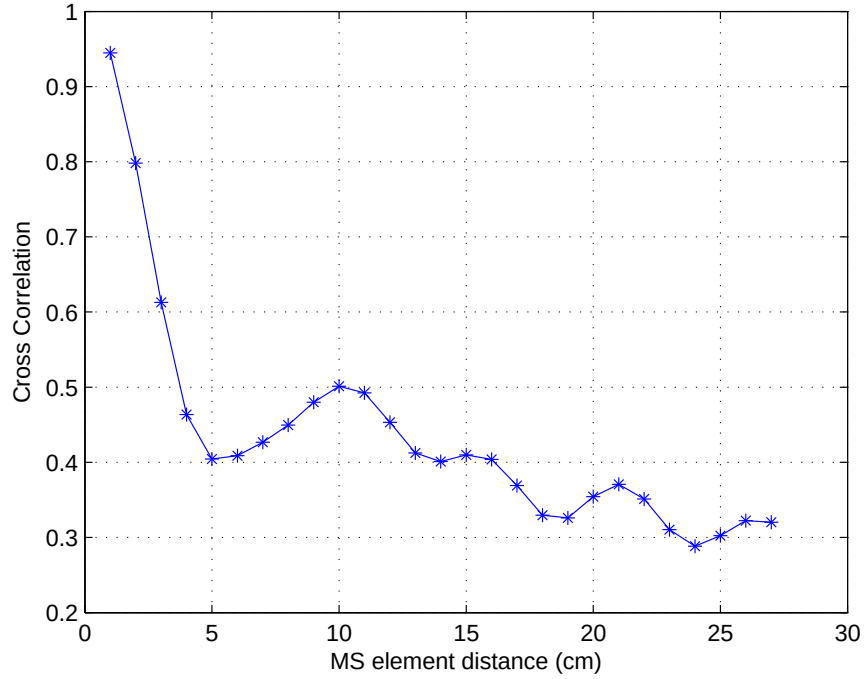

Figure 5.8: Cross correlation amplitude for different MS element distances.

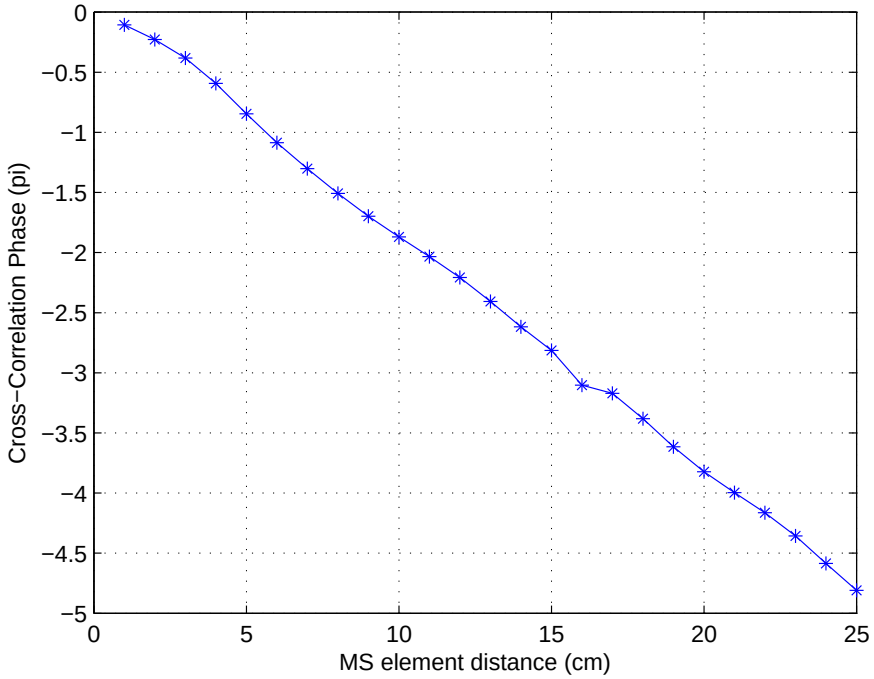

Figure 5.9: Cross correlation phase for different MS element distances.

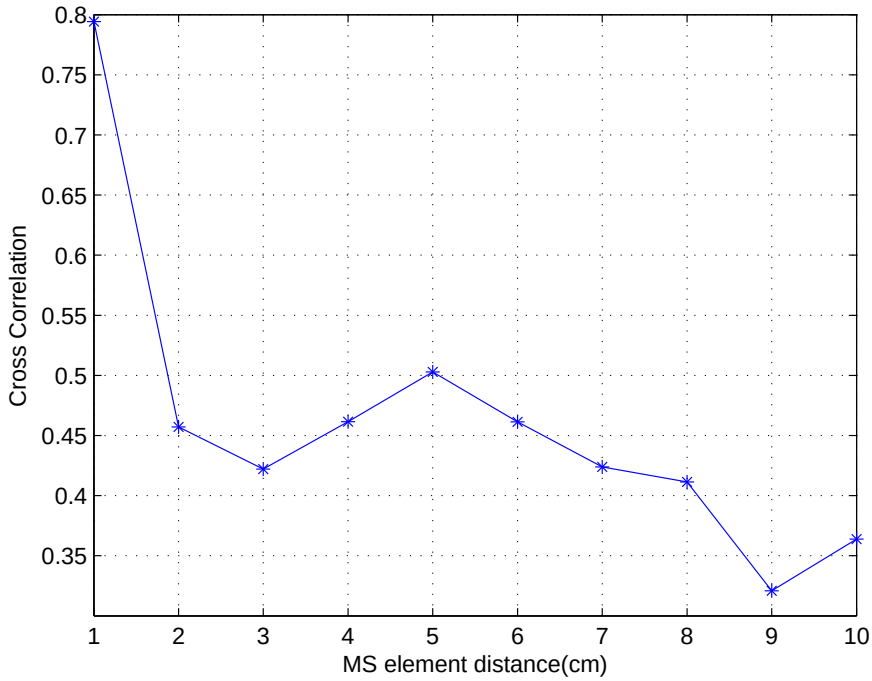

Figure 5.10: Cross correlation amplitude for different MS element distances (F_c=6e9).

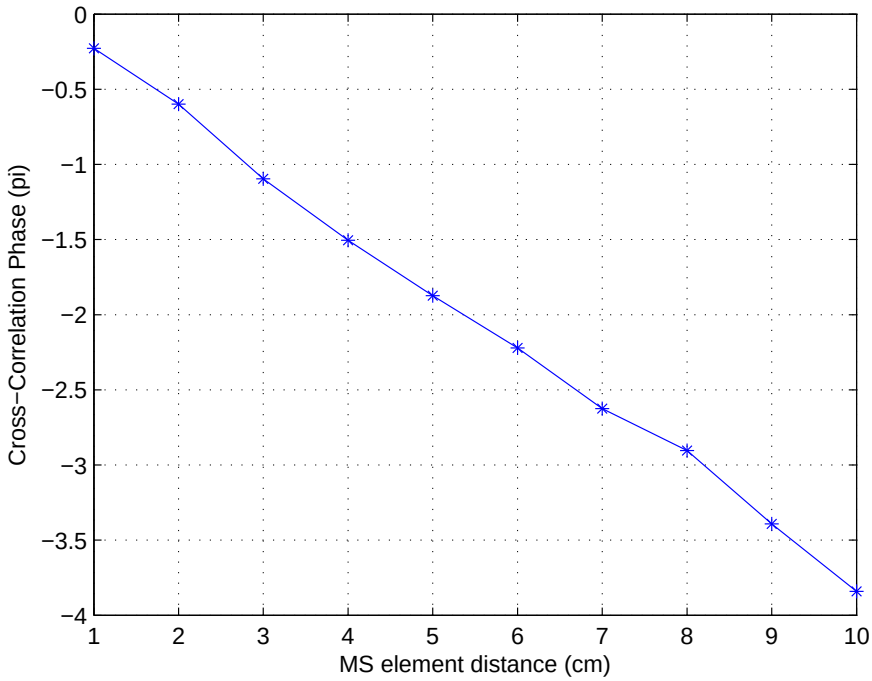

Figure 5.11: Cross correlation phase for different MS element distance (F_c=6e9).

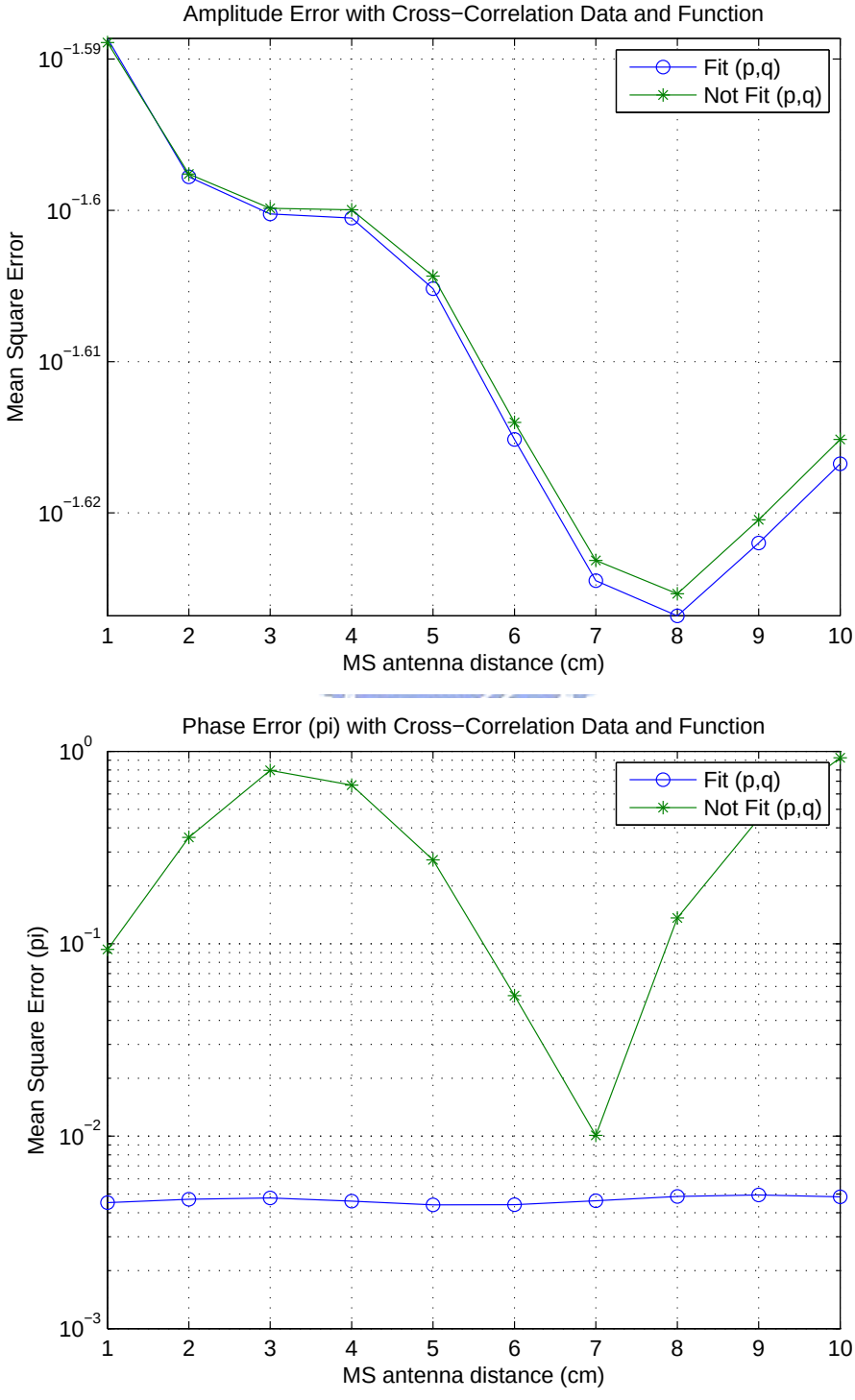

Figure 5.12: Mean square error of Fit Function

defined for oversampling factor which is the number of time samples per half wavelength. So if we fixed the total sample number ($wimpar.NumTimeSamples = 1000$), and mobile station moving distance is ($wimpar.NumTimeSamples$) $\div$ ($2 \times wimpar.SampleDensity$) $\times$ ($wavelength$). For example, we set the $CenterFrequency = 3e9$ Hz, $wavelength = 0.1$ m and $wimpar.SampleDensity = 50$, then we could know the mobile station move total distance is 1 m in the time period to transmit the 1000 sample ($wimpar.NumTimeSamples = 1000$). Then we use this way to discuss the distance effect on channel coefficients cross-correlation.

Figs. 5.13 and 5.14 were the simulation result for amplitude and phase of channel cross-correlation. We set the $wimpar.SampleDensity = 1000 \sim 100$ and $wimpar.SampleDensity = 100 \sim 10$, then the mobile station moving distance are rethe $0.05 \sim 0.5$ (m) and $0.5 \sim 5$ (m) , respectively. We can see the degree of cross-correlation is lower, when MS moving distance farer. But when the moving distance excess some distance, channel cross-correlation may not change a lot.

Fit Cross-Correlation Function

Fig. 5.15 is the fitting cross-correlation simulation result, we could also see the mse of fitting p and q parameters in (5.3) was lower than that only fitting auto-correlation equation parameter. In phase figure, the mse_{phase} sometimes was too high. And we inferred that its cross-correlation phase term was not closely to linear line, but the most auto-correlation phase term was. Because we based on auto-correlation parameter to fit cross-correlation, their mse_{phase} must be much higher in this case. So our suppose cross-correlation equation may not fit used, when cross-correlation phase curve is not linear.

5.3.3 Angle of Arrival and Angle of Departure

In the WINNER channel model, we can not decide the cluster position directly, but we can base on the angle of arrival (AoA) and angle of departure (AoD) then to get the position we want. In this section, we reset the angle of arrival and departure to discuss the spatial

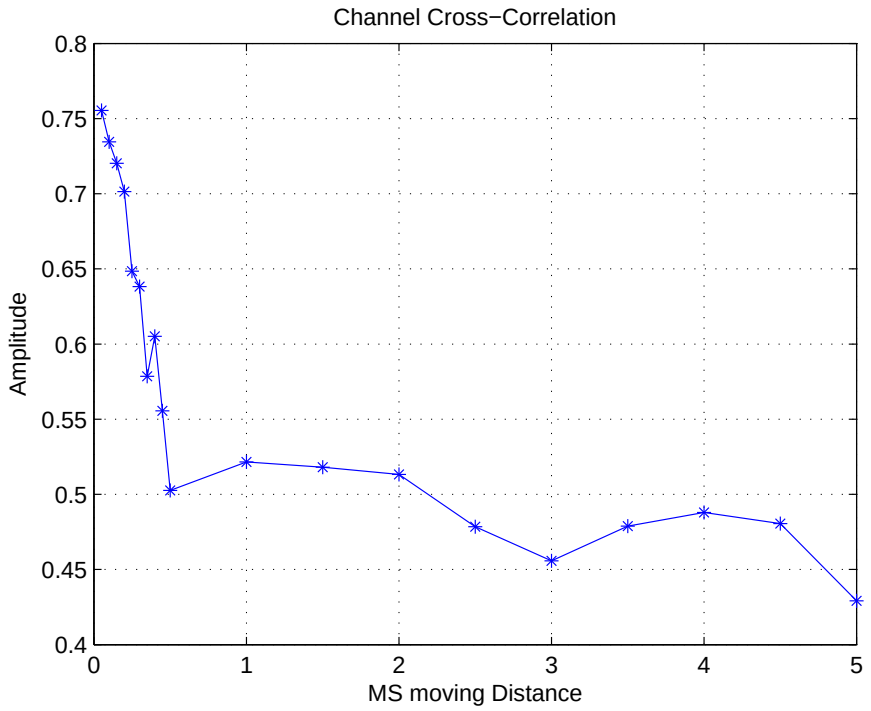

Figure 5.13: Cross correlation amplitude for different MS move distances.

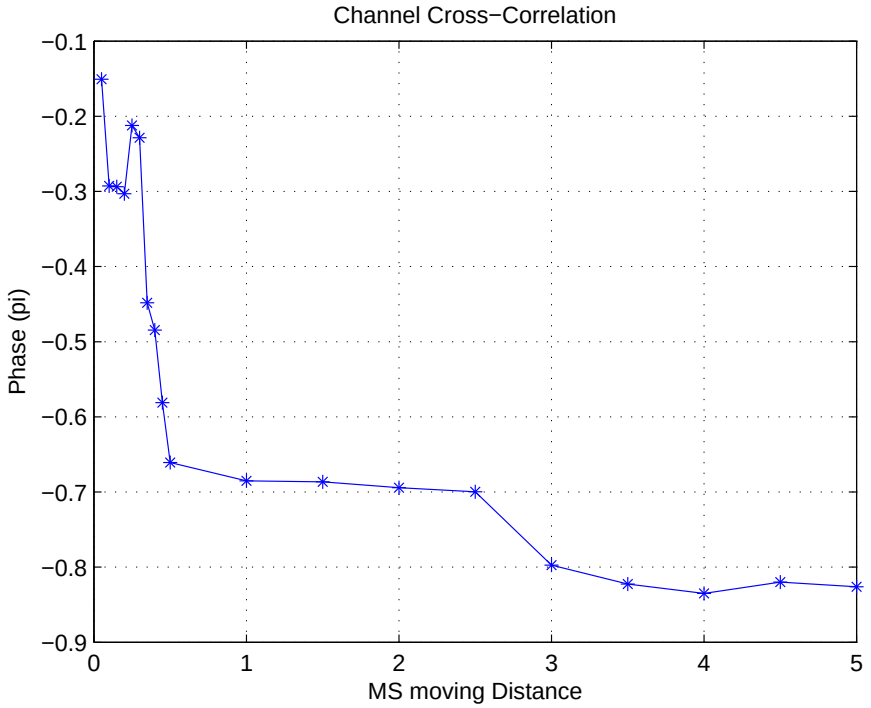

Figure 5.14: Cross correlation phase for different MS move distances.

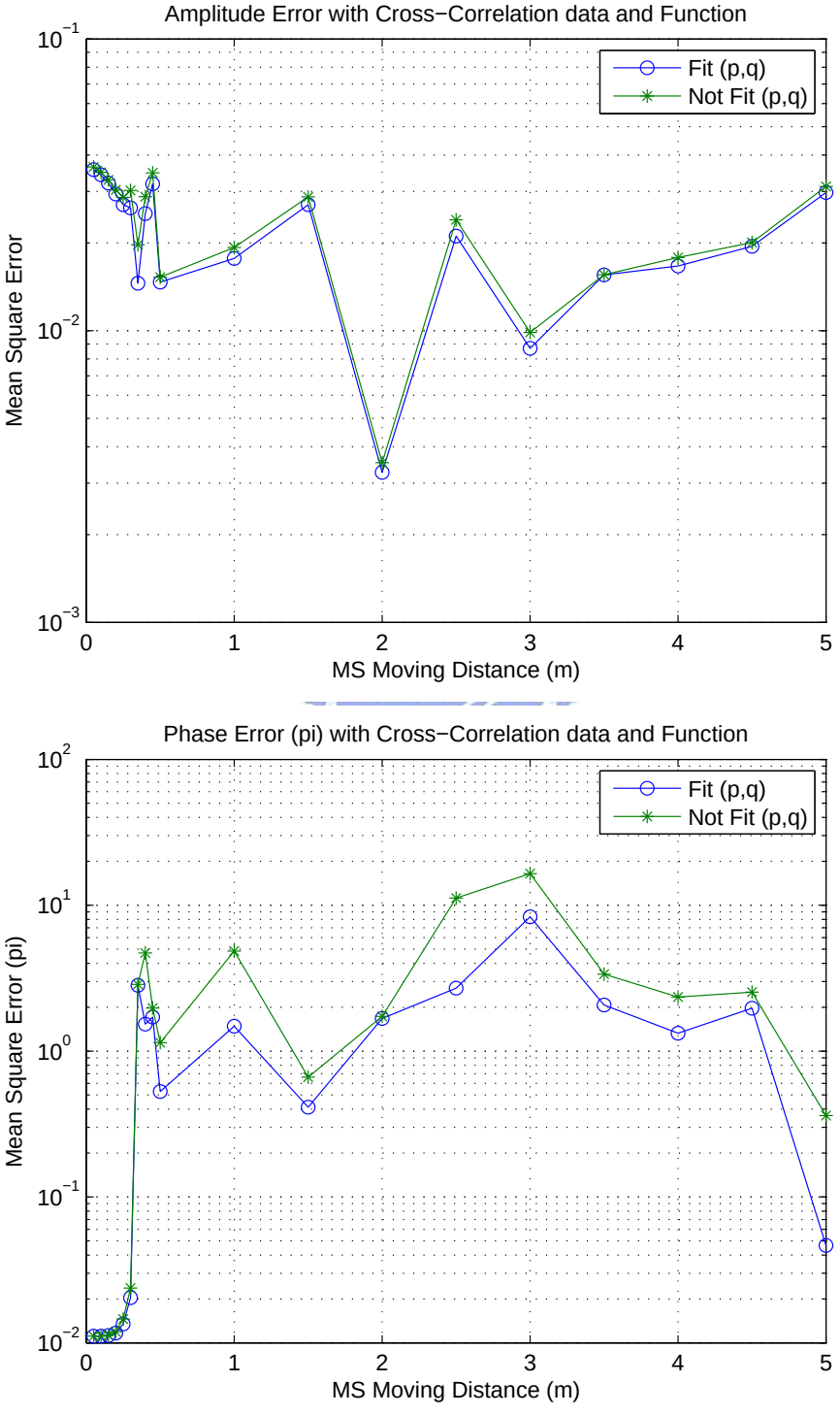

Figure 5.15: Sum square error of fit function

$$
\begin{aligned}
&mod(i,2) == 1 \\
&\qquad AoD_{path} &&= AOD_{LOS} + rand \times 10 + 90 \\
&\qquad AoA_{path} &&= AOA_{LOS} + rand \times 10 \\
&mod(i,2) == 0 \\
&\qquad AoD_{path} &&= AOD_{LOS} + rand \times 10 \\
&\qquad AoA_{path} &&= AOA_{LOS} + rand \times 10 + 90
\end{aligned}
$$

Figure 5.16: Simply equation to reset AoA and AoD.

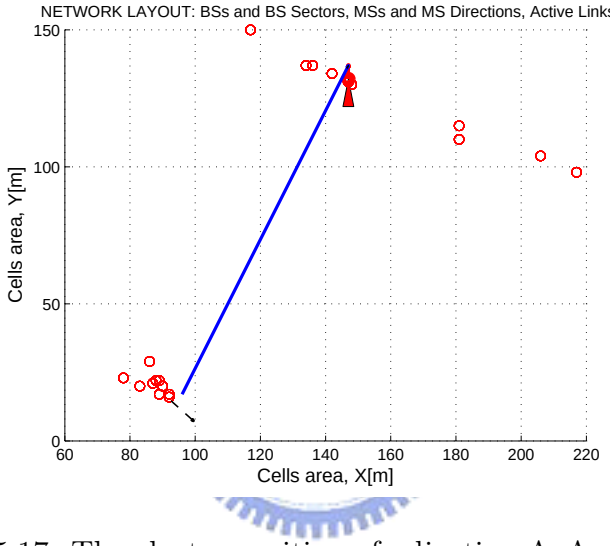

Figure 5.17: The cluster position of adjusting AoA and AoD.

channel correlation. Fig. 5.17 is our simply reset the AoA and AoD result based on (5.16). In the (5.16), we only considered the cluster position around BS and MS.

Table 5.4 is our first simulation case of one BS antenna element and two MS antenna elements, and we adjust MS antenna elements distance to discuss channel correlation and fit result. Tab. 5.5 is the summary table of fitting result for different cases, and the Fig. 5.18∼5.20 are the simulation figure of the WINNER channel cross-correlation curve in frequency domain and its fitting result curve. In order to convenient to discuss the adjusting angle effect, we also list not adjusting AoA and AoD cases, and their parameter are same as Table 5.5. According to Table 5.5, we realize the if the clusters are more centralized around BS and MS, then their auto-correlation are more similarity and have better curve fitting result.

Table 5.4: Channel Environment Parameter to Test Fit Function

Parameters	Values
Scenario	C2
CenterFrequency	3e9
NumTimeSamples	10000
SampleDensity	5
BS elements distance	5 (m)

Table 5.5: Fit result for adjust AoA and AoD for 1BS2MS

Adjust AoA and AoD				
MS antenna elements distance (cm)	p	q	MSE_p	MSE_q
1	0.9999	-0.4586	0.01483	0.00942
5	0.9994	-2.296	0.01485	0.009745
10	0.9985	1.698	0.01487	0.01027
Not adjust AoA and AoD				
MS antenna elements distance (cm)	p	q	MSE_p	MSE_q
1	1.005	-0.3982	0.0165	1.52516
5	1.014	2.364	0.0163	2.5783
10	1.038	3.956	0.01405	1.609

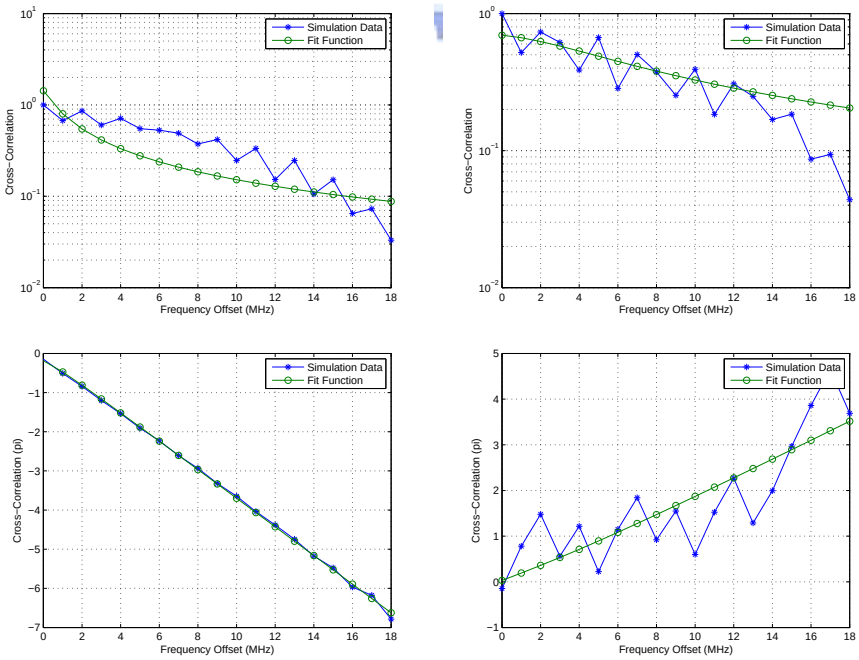

Figure 5.18: Fit cross-correlation for adjust angle and not adjust angle in MS antenna distance 1 (cm).

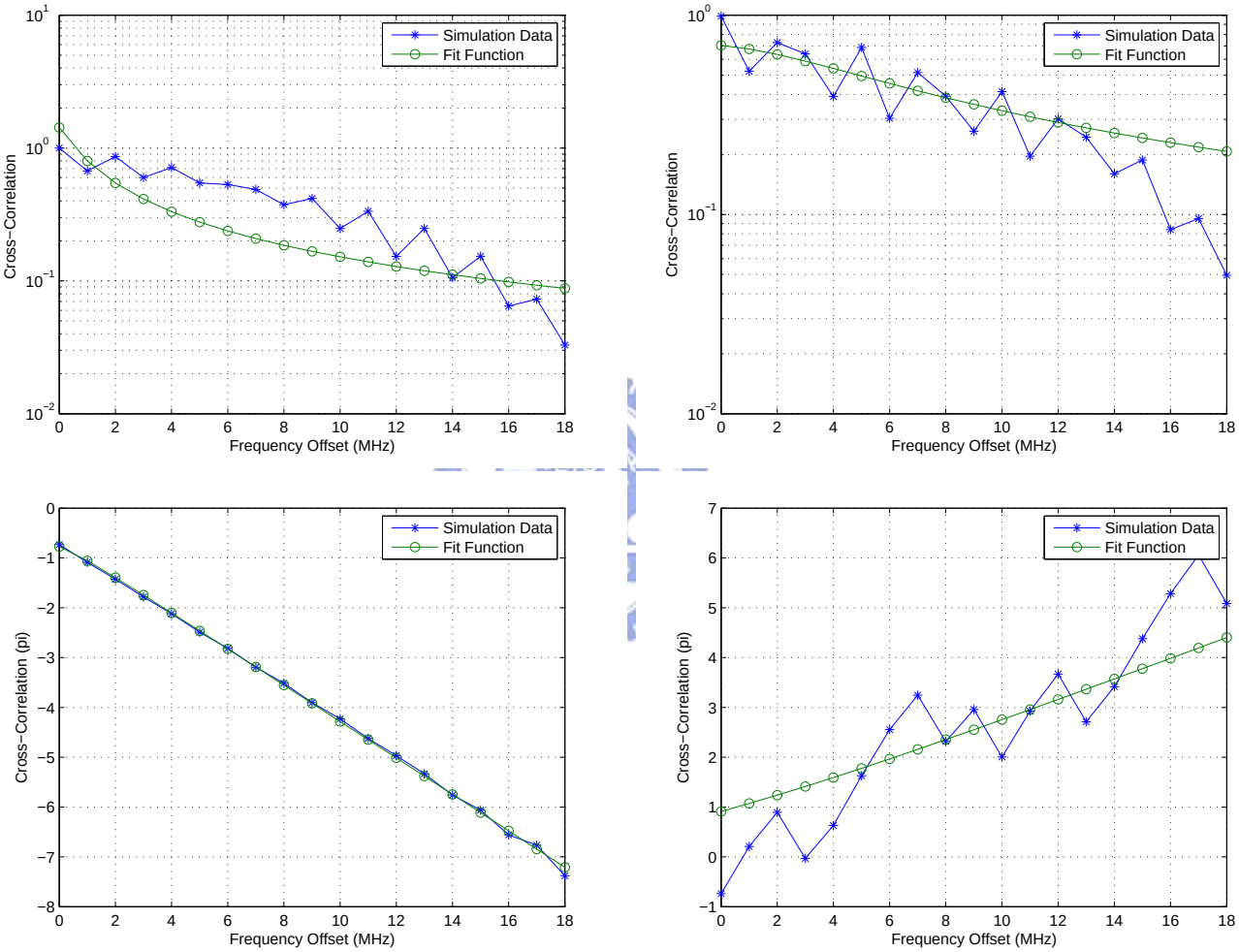

Figure 5.19: Fit cross-correlation for adjust angle and not adjust angle in MS antenna distance 5 (cm).

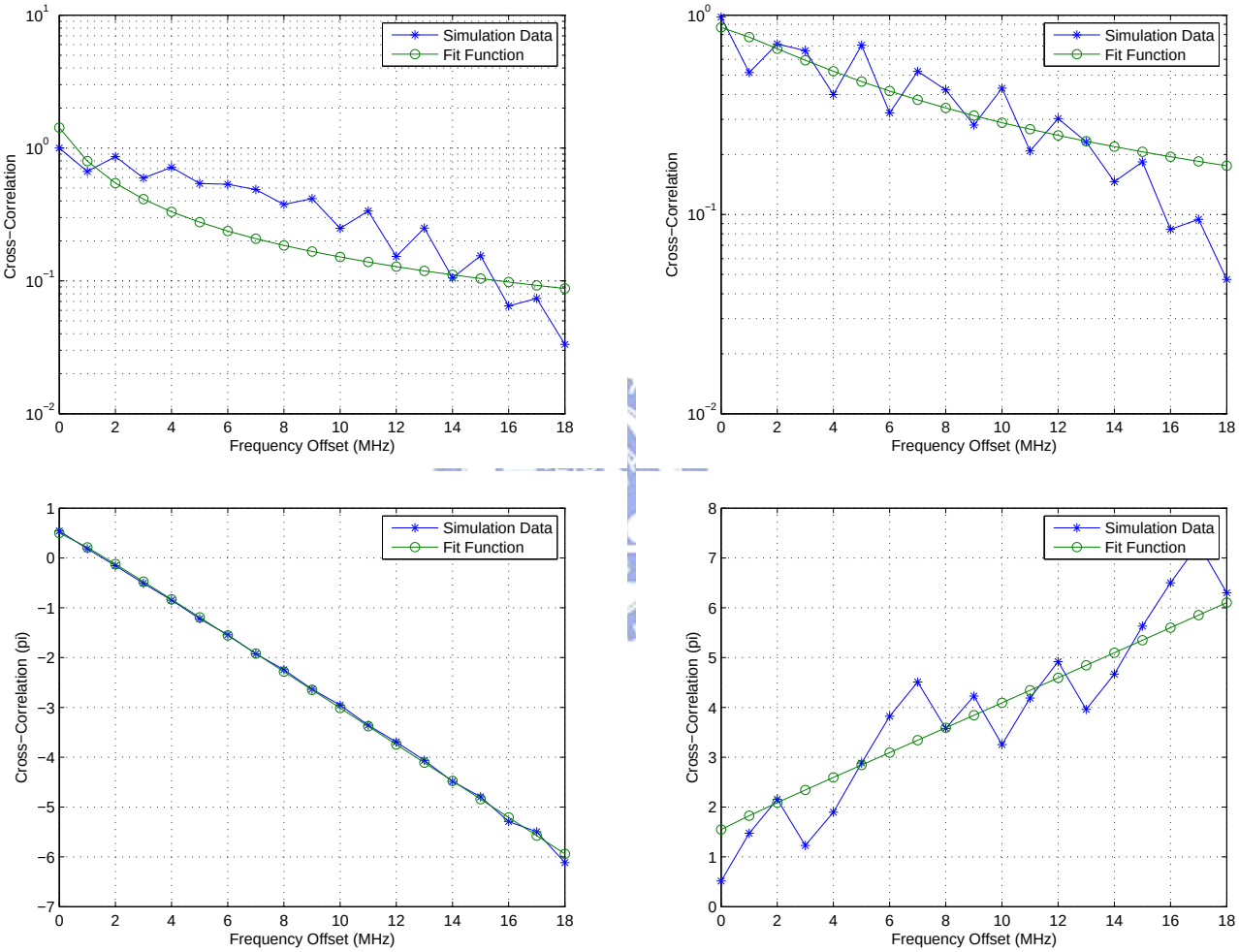

Figure 5.20: Fit cross-correlation for adjust angle and not adjust angle in MS antenna distance 10 (cm).

Chapter 6

Conclusion and Future Work

6.1 Conclusion

In this thesis, we first presented the several channel modeling technique. Second, in order to reduce the Sum-of-Sinusoids channel technique, we listed four skill and verify. Third, we integrated IEEE 802.16e PHY layer block function and analyze each block input and output power establish the connection between PHY and MAC layer. Final, we discussed the some reason to affect channel cross-correlation, and we also fitted auto-correlation and cross-correlation function to discuss their relation.

In order to simulate more actual channel condition, we studied WINNER II channel model and learn to use WINNER public MATLAB code. Additional, we want to implement on DSP in the future, we verified three kinds of polynomial technique could reduce channel simulation complex and their simulation time a lot. We also verified the winner channel model and auto-regressive approximation error were closely to Gaussian distribution, so we only needed some of AR model parameter and random number generator could simulate the WINNER channel well and do not need so much time.

We integrated IEEE 802.16e PHY layer system with c program, and analyzed input and output each function block power level. Second, we established the simple mechanism to communicate physical layer and MAC layer.

Final, we discussed some reason to affect spatial channel correlation. And verified cross-correlation and auto-correlation function were correlated, when the channel cross-correlation

was high.

6.2 Future Work

There are several possible extensions for our research:

- Discuss the channel parameter set in WiMAX channel simulation.
- Implement approximation technique and optimize their performance on DSP.
- Simulate more channel environment or consider different channel environment parameter to verify our suppose channel cross-correlation equation.
- Change the fit equation could be used more general case
- In this thesis, we do not consider the antenna polarized arrays, path-loss and shadowing model. The simulation can be involved in the future.

Bibliography

[1] Matlab sofeware documentation of WIM2 model V1.0, April 2008, http://www.ist-winner.org.

[2] D5.4, "Final Report on Link Level and System Level Channel Models, ver 1.4 , November 2005.

[3] P. Dent, G.E. Bottomley and T. Croft, "Jakes' fading model revisited", *Electronics Letters*, vol. 29, no. 13, pp. 1162–1163, June 1993.

[4] 3GPP TR 25.996 V6.1.0, *3rd Generation Partnership Project; Technical Specification Group Radio Access Networks; Spatial Channel Model for MIMO Simulations (Release 6)*. September 2003.

[5] IST-WINNER II, D1.1.2, "WINNER II Channel Models, ver 1.0, Sep. 2007, http://www.ist-winner.org.

[6] M. Narandzic, C. Christian, R. Toma, T. James, P. Kyosti, and Xiongwen Zhao, "Comparison of SCM, SCME, and WINNER channel models, *IEEE 65th Veh. Technol. Conf.*, April 2007, pp. 413–417.

[7] Kareem E. Baddour, and Norman C.Beaulieu, "Autoregressive modeling for fading channel simulation, *IEEE Trans. Wireless Communication*, vol. 4, no. 4, pp. 1650–1662, July 2005.

[8] PCI data rate message home page: http://www.tomshardware.tw/681,review-681-4.html.

[9] Sundance home page: http://www.sundance.com/default.asp.

[10] Chih-Wei Wang, "Research in and DSP implementation of channel estimation techniques for IEEE 802.16e OFDMA uplink and downlink," M.S. thesis, Dept. Electronics Eng., National Chiao Tung Unversity, Hsinchu, Taiwan, R.O.C., June 2007.

[11] IEEE Std 802.16-2004, *IEEE Standard for Local and Metropolitan Area Networks—Part 16: Air Interface for Fixed Broadband Wireless Access Systems*. New York: IEEE, June 24, 2004.